Contract Report Series 80-3 [Part 3]

KITIMAT PHYSICAL OCEANOGRAPHIC STUDY 1977-1978
PART 3
ESTUARINE CIRCULATION

by

Ian Webster

Dobrocky SEATECH Ltd.

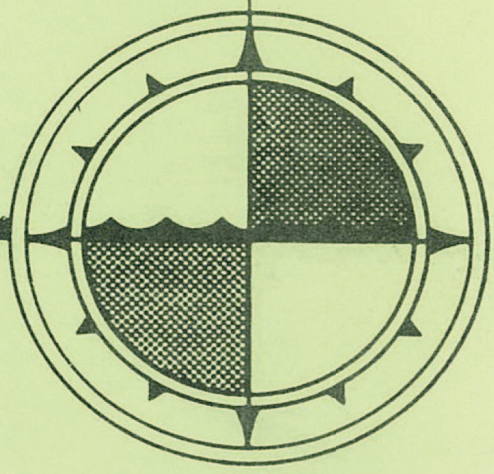

For

INSTITUTE OF OCEAN SCIENCES
Sidney, B.C.

Contract Report Series 80-3 (Part 3)

KITIMAT PHYSICAL OCEANOGRAPHIC STUDY 1977-1978

PART 3

ESTUARINE CIRCULATION

by

Ian Webster

Dobrocky SEATECH Ltd.

For

Institute of Ocean Sciences

Sidney, B.C.

1980

This report was prepared by Ian Webster of Dobrocky SEATECH Ltd. under contract to the Institute of Ocean Sciences. The contents of this report are the responsibility of the Contractor.

ACKNOWLEDGEMENTS

The author would like to thank all those persons who assisted in the preparation of this report. Thanks are due to S. Narayanan who provided details of her tidal circulation model which are outlined in this report and to D. F. Winter who adapted his estuarine circulation model to the Kitimat system. Other important contributions were made by D. M. Farmer who provided valuable advice during the design stages of the project and by W. Buckingham who assisted in the compilation of this report. Thanks are also due to the typists of the report, K. Tolhurst and L. Erechar, and to H. Pite who drafted the diagrams.

ABSTRACT

This report is one of a series describing the implementation and results of a study of the circulation in the channels which form the seaward approaches to the port of Kitimat, British Columbia. The following report first summarizes the conduct of the study. The importance of prominent baroclinic tides to near surface currents and to the problem of determining water structure is discussed. Also examined are the temporal and spatial variations in water structure throughout the study area and their implications to the estuarine circulation and to deep water exchange. The effects of wind on water movements and water structure in Douglas Channel are described. Observations of the tidal flow passing over the shallow sill in Verney Passage suggest that an internal hydraulic jump forms. A description of these observations is included in the report.

TABLE OF CONTENTS

LIST OF FIGURES

LIST OF TABLES

PREFACE

The purpose of the present study was to gain an understanding of features of the tidal, estuarine, and wind driven circulations in the seaward approaches to the port of Kitimat. To collect sufficient data to describe these circulations in such a complex system of channels as the one studied was recognized at the outset as being beyond the available resources of the study. Nevertheless, much information on these circulations in the region was learned which is of great value in itself, but perhaps is even more valuable as a framework from which future studies can be designed and interpreted. Major deficiencies in our understanding of the circulations remain which could be resolved by further work both in the field and on data which have already been collected. Time constraints dictated that most of the data collected during the study could not be examined in detail. The data analysis procedures were chosen to outline those features of the data necessary for the application of a tidal circulation model and for descriptions of the estuarine and wind driven circulations which were mostly non-dynamical. It was hoped that by providing a generalized description of the circulations in the channel approaches to Kitimat rather than concentrating on several smaller scale phenomena, which may be more scientifically interesting, the utility of the reporting of the study results would be maximized.

The implementation and results of the study are presented in the six volumes:

Kitimat Physical Oceanographic Study 1977 - 1978
Data Collection and Analyses

Kitimat Physical Oceanographic Study 1977 - 1978
A Manual for General Data Access

Kitimat Physical Oceanographic Study 1977 - 1978
Estuarine Circulation

Kitimat Physical Oceanographic Study 1977 - 1978
Tidal Circulation Model

Kitimat Physical Oceanographic Study 1977 - 1978
The Response of Douglas Channel to Meteorological Forces

Kitimat Physical Oceanographic Study 1977 - 1978
Temporal Variations of the Baroclinic Tide in Douglas Channel

1. INTRODUCTION

The port of Kitimat, situated on the central British Columbian coast, is the site of a large aluminum smelting plant and a large pulp mill. Primarily in connection with these industries the port handled coastal and foreign cargoes of over one million tons during 1975. There is a strong possibility of further development in the Kitimat area including tanker port facilities, steel mill, coal port, oil refinery, and offshore drilling, all of which will make Kitimat a major centre of industrial activity. Both the present industry and future developments are apt to have a significant impact on the ocean environment in the seaward approaches to Kitimat. Fundamental to the assessment of the assimilative capacity of any ocean system to industrial or municipal discharges is an understanding of the water circulation patterns. The water circulation governs the dispersal and removal of discharged wastes whose concentration in turn affects the characteristics and quantity of the biological communities in the area. Because of the importance of knowledge of the water circulation in environmental impact assessment of potential and existing development at Kitimat, Dobrocky SEATECH Limited undertook a physical oceanographic study of the complex of channels which forms the seaward approaches to the port. This complex will be referred to as the Kitimat system in this report.

Typically, the circulation in inlets along the British Columbian coast is driven by a combination of tidal forces, wind stress on the surface, and by pressure forces arising from variations in density along the inlet's length. The tidal forces which originate with the gravitational pulls of the moon and the sun result in tidal currents. Although these currents, which run primarily back and forth along the channel lengths, may not be the major agent of net advection from an inlet system, they are usually important sources of energy for longitudinal, lateral, and vertical mixing processes. Also, if the tidal currents are large they may be of considerable importance to navigation especially in narrow twisting channels. The force of the wind on the surface of an inlet is capable of causing water movements there. The intensity of the wind driven circulation is dependent both on the strength and duration of the wind in a particular direction. Since the wind climate in a particular location is usually seasonally dependent, one might expect the same to be true of the component of circulation which is driven by the wind. Most inlets along the British Columbian coast have freshwater discharges along their sides and at their heads which gives rise to a third mode of circulation. This flow which will be termed the estuarine circulation has an intensity which is strongly dependent on the seasonal fluctuations of freshwater discharge. Both the wind driven and estuarine circulations are important agents for the exchange of the surface waters of the inlet with water external to the inlet.

Field data were collected during SEATECH's oceanographic study of the Kitimat system pertinent to the examination of the 3 types of circulation just mentioned. The seasonal dependence of the wind driven and estuarine circulations necessitated that the observations in the system take place over a minimum of a year's period. The collection of sufficient data to adequately document this circulation in the maze of interconnecting channels

which forms the Kitimat system was recognized as being unrealistic. Rather, data collected in key locations would be used as a basis for construction of two numerical models of the system, one of which will be termed the Tidal Circulation model and the other the Estuarine Circulation model. The Tidal Circulation model, which considers tidal motions only, is used to extend tidal current and tidal height predictions to the extensive areas of the system in which direct measurements were not obtained. Conversely, the Estuarine Circulation model is a steady state model which doesn't consider tidal motions at all. The Estuarine Circulation model, which requires as input the observed density structure in the system, freshwater discharge data and wind data, is a diagnostic model rather than a predictive one. Its immediate aim was to quantify the circulations due to freshwater discharge and the wind, but it was hoped that it would also provide insight into the functioning of the system as it responds to the wind and estuarine driving forces. It is recognized that the circulations due to the tides, the wind and freshwater runoff interact in a nonlinear fashion with one another but, unfortunately, a time dependent model which incorporates all 3 circulation modes is not within the resources of the study.

The results of SEATECH'S study of the physical oceanography of the Kitimat system are reported in 6 separate volumes. The following report performs a dual function. First, it provides an outline of the studies' objectives, its implementation and its results. Also included is a description of some of the pertinent features of the physical geography of the Kitimat area. The other function of the report is the examination of the estuarine and wind driven circulations of the Kitimat system. The current meter records showed that major changes in the current regime within the inlet system can occur over periods of a matter of days, hence the response of the system to influences having periods of several days is examined. Likewise, the longer term variations in water structure and circulation which result from seasonal variation in solar insolation, wind regimes, and freshwater discharges are described. The Estuarine Circulation model is used as a diagnostic tool in the latter presentation.

2. PHYSICAL GEOGRAPHY OF THE KITIMAT SYSTEM

2.1 Topography

The location of the section of the British Columbian coast which will be termed the Kitimat system is shown in Figure 1. The Kitimat system is bounded by the mainland of British Columbia in the north and by Pitt Island, Campania Island, and Princess Royal Island in the south (see Figure 2). There are 4 entrances to the system, namely Grenville Channel and Princess Royal Channel on its western and eastern sides respectively and Otter Channel and Campania Sound at its southern end. Of these entrances, Campania Sound and Otter Channel are certainly the most important as they are wide and connect fairly directly to Hecate Strait. Grenville Channel and Princess Royal Channel, which are both long and narrow, ultimately connect to Hecate Strait and Queen Charlotte Sound, respectively. The geometry within the Kitimat system is complicated by the presence of numerous islands and of inlets which adjoin its sides. If the axis of the system is considered to be the waterways between Campania Sound and Kitimat then Hawkesbury Island and Gil Island roughly bisect the system along its length. The channels to the west of these islands, from north to south, are Douglas Channel and Squally Channel; those on the eastern side are Devastation Channel, Verney Passage, and Whale Channel. The distance between Kitimat and Campania Sound along these channels is approximately 140 km. Ursula Channel on the eastern side and McKay Reach on the southern side of Gribbell Island form an alternate route for water movements in the area to the southeast of Hawkesbury Island. Of the numerous inlets which adjoin the sides of the Kitimat system, Gardner Canal is by far the most important. This inlet, which has a length of 90 km, joins the eastern side of Devastation Channel.

2.2 Bathymetry

Figure 3 shows the water depths along sections of the Kitimat system. The positions in each channel are referenced using the locations of some of the CTD stations which were occupied during the study. The interior of the Kitimat system can be considered to be divided into 3 major basins by the presence of sills. The locations and depths of these sills are shown in Figure 4. One of these basins is defined by sills which cross Otter Channel, Campania Sound, Grenville Channel, the northern end of Princess Royal Channel, the northern end of Ursula Channel, Verney Passage, and Douglas Channel. The sills which cross Verney Passage and Ursula Channel are particularly shallow being only 31 m and 35 m deep, respectively. This basin thus includes the channels around Gil Island and Gribbell Island, the southern half of Douglas Channel and part of Grenville Channel. In Whale Channel and Squally Channel on the 2 sides of Gil Island, depths of over 550 m are attained which are the greatest found in any part of the Kitimat system. These 2 channels are connected to a depth of 490 m around the northern end of Gil Island. The sill of depth 240 m which crosses Douglas Channel between stations CTD 27 and CTD 28 forms one of the southern boundaries of a second basin. This basin, which has a maximum depth of 400 m, includes the northern half of

Douglas Channel, Kitimat Arm and Devastation Channel as far south as its sill. This sill of depth 110 m crosses Devastation Channel just north of its confluence with Gardner Canal. A third major basin is found in the inner section of Gardner Canal defined by a sill which crosses the channel at a depth of 100 m between stations CTD 19 and CTD 20. Depths in this basin reach 500 m. Water movements in and out of Gardner Canal are further restricted by the sills which cross Devastation Channel, Verney Passage and Ursula Channel.

3. DATA COLLECTION AND DATA ANALYSES

The following summarizes the major features of the data collection and data analyses for the oceanographic study of the Kitimat system undertaken by SEATECH. A more complete discussion is available in the separate report entitled "Kitimat Physical Oceanographic Study 1977-1978 - Data Collection and Analyses."

3.1 Data Collection

During the period July, 1977 to June, 1978, 5 cruises were undertaken to the Kitimat system on board the vessel "Sea Lion." On each cruise, roughly 10 days were spent in the study area servicing instrumentation that had been left in place between the cruises and making water structure measurements throughout the system by CTD casts and by hydrocasts. The 5 periods spent in the study area were July 8 to July 16, 1977; September 25 to October 5, 1977; December 5 to December 17, 1977; March 5 to March 15, 1978; and June 8 to June 13, 1978. These cruises will be termed the July (1977), September (1977), December (1977), March (1978) and June (1978) cruises respectively. All times referenced in this report are Pacific Standard Time (PST).

The instrumentation left in place between the cruises included current meters, tide gauges, thermistor chains and weather stations. Each of these instruments recorded data internally on magnetic tape at preselected intervals which were 15 minutes for the current meters and tide gauges and 30 minutes for the thermistor chains and weather stations. The current meters recorded measurements of temperature and conductivity in addition to current speed and direction. Each current meter mooring contained 2 or 3 current meters located at different depths. The tide gauges were placed in concrete blocks at a depth of between 10 m and 20 m and recorded water pressure and temperature. Each thermistor chain was 50 m long and contained 11 thermistors at 5 m intervals. The thermistor chains were hung vertically from a flotation buoy on the surface. A measurement of temperature was recorded from each thermistor at the end of every sampling interval. The weather stations were intended to make measurements of wind speed, wind direction, and precipitation. Unfortunately, mechanical and electrical problems occurred which prevented good quality data being collected from them. However, the data recovery rate from the current meters, tide gauges and thermistor chains was high. Figure 5 summarizes the installations of these instruments for which good quality data were recovered; Figure 6 shows the locations of these installations.

A CTD is an instrument lowered over the side of a ship to determine temperature and conductivity as functions of pressure. A total of 39 regular CTD stations were designated in the study area. On each cruise, CTD casts were made at least once at most of these stations. In addition, in areas where the time variability of the water structure was likely to be of particular importance, time series of CTD casts were collected. To supplement the CTD work, 8 hydrocasts were carried out on

each cruise. These hydrocasts served the dual function of verifying the operation of the CTD and of collecting samples from the deeper water for a dissolved oxygen analysis. The locations of the CTD stations and the hydrocast stations are shown in Figure 7.

3.2 Data Analyses

Once ashore, the data from most of the instrumentation used in the study underwent further processing on the Univac computer at the Institute of Ocean Sciences, Patricia Bay. The data from the current meters, tide gauges, thermistor chains, and weather stations were all calibrated, edited and plotted as time series. Subsequent processing of the data from the current meters and the tide gauges included harmonic analyses and digital filtering. The harmonic analyses were applied to the current velocity data and the water pressure data to determine the magnitudes and phases of the tidal constituents in these records. These determinations were used in the construction of the Tidal Circulation model for the Kitimat system. The current velocity data and the water pressure data were also low pass digitally filtered to remove fluctuations having periods less than or equal to the tidal period. This filtering procedure reduced the amplitude of a fluctuation having a period of 3 days by 50%. A digital filter having a similar effect was applied to the temperature records from the thermistor chains. The filtered data from each thermistor chain were then contoured to produce a time series plot of isotherm depths.

The initial processing of the temperature, conductivity, and pressure data from the CTD included their calibration and editing. Subsequently, these data were combined to produce plots of temperature, salinity and sigma-t (density) as functions of depth for each cast. Laboratory analyses were carried out on water samples collected by hydrocast to determine salinities and dissolved oxygens. Temperatures were read from reversing thermometers attached to the hydrocast sampling bottles.

4. TIDAL CIRCULATION

Features of the tidal heights and tidal currents observed during the study are described in the following. Also included is a brief description of the numerical tidal model developed to describe the barotropic currents throughout the Kitimat system. The development of the model and the results obtained are described in more detail in "Kitimat Physical Oceanographic Study 1977-1978 - Tidal Circulation Model".

4.1 Tidal Heights

Tidal variations in pressure measured by the tide gauges were converted to equivalent water level variations using the relationship: 1 m change in water level = 1 dbar pressure change. The exact relationship between pressure and water level changes is determined by the water density structure above the tide gauge. In view of the variations in water structure actually observed in the Kitimat system during the study, the accuracy of the '1 m = 1 dbar' relationship is estimated to be better than ± 0.5%.

Observed tidal height ranges were large everywhere, averaging about 4 m. In some sections of the Kitimat system, daily tidal ranges were observed to exceed 7 m during spring tides. The tides were of the mixed semi diurnal type characterized by 2 daily highs and 2 daily lows of unequal amplitude (see Figure 8). The harmonic analyses of the time series of water heights performed on tide gauge records of 3 months duration differentiated the contributions of 35 tidal constituents. The 5 constituents having the largest amplitudes were the M_2, K_1, S_2, N_2 and O_1 constituents. The computed amplitudes of these constituents from a tide gauge near Kitimat (TG 1) and one in Campania Sound (TG 2) for the period September to December, 1977, are listed in Table 1.

Table 1.

Tidal Constituent Amplitudes at TG 1, TG 2, September to December, 1977

Tidal Constituent	Constituent Period (hrs.)	Constituent Amplitude (m)	
		TG 1	TG 2
M_2	12.42	1.69	1.56
S_2	12.00	0.55	0.51
K_1	23.93	0.49	0.48
N_2	12.66	0.35	0.33
O_1	25.82	0.28	0.29

The M_2 tidal constituent is the largest constituent by far having an amplitude roughly equal to the sum of the amplitudes of the other 4 constituents. For the 2 tide gauges at TG 1 and TG 2, a comparison of the computed amplitudes of constituents between the 3 installation periods, September to December, 1977; December, 1977 to March, 1978; and March to June, 1978, revealed that the M_2, S_2 and O_1 amplitudes varied by 5% or less, whereas the K_1 and N_2 amplitudes varied over a 20% range. The corresponding comparison of tidal phases at the 2 tide gauges over the 3 periods resulted in variations of less than 5^o for both the M_2 and O_1 constituents, of between 15^o and 20^o for the S_2 and N_2 constituents, and of around 30^o for the K_1 constituent. Harmonic analyses performed by A. Douglas (Institute of Ocean Sciences) on tide gauge records collected at Kitimat over the same period yielded similar phase variations even when inference was included in the analysis scheme. The tidal heights and tidal phases showed a degree of variation throughout the Kitimat system. The largest tides were observed in Grenville Channel and the smallest in Princess Royal Channel. In these 2 channels, the amplitudes of the M_2 constituents were 2.0 m and 1.5 m, respectively. M_2 tidal height phases computed from records collected simultaneously in different parts of the study area were all within 10^o of one another.

4.2 Tidal Currents

As expected, the large tidal ranges observed were associated with vigorous tidal currents in the channels comprising the Kitimat system. In most cases, the tidal currents dominated the contributions from the wind driven and estuarine circulations. Figure 8 shows the north/south component of current velocity observed by the current meter at 165 m depth on mooring CM 2 for the same time period as the tide gauge record shown above it. The harmonic analyses of current meter data showed that everywhere the M_2 tidal constituent dominated the tidal current. The ratio of the amplitude of a selected tidal current constituent to the sum of the amplitudes of all the tidal current constituents at diurnal frequencies and higher was estimated for 10 records from current meters between 30 m and 50 m depth. For the M_2 constituent, this ratio varied between 0.18 and 0.41, the average being 0.30; for the 4 other largest constituents, the average ratios were 0.10 for S_2, 0.07 for N_2, 0.06 for K_1 and 0.04 for O_1.

It has been shown in general that the tip of a 2-dimensional vector which has its 2 coordinates varying sinusoidally at frequency, f, traces out an ellipse traversing either in a clockwise or in an anticlockwise direction at frequency, f. (Mooers, 1973) From the current velocity data from each meter, a tidal ellipse was determined. The lengths of the major and minor axes and the orientations of the ellipses were derived from the north/south and east/west velocity amplitudes and phases at each tidal frequency. As expected, the ellipses were oriented such that their major axes were aligned with the channel axes; that is, the major component of the tidal flow in the channel was back and forth along the channel. For each ellipse, the ratio R, of the magnitude of the minor axis to the magnitude of the major axis was determined for the

M_2 tidal constituent. For a purely back and forth motion, R would be 0, whereas for a circular motion R would be 1. The values of R observed for the M_2 constituent in the Kitimat system were less than 0.1 (ellipse eccentricity greater than 0.99) except for the 8 instances listed in Table 2. Also listed in Table 2 are the R values from the other current meters on the same moorings for comparison and the sense of rotation in the ellipse. Except for an R value of 0.27 at the 110 m depth current meter at CM 1 in Kitimat Arm, the remaining occurrences of R values greater than 0.1 were located in the channels south of Wright Sound. In tidal flows in channels, values of R different from 0 are expected to arise from the inertial interaction of currents with the topography and from apparent inertial forces resulting from the earth's rotation (Coriolis force). In the development of the Tidal Circulation model, it became evident that the inertial forces were more important in the region to the south of Wright Sound than in the region to the north. The predominance of clockwise rotation for the tidal ellipses in the former region suggests that Coriolis force may be responsible for some of the high R values. In the northern hemisphere, the Coriolis force is expected to cause a clockwise rotation in the tidal ellipse. In Kitimat Arm at CM 1, the total magnitudes of the currents were not much larger than 2 or 3 cm/sec. In such low currents, the direction sensitivity of the current meter is much reduced which may in turn result in apparent cross current flows when there are none. Also, since the width of the channel at CM 1 was around 3 km and the horizontal tidal excursion would have been 0.5 km or less, flows in Kitimat Arm would not have been well confined by the topography. Hence, cross channel flows could have been proportionally larger with respect to the longitudinal flows.

Comparisons of the tidal constituents from current meters at different depths revealed that both the amplitudes and phases of each constituent varied with depth. Evidently, the tidal currents were made up of contributions from the purely barotropic mode and baroclinic modes of tidal circulation. The barotropic tide is essentially a long wavelength, surface wave. In a depth of 200 m, the semi diurnal lunar constituent, M_2, of period 12.42 hrs., has a wavelength of 1400 km. The velocity field associated with such a wave has almost no depth dependence. Conversely, a baroclinic tide, also termed an internal tide, produces only small height changes in the water surface. Rather, it produces vertical movements of density layers within the body of the fluid; the fluid must be density stratified for baroclinic wave propagation. The currents associated with such a tide change magnitude with depth and may undergo one or more 180° phase changes over the water column. Provided the effect of the earth's rotation is neglected, for each frequency below the Brunt-Väisälä frequency, N, ($N = \left(-\frac{g}{\rho}\frac{\partial \rho}{\partial z}\right)^{\frac{1}{2}}$); where g is the gravitational acceleration constant, ρ is density and z is depth) the momentum equation of fluid mechanics allows a series of eigenvalue internal wave solutions in addition to the surface wave or barotropic solution (Phillips, 1966). For a specified vertical density profile, horizontal velocity profile and frequency, the internal wave solution can be found using numerical techniques assuming all horizontal

Table 2.

Occurrences of R Values Greater than 0.1 in Tidal Current Ellipses

Current Meter Mooring	Meter Depth (m)	Time Period	Minor Axis/ Major Axis	Sense of Rotation
CM 1	45	July-Sept.	0.03	Anticlockwise
	110	July-Sept.	0.27	Anticlockwise
	175	July-Sept.	< 0.005	Clockwise
CM 4	35	July-Sept.	< 0.005	Clockwise
	150	July-Sept.	0.14	Clockwise
	265	July-Sept.	0.09	Anticlockwise
CM 4	150	Sept.-Dec.	0.02	Anticlockwise
	265	Sept.-Dec.	0.18	Clockwise
CM 8	40	Dec.-March	0.23	Clockwise
	135	Dec.-March	0.12	Clockwise
	230	Dec.-March	0.29	Clockwise
CM 9	420	Dec.-March	0.15	Clockwise
CM 15	30	March-June	0.13	Anticlockwise
	245	March-June	0.01	Anticlockwise
	445	March-June	0.03	Clockwise

gradients of density, velocity and water depth are zero. Internal wave solutions exist at the semi diurnal period ($\sim$ 12 hours) providing the density gradient is greater than 5×10^{-8} sigma-t units/m over a portion of the water column. This criterion was met everywhere in the Kitimat system at all times of the year. When the effect of the earth's rotation is included, the frequencies for free internal gravity waves must be greater than the local inertial frequency. At 53°N, which is about the latitude of the Kitimat system, this criterion allows free semi diurnal internal waves, but not free diurnal internal waves.

Using the actual density gradient determined from a CTD cast at station CTD 28 in Douglas Channel in September, 1977, the solution was found for the first and second modes of the internal tide at the M_2 period neglecting the effect of the earth's rotation. The normalized, vertical displacement amplitude and horizontal velocity amplitude functions for the 2 baroclinic solutions and for the barotropic solution are shown in Figure 9. The vertical displacement function reaches a maximum at a depth of 125 m for the first mode; for the second mode 2 maxima occur one at 40 m depth and the other at 225 m depth. The phase of the horizontal velocity changes by 180°at each of the amplitude maxima. H. Freeland (Institute of Ocean Sciences, Patricia Bay) has formulated a technique for decomposing measured current velocities at a particular frequency into contributions from the barotropic mode and from various baroclinic modes. The method requires that currents are measured at a series of depths throughout the water column. When the modal separation technique was applied to current meter data for the period July to September from depths of 5 m, 17 m, 30 m, 165 m and 305 m from sites close to station CTD 28 (moorings CM 2 and CM 3), the results indicated that a large proportion of the current velocity energy at the M_2 period lay in the first baroclinic mode. The observed horizontal velocity profile was fitted by a linear combination of a barotropic current which had an amplitude of 11 cm/sec and a first mode baroclinic current which had an amplitude of 9 cm/sec at the surface. The phases of the fitted barotropic and baroclinic currents were 3° different from each other. The second baroclinic mode could not be clearly distinguished from the noise level of the separation process. The actual M_2 current amplitudes are compared to the fitted amplitudes in Table 3.

Table 3.

Comparison of Observed and Fitted M_2 Current Amplitudes at CM 2, July to September, 1977

Current Meter Depth (m)	Observed M_2 Current Amplitude (cm/sec)	Fitted Barotropic + First Mode Baroclinic Amplitude (cm/sec)
5	20	19
17	18	15
30	14	14
165	8	11
305	8	7

Figure 10 shows a time series plot of isotherm depths derived from contouring data from a thermistor located at TMS 2 close to station CTD 28. Depth fluctuations of the order of 10 m in vertical extent were evident at the semi diurnal period for the 8°C isotherm. There appeared to be depth fluctuations of the 9°C isotherm at the semi diurnal period also, but their vertical extent was of the order of 2 to 3 m. The velocity eigenfunction for the first mode calculated from the density profile taken at CTD 28 on the September, 1977 cruise had a normalized amplitude of close to 1.0 at 5 m depth and -0.15 at 165 m depth. Thus, the velocity measured by the current meter at 165 m depth at CM 2 should have been within 20% of the barotropic velocity (assuming the contribution from the second mode was small). An estimate of the first mode of the north/south component of baroclinic velocity can be taken as the difference of the north/south velocity component at 5 m depth at CM 3 and the north/south velocity component at 165 m depth at CM 2. (The moorings were about 0.5 km apart and both within 1 km of TMS 2.) This velocity difference is shown plotted in Figure 10.

The 5 m amplitude of the 'baroclinic' semi diurnal north/south velocity was of the order of 20 cm/sec. If such a baroclinic tide were propagating as a purely travelling wave, it would have produced vertical excursions of the 9°C isotherm ($\sim$8 m depth) of 3 m and of the 8°C isotherm ($\sim$ 35 m depth) of 13 m. These fluctuations of isotherm depths are approximately what were observed.

However, from a visual examination of the isotherm and north/south velocity time series the former is estimated to have led the latter by 80°. The phase difference between isotherm depths and north/south velocity would be either 0° or 180° for a pure travelling internal wave depending on its direction of propagation. For a pure standing internal wave this phase difference would be either 90° or 270°. Thus, the phase relationship observed between isotherm depths and north/south velocity suggests the presence of a standing internal wave in Douglas Channel rather than a travelling internal wave.

The normalized displacement and velocity eigenfunctions for the internal tide have been developed from equations for small perturbations. When the magnitude of the vertical displacement function for an isotherm is calculated to be more than 35% of the mean depth of the isotherm, as it was in this case, then small perturbation theory is not strictly applicable. Also, since the M_2 frequency (0.081 cycles/hour) is not much higher than the local inertial frequency (0.067 cycles/hour), it is likely that the rotational effect of the earth on the characteristics of the internal tide in Douglas Channel was considerable. Although a close examination of the nature of the internal tide in Douglas Channel should consider both rotational effects and nonlinear amplitude effects, it is evident that the internal tide can account for the major part of the observed fluctuations in isotherm depths.

An alternative explanation for the observed fluctuations would be for these to have resulted from the tidal advection of water having a horizontal temperature gradient past the thermistor chain. During

September, 1977, the temperature gradient in Douglas Channel between 20 m and 50 m depth was positive southwards. Such a temperature gradient would cause the apparent isotherm depths at a stationary site to lead the north/south tidal velocity component by 90^{o} versus 80^{o} which was observed. However, the prevailing temperature gradient in Douglas Channel deduced from filtered data from the thermistor chains at TMS 1 and TMS 2 is not thought to have been large enough to have produced the major part of the observed isotherm fluctuations at TMS 2.

Whenever longer term current velocity data were recovered from 3 or more current meters at the same location, modal separation was carried out to separate the M_2 tidal constituent energy into a barotropic and a first mode baroclinic contribution. The magnitude and phase of the estimated baroclinic contribution were then computed for a depth of 5 m and added to the barotropic contribution which should be almost constant with depth. It should be noted that this calculation was carried out for current meters which were installed at depths of 30 m and deeper. The 5 m depth barotropic and baroclinic currents and their sums for the M_2 tidal constituent are listed in Table 4 for the different mooring installations. It can be seen that in most cases the baroclinic contribution is of similar size to the barotropic contribution. Sometimes, when the phases of the 2 are close as they are at CM 2 in the period July to September, 1977, they combine additively to produce a larger M_2 tidal current; sometimes when the contributions are out of phase they act against one another to produce a smaller M_2 current as they do at CM 15 from March to June, 1978. A major feature of the baroclinic current at CM 2 where a whole year of record is available is its apparent variability. The magnitude of the baroclinic current, estimated as 9 cm/sec from July to September, 1977, is reduced to 1 cm/sec in the period March to June, 1978. In each of these cases, the baroclinic current has been estimated from a 3 month section of record and so represents an average. If shorter sections of record were to be examined the variability of the baroclinic current would certainly be larger. For example, in the period September 29 to October 1, 1977, the semi diurnal baroclinic current was estimated to have had an amplitude of 20 cm/sec at the surface at CM 2, whereas from October 2 to October 6, 1977 at the same location this amplitude was reduced to around 8 cm/sec. In the former period, the non tidal flow at 5 m depth was around 10 cm/sec or less, whereas in the latter period it exceeded 40 cm/sec. Since the phase speed of the first mode of the internal tide was calculated to be close to 1 m/sec, currents of 40 cm/sec magnitude are likely to have had a major influence on the characteristics of the tide. There is little reason to suppose that the baroclinic currents at the other current meter sites might not undergo variation of similar magnitudes.

4.3 Tidal Circulation Model

4.3.1 Model Description

The tidal model developed for the Kitimat system was 1-dimensional in the sense that the tidal height, h, and the tidal current, u, were functions only of x, the distance along each channel, and time, t. The variable, u, thus represents the velocity averaged over the width and

Table 4.

Estimated M_2 Tidal Currents at 5 m Depth

Current Meter Mooring	Time Period	Barotropic Contribution		First Mode Baroclinic Contribution		Resultant Current	
		Amplitude (cm/sec)	Phase (deg)	Amplitude (cm/sec)	Phase (deg)	Amplitude (cm/sec)	Phase (deg)
CM 2	July to Sept.	10	190	9	187	19 (20)*	188 (180)*
CM 2	Sept. to Dec.	9	186	5	212	14 (15)*	195 (175)*
CM 2	Dec. to March	8	178	7	261	11	216
CM 2	March to June	8	137	1	218	8	141
CM 4	July to Sept.	23	191	5	186	27	189
CM 5	Sept. to Dec.	7	180	5	325	4	224
CM 6	Sept. to Dec.	5	54	4	315	5	16
CM 8	Dec. to March	12	90	6	68	17	83
CM 15	March to June	8	172	12	355	4	360

* Observed at CM 3

depth of the channel. If A is the cross sectional area of the channel and B is the channel width (both functions of x), then the tidal transport, q, is:

$$q = u\ (A + Bh)$$

The equation of continuity is expressed as:

$$\frac{\partial q}{\partial x} + B\ \frac{\partial h}{\partial t} = 0 \qquad 1)$$

The fluid has been assumed to be of uniform density and incompressible.

The 1-dimensional momentum equation is:

$$\frac{\partial u}{\partial t} + \frac{u\partial u}{\partial x} = -g\ \frac{\partial h}{\partial x} - F_c \qquad 2)$$

where g is gravitational acceleration and $F_c = F_c(u)$ is a frictional term. The problem of modelling the tides is reduced to finding the solution of 1) and 2) subject to appropriate conditions which include the matching of tidal heights and transports at channel junction points within the system and the specification of the boundary conditions. The boundary conditions used were the time varying tidal heights at the entrances to the system, namely Campania Sound, Otter Channel, Grenville Channel and Princess Royal Channel. The solution was accomplished using a conventional time stepping technique. The model was tuned to agree with barotropic current and tidal height observations in the interior of the system by making the degree of bottom friction a function of position.

4.3.2 Model Results

The model was run in several configurations one of which involved using a linearized version of the momentum equation (equation 2) as one of the governing equations. The linearization included dropping the second term and using a linear friction term, namely $F_c = \lambda u$. Solutions were found for the model for each of the tidal constituents M_2, S_2, K_1, N_2, and O_1 separately; the total solution for the linearized system is the sum of the constituent solutions. The model was also run using the nonlinear version of equation 2 with a friction term of the form $F_c = \lambda\ u|u|$. A comparison of the results with the solution for the linearized system over 48 hours showed these to be similar. Evidently, the nonlinear terms are of limited importance particularly in the sections of the Kitimat system north of Wright Sound.

Figure 11 shows the tidal transport amplitudes obtained from the linear solution for the M_2 constituent. The transports through each of Grenville Channel, Otter Channel and Princess Royal Channel into the Kitimat system are of similar magnitude, whereas that through Campania Sound is of the order of 8 times as large. An examination of the corresponding transport phases (Figure 12) shows that when the tide floods north through Campania Sound and Princess Royal Channel, the transports through Otter Channel and Grenville Channel are both in

directions out of the Kitimat system. The currents north of Gil Island were approximately in phase with those through Campania Sound. A tidal current node exists in Devastation Channel just north of the entrance to Gardner Canal. At this point, the current which floods southwards along Devastation Channel from around the north end of Hawkesbury Island meets the northward flood through Verney Passage and Ursual Channel. The tidal flow in and out of Gardner Canal occurs through Verney Passage and Ursula Channel rather than through Devastation Channel. Tidal currents were actually observed to be much weaker in Devastation Channel than in Verney Passage.

5. WIND DRIVEN AND ESTUARINE CIRCULATION

Pickard (1961) considers estuarine circulation to be an established and expected mode of circulation in British Columbian inlets. The estuarine circulation mode is important in inlets with large amounts of freshwater runoff which is the case in the Kitimat system for much of the year. In the idealized estuarine circulation mode, freshwater discharging into the sides and head of an inlet forms into a brackish surface layer which floats on a denser, saline layer underneath. Continuity of volume and dynamical considerations require that this surface layer move seaward. The salinity of the layer generally increases in the seaward direction due to the turbulent entrainment of salty water from below. For the most part, water below the upper layer is derived ultimately from saline oceanic water external to the inlet although it may be freshened somewhat during its progress seaward as a consequence of turbulent mixing between the layers. In the idealized estuarine circulation system, a slow landward flow of saline oceanic water is required to replace that which is entrained into the upper layer and carried out of the inlet.

On the basis of the observed salinity structure of the water column and of some near-surface current meter measurements, it is evident that the estuarine mode of circulation is a major feature in most of the sections of the Kitimat system. The intensity of this circulation is determined by the seasonal variations of freshwater discharge into the sides of the system. In the following, the seasonal variations of the estuarine circulation are described. The stress of the wind on the surface of the water can cause large near-surface water movements which modify the apparent nature of the estuarine circulation. The effect of the wind on the near-surface circulation of Douglas Channel is discussed. The application of a numerical estuarine circulation model to the sections of the Kitimat system landward of Wright Sound is described.

5.1 River Discharge

Pickard describes Douglas Channel and Gardner Canal as being inlets of the stored runoff types. Such inlets receive their peak freshwater discharges in the period May to July corresponding to the melting of snow on higher inland elevations. The 2 gauged rivers which discharge into the Kitimat system are the Kitimat River and the Kemano River which discharge into the head of Douglas Channel and into Gardner Canal, respectively. It was observed, when in the study area, that a lot of freshwater flowed into the sides of the channels forming the Kitimat system. A comparison of the relative areas of the watersheds which drain into the Kitimat and Kemano Rivers with those draining into the large number of ungauged rivers and streams suggests that the latter group contributes considerably more freshwater into the system than the 2 gauged rivers. If one makes the crude assumption that the discharge is proportional to the watershed area then the total discharge along the sides of Douglas Channel is about 3 times that of the Kitimat River. A similar calculation shows that the discharge into Gardner Canal is about 17 times that of the Kemano River. Figure 13 shows the estimated monthly averaged rates of discharge into Douglas Channel and into

Gardner Canal for 1977. River discharge data were available for the Kitimat River but not for the Kemano River for the first half of 1978. A comparison of the monthly averaged discharges of the Kitimat River between 1977 and 1978 showed these to be similar for corresponding months. Presumably, the discharges into Gardner Canal were also similar between the 2 years.

5.2 Water Structure Sampling Problems

It was evident from preliminary examinations of time series data from the current meters and thermistor chains that depths of isohalines and isotherms varied almost continuously in response to the effects of wind, of the horizontal advection of water masses by the tides, and of internal waves having periods ranging up to tidal periods. Any estimates of the prevailing depths of particular isohalines or isotherms throughout the Kitimat system based upon a single CTD cast at each location are therefore subject to aliasing uncertainties. The time series of contoured isotherm depths from TMS 2 obtained during the September cruise (see Figure 10) illustrated a range of phenomena which would cause aliasing problems at that site. The semi diurnal internal tide (discussed in section 4.2) caused the 8°C isotherm to undergo depth variations averaging about 10 m in extent. Over a 6 hour period during the 4 day long record, this isotherm was observed to change depth from 20 m to 50 m. Six hours was about the length of time required to complete a series of CTD casts along the length of Douglas Channel. The phase speed of the first semi diurnal mode of the internal tide was about 1 m/sec which gives it a wavelength of about 40 km. The distance between CTD stations in Douglas Channel was of the order of this wavelength. Because the spatial and temporal separations of the CTD stations were of similar size to the spatial and temporal characteristics of the internal tide, aliasing could cause the perception of the slope of an isohaline, along the length of Douglas Channel to be quite erroneous. Not enough is known about the propagation characteristics of this internal tide to account for its effect on data at most of the stations throughout the Kitimat system. As Figure 10 shows, the vertical displacements of the isotherms at the semi diurnal frequency were much smaller near the surface. The 9°C isotherm varied between depths of 5 m and 12 m but only 2 or 3 m of this 7 m depth excursion appears to be attributable to the internal tide. The major proportion of the depth variance of the 9°C isotherm occurred over a range of non tidal frequencies. Variance was evident in the record right up to the Nyquist frequency of 0.25 cycles/minute. The average vertical density gradient over the surface 15 m observed at a nearby CTD station (CTD 28) around this time was 0.13 sigma-t units/m. The Brunt Väisälä frequency frequency calculated from this density gradient is 2 cycles/minute, which is higher than the Nyquist frequency of the thermistor chain. Thus, the high frequency variance in the thermistor chain record could result from propagating internal waves. The appearance of the 10°C isotherm at the surface for short periods on October 1 and October 2 coincided with 2 high tides in Douglas Channel. Certainly, these were cases in which warmer surface water was advected by the tides to the thermistor chain location. In this part of Douglas Channel, it is

thought that although the surface tide transported water back and forth over a 5 km length of the channel, the horizontal temperature gradients were not very large so that tidal advection caused relatively minor aliasing problems. In other parts of the system such as in Campania Sound, tidal advection seems to have had a considerable influence on the observed water properties.

5.3 Water Structure and Circulation to 50 m Depth

Due to the influx of freshwater and solar radiation through the water surface, the largest horizontal and vertical gradients of temperature and salinity throughout the Kitimat system tended to occur in the top 50 m. Accordingly, features of spatial and temporal water structure variations in the top 50 m will be discussed separately from those occurring in deep water, namely, below 50 m depth.

5.3.1 Salinities at 1 m Depth

In the inner reaches of the system, that is in Douglas Channel and Gardner Canal, the vertical salinity structure was characterized as having a surface, relatively low salinity layer with a thickness of the order of 10 m. Such layers are usually found in inlets along the British Columbian coast with appreciable freshwater inputs. In the remaining sections of the Kitimat system, this layer was more diffuse and sometimes non-existent. Figures 14 to 18 show the salinities observed at 1 m depth throughout the Kitimat system on each of the 5 cruises to the study area. Despite the large spatial and temporal variations of the 1 m salinities, salinities at 50 m depth almost everywhere fell in the range 31.0‰ ± 0.5‰. The pattern of surface salinities was as expected considering the nature of the freshwater discharge into the system. Gardner Canal, having the largest freshwater input consistently had the lowest surface salinities all year round. Douglas Channel also had relatively low surface salinities though these were not as low as salinities in Gardner Canal. Generally speaking, the salinities increased towards the entrances of the Kitimat system from their lowest values at the eastern end of Gardner Canal and at the northern end of Douglas Channel. It is expected that the surface layer involved in an estuarine circulation increases in salinity in its direction of flow. However, a surface salinity based upon a single CTD cast is subject to an aliasing uncertainty which may reverse the apparent direction of a surface horizontal salinity gradient. The lowest surface salinities throughout the system were observed on the cruises in July, 1977 and June, 1978 which were coincident with the season of highest freshwater discharge (see Figure 13). On these 2 occasions separated by almost a year, the surface salinity distributions were quite similar. Surface salinities tended to be progressively higher on the September, 1977 cruise, on the March, 1978 cruise and on the December, 1977 cruise which was the order of decreasing freshwater discharges.

5.3.2 Douglas Channel Observations

5.3.2.1 Water Structure

Figure 19 shows the salinity profiles taken at stations along the length of Douglas Channel in July, 1977. If the thickness of the upper layer is defined as the depth of maximum negative curvature of the salinity profile then it can be seen that this thickness does not change much from a value of around 10 m along the channels' length. However, the integrated quantity of freshwater in the top 50 m of the water column decreased markedly towards the mouth of Douglas Channel. The increase of salinity, the reduction of freshwater content, and the approximate constancy of the upper layer thickness along the channel's length are features observed in the salinity profiles of the September, 1977; March, 1978; and June, 1978 cruises. Figure 19 also shows the salinity profiles observed at CTD 26 on each of the 5 cruises to the study area. The existence of a distinct, low salinity, surface layer in Douglas Channel in July, 1977 and June, 1978 was indicative of a well developed estuarine circulation mode at these times. Less distinct surface layers occurred in September, 1977 and in March, 1978, whereas in December, 1977 the salinity difference between the surface and 50 m depth was about 1.0‰ or less. Observations of salinity by the current meter at 5 m depth at CM 3 up to the middle of December, 1977 indicated that low salinities occurred in the period between the beginning of the record and the end of July and in a second period between the middle of October and the middle of November. It appears that the September cruise was undertaken prior to the peak of freshwater discharge into Douglas Channel which occurred in October. Small vertical salinity gradients in December would be expected in view of the small freshwater discharge into Douglas Channel that month. Also, strong northerly wind conditions occurred in Douglas Channel a day or so prior to when the December observations were taken which would have increased surface salinities by blowing the surface layer out of the channel and by encouraging vertical mixing of surface water with more saline water below. At the stations to the north of CTD 26, a thin ($\sim$ 1 m thickness) surface layer appeared to be forming which had a salinity of about 1‰ less than that in the deeper water.

Figure 19 shows the temperature profiles in the top 50 m of the water column from station CTD 26. During the cruises in July, 1977; September, 1977; and June, 1978, a warm, surface layer identifiable with the low salinity, surface layer existed. The freshwater that was discharged into Douglas Channel appeared to have been warmed by the sun on its way to the inlet. Once in the inlet, it mixed with cooler, more saline water from below. An approximately linear relationship between temperature and salinity with a negative slope resulted. In the July, 1977 and June, 1978 cruises, the temperature at a given salinity was higher at the southern end of Douglas Channel than at the northern end. Presumably, the surface layer was heated by the sun in its passage south. Vertical temperature gradients were observed to be smallest in the cruise of December, 1977. Although Figure 19 shows that December temperatures decreased from the surface to depth at CTD 26, thermistor

chain data taken in Douglas Channel (TMS 1 and TMS 2) indicated that the prevalent near surface, temperature gradients were positive downwards starting about the middle of October through to April of the following year. The lowest temperatures in the top 50 m of the water column in Douglas Channel were observed on the March, 1978 cruise, but thermistor chain data indicated that temperatures had already begun to increase throughout this layer at this time.

5.3.2.2 Wind Driven Circulation

Continuous records of wind speed and direction have been made at Kitimat Townsite since November, 1967 by the Atmospheric Environment Service, Environment Canada. However, the relationship between winds observed at Kitimat and at other positions throughout the Kitimat system has not been well studied. The rows of mountains on either side of the various channels would be expected to direct the winds along the channel axes. Observations of wind directions taken on board ship during each cruise in the Kitimat study indicated that this was the case. The relationship between wind strengths within the channel system has been described by Phillips (unpublished manuscript) as being chaotic and not well understood. Kitimat lies in a valley defined by the northward continuation of the 2 rows of mountains which flank Douglas Channel and Kitimat Arm. Accordingly, it is conjectured that the wind observations taken at Kitimat Townsite are representative of the winds along Douglas Channel. From Wright Sound south, it is unlikely that this is as valid a conjecture because of the increased complexity of the system. Also, as the outer coast is approached, an increasing influence of the wind regime there could be expected. Figure 20 shows the daily averaged north/south component of wind velocity observed at Kitimat Townsite for the period July 1 to December 31, 1977. Historical records from the anemometer at Kitimat Townsite indicate a predominance of northerly and southerly winds reflecting the channeling effect of the valley in which Kitimat is situated. Also shown in Figure 20 are the north/south gradients of atmoshperic pressure for the region estimated every 6 hours. The pressure gradients were calculated from barometric pressures observed at Langara Island, Smithers and Port Hardy which bracket the study area (see Figure 1). The gradients were assumed to be constant between the observing stations at a given time. Visual examination indicates there was a high degree of correlation between winds observed at Kitimat and the north/south pressure gradient. A lesser degree of correlation was noted with the east/west pressure gradients estimated using the same scheme. The transfer function between the magnitudes of pressure gradient and wind speed evidently changed over the period July to December. Whereas in November and December, an approximate relationship was:

$$\text{N/S Wind velocity (m/sec)} \simeq 0.008 \times \text{N/S Pressure gradient (mbar/km)}$$

the factor 0.008 roughly doubled in the summer months. A major feature of the wind record was the occurrence of prolonged periods of strong northerlies commencing in the middle of November. These northerlies, termed katabatic winds, are a feature of the British Columbian coast. They are outflows of cold air from the interior of the province (Phillips, unpublished report) during winter months.

The low pass filtered currents at 5 m depth from CM 3 near the southern end of Douglas Channel (see Figure 20) showed a very large degree of variability. Up to the end of September, 1977, the currents tended to be in a southerly direction with speeds which varied up to 25 cm/sec; an average for this period would be closer to 10 cm/sec. The prevailing winds at this time were southerly, that is opposing the direction of average current flow. Variations in strength and direction of the wind clearly had a major effect on the 5 m currents; the stronger the southerly wind was, the weaker the southerly current tended to be. On occasion, the 5 m currents reversed themselves for short periods to flow north. From the end of September to the middle of November, the character of the wind, pressure gradients and 5 m currents changed markedly. The wind underwent a series of fluctuations having periods of 4 or 5 days which were reflected in both the pressure gradients and in the 5 m currents. Although the wind fluctuations were no larger than they were in the previous months, the pressure gradient fluctuations and the current fluctuations were both considerably larger. This suggests that the pressure gradient fluctuations may be more indicative of wind speeds in Douglas Channel than the Kitimat wind measurements. Filtered currents up to 30 cm/sec were observed to occur in the northerly direction and up to 40 cm/sec in the southerly direction. The average wind direction for this period was still towards the north, whereas the average current direction was still southerly. The fluctuations of the 5 m currents were positively correlated with the fluctuations in wind direction. The onset of katabatic winds in mid-November had a dramatic effect on the 5 m currents. Between November 15, 1977 and December 31, 1977, 3 periods of more than 10 days duration each of large southerly currents occurred which were clearly the result of periods of strong northerly winds. During all 3 periods, the current strengths exceeded 40 cm/sec for at least a couple of days. In between these 3 periods were 2 periods of northerly currents which were associated with the reversal of the wind direction to southerly in the first instance and to the occurrence of variable winds in the second. The north/south pressure gradients suggest that southerly winds predominated in the second instance, but that these winds were less strong than during the first occurrence of southerly winds. Also shown in Figure 20 are the filtered north/south current components obtained from the 17 m depth current meter at CM 3, the 30 m depth current meter at CM 2 and the 165 m depth current meter also at CM 2. The magnitudes of the filtered currents decreased markedly with depth but the temporal variability of these currents remained large. Up to the end of September, the currents at 17 m depth tended to be southerly with speeds ranging up to 20 cm/sec. In the following one and one half months, northerly currents occurred with a greater frequency so that the average current could be considered to have been closer to zero or even to have had a northerly bias. In the period from the middle of November to the end of the data record on December 10, 1977, the 17 m currents reflected the currents at 5 m on the same mooring. Although the onset of large southerly currents at 17 m depth was delayed by 3 days over that at 5 m depth, the 17 m currents subsequently closely followed those at 5 m depth in both phase and amplitude. The relationship between the 2 current records from July to mid-November does not seem as clear. Both positive and negative correlations existed between the fluctuations at the 2 depths in

roughly similar proportions. That both kinds of correlation can exist is not surprising considering that both meters could either have been in the same near surface wind driven layer or the bottom meter could have been located in a layer of return flow below the wind driven layer in which the top meter was located. The currents seen by the 2 meters would have been in the same direction in the first case and in the opposite direction in the second.

The fluctuations in the filtered currents at 30 m depth roughly followed those at 17 m depth but their magnitudes were reduced by a factor of 2 over those at the shallower depth. Up until the end of August, the currents at 30 m depth tended to flow south at rates which were much less than the southerly flows at 17 m depth. After August, the currents had a northerly bias. The onset of katabatic winds in mid-November produced southerly currents over 25 cm/sec at 30 m. It is interesting to note that after the initial onset of the northerly katabatic winds the 30 m currents first turned north. After 5 days, these currents turned towards the south to follow the currents at 5 m and 17 m. Presumably, after the onset of the katabatic winds the 30 m current meter first saw the return flow from the surface wind driven flow. As time progressed, the wind driven layer became thicker and thicker until it reached 30 m depth and caused a reversal of the flow at that depth.

The filtered currents at 165 m depth were of the order of 5 cm/sec or less. A comparison of these currents with those at 17 m and 30 m depths shows that their fluctuations tended to be 180° out of phase with those at the shallower depths. The average 165 m flow was northerly up until the end of August and southerly after this time. The response of the currents to the onset of the katabatic northerlies was to flow north, that is in the opposite direction to the currents at 5 m, 17 m and 30 m depths.

Figure 21 shows the contoured isotherm depths at TMS 1 and TMS 2 and the north/south component of wind speed observed at Kitimat for the period between July and December, 1977. The change of the thermal stratification of the top 20 m of the water column in response to the decline in solar radiation as winter was approached can be seen in both thermistor chain records. Changes in the depths of isotherms in the top 20 m over periods of a few days were strongly correlated with variations in the north/south component of wind velocity. However, the response of the thermal structure to the wind up to the end of September appeared to be different from the response from the beginning of November on. In the first period, a series of dips in the near surface isotherms of the order of 5 m in vertical extent were evident which coincided with occurrences of southerly winds. The response of the isotherms at TMS 2 was the opposite; that is, when the isotherms deepened at TMS 1 they rose towards the surface at TMS 2. Evidently, the southerly winds caused an accumulation of water at the northern end of Douglas Channel at the expense of the southern end. After the beginning of November, the depths of the isotherms at both TMS 1 and TMS 2 underwent a continuous series of fluctuations which increased

markedly in magnitude with time. In this period, southerly winds caused increases in isotherm depths at both stations and northerly winds the opposite. The fluctuations in isotherm depths were larger at TMS 1 than those at TMS 2. The slopes of the isotherms and, presumably, of the isohalines along the channel changed continuously in response to the wind stress acting on the water surface. The onset of katabatic winds in mid-November had a dramatic effect on the observed temperature structure. During the first period of strong northerlies, the 7.75°C isotherm appeared on the surface at TMS 1, whereas during the following period of southerlies it was depressed to almost 50 m depth. The change of depth of the 7.75°C isotherm at TMS 2 over the same period was around 20 m. The increase in the size of the fluctuations of isotherm depths caused by the wind in the winter months can be attributed mainly to the reduction in the vertical density gradients of the top 50 m over what they were in the summer. The longitudinal slopes of the isopycnals required to produce a pressure gradient to balance the pressure gradient set up by the shear stress of the wind acting on the surface of the channel were therefore less in summer than in winter and so too would be the fluctuations in isotherm depths. On the basis of the comparison of the north/south pressure gradients between summer and winter, it seems likely that the wind speeds throughout most of the Kitimat system were higher in winter than in summer. If this was the case the winter winds would have caused larger fluctuations in isotherm depths than the summer winds.

5.3.3 Gardner Canal Observations

The estuarine mode of circulation appeared to be best developed in Gardner Canal. Not only did Gardner Canal have more freshwater input than Douglas Channel at all times of the year, but the width of Gardner Canal is roughly half that of Douglas Channel so that the effect of this input should have been correspondingly larger. Figure 22 shows the salinity profiles observed along the western 2/3 of Gardner Canal in July, 1977 during the season of high freshwater input. These profiles were characterized by having a brackish surface layer which changed its form along the length of the inlet. At the 2 most eastern stations, CTD 33 and CTD 34, the surface 5 m had a salinity of less than 1‰. Below 5 m depth, the salinity rapidly increased to reach a value of 30‰ at about 15 m depth. At stations further west along the inlet, the salinity of the surface layer increased and the depth at which the salinity began its sharp increase decreased. Nevertheless, the surface salinities at the mouth of Gardner Canal, at station CTD 18, were still less than 10‰ and the salinity profiles were all very similar below 15 m depth. Figure 22 shows the vertical profiles of salinity to 50 m depth observed at station CTD 33 on the 5 cruises to the study area. On each of the cruises, a brackish surface layer was evident whose average salinity increased towards the mouth of the inlet. This layer appeared to be most poorly developed in December, 1977. On this cruise at stations CTD 33 and CTD 34, a distinct, thin (1 or 2 m thickness) layer of low salinity (less than 20‰) was observed which was not evident at the stations closer to the mouth although at the latter stations near surface salinities were still several parts per thousand less than they

were at 50 m depth. The December CTD measurements in Gardner Canal were taken only 3 days after the end of a period of katabatic winds. Wind observations taken in Gardner Canal during the period of katabatic winds indicated these winds flowed along the inlet towards its mouth. Likely, the surface layer which existed prior to these winds was either blown out of the inlet by them or mixed with deeper, more saline water. Perhaps the thin surface layer which appeared at stations CTD 33 and at CTD 34 was the first stage in the re-establishment of a thicker surface layer. The estimated rate of freshwater discharge into Gardner Canal in December, 1977 which was 0.2×10^3 m^3/sec was enough to fill a volume of Gardner Canal which is 50 km long, by 2 km wide, by 1 m deep in a period of 6 days. Thus, the volume of discharge into Gardner Canal was of the right order of size for producing the observed thin surface layer in the inner sections of the inlet. The low salinity surface layer was progressively better developed in March, 1978 and September, 1977 which are periods of low and medium freshwater discharges, respectively; the surface layer was observed to be best developed in July, 1977 and June, 1978. At these 2 times, the salinity structures of the top 50 m in Gardner Canal were similar. Although freshwater discharge data are not available for June, 1978, they are thought to be similar to those in July, 1977. In 1977, the discharge into Gardner Canal was maintained at a fairly constant level for June, July and August which was around 1.6×10^3 m^3/sec. The temperature profiles observed at station CTD 33 (see Figure 22) displayed the main features of the seasonal changes of the temperature structure of the top 50 m of the water column in Gardner Canal. Generally, the depths of large temperature change coincided with those of large salinity change. In July, 1977; September, 1977; and in June, 1978 the brackish surface layer was warmer than the more saline water below it and cooler in December, 1977 and in March, 1978. The average temperature of the upper 50 m was lowest in March, 1978 as it was in Douglas Channel.

5.3.4 Devastation Channel and Verney Passage Observations

5.3.4.1 Estuarine Circulation

The nature of the estuarine circulation in the channels along the eastern side of Hawkesbury Island is complicated by geography and by an apparent strong interaction with tidal currents. The brackish surface layer which flows out of Gardner Canal as part of its estuarine circulation must divide into a proportion which flows north into Devastation Channel and one which flows south into Verney Passage. The momentum of such a flow would tend to carry it northwards into Devastation Channel, but observations suggest that at least some of it goes the other way. If local sources of freshwater are small as they are along Devastation Channel and Verney Passage, then the surface layer should be flowing in the direction of increasing salinities. Vertical mixing between a brackish surface layer and more saline water below can only increase salinities in the surface layer. The salinities at 1 m depth increased along both Verney Passage and Devastation Channel in directions away from the mouth of Gardner Canal in July, 1977; September, 1977; and June, 1978. The southward flow of the brackish surface layer in Douglas Channel probably had a blocking effect on the

northward flow in Devastation Channel. Likely, the proportion of surface layer flow into Devastation Channel and Verney Passage changed in response to changes in the relative intensities of the estuarine circulations in Douglas Channel and Gardner Canal. During 1977, the ratio of the discharge into Gardner Canal with that into Douglas Channel varied from about 5 in August to about 1 in November. It is likely, too, that the wind stress on the water surface will normally be unbalanced on the 2 sides of Hawkesbury Island and so tend to drive the surface flow one way or another around the island. Likewise, the nonlinear interaction of the tidal currents with the sides and bottoms of the channels on both sides of Hawkesbury Island could give rise to a net circulation around the island. On the basis of low pass filtered current measurements taken in Verney Passage and Devastation Channel in the period between September and December, 1977, it appeared that any net tidal circulation would have been less than 1 cm/sec. Wind stress is expected to have had a greater influence on surface water movements in Devastation Channel and Verney Passage judging by its importance in Douglas Channel.

Turbulent mixing arising from strong tidal currents appears to have been a major agent responsible for the rapid increase in surface layer salinities westward along Verney Passage. The tidal model predicts that the tidal transport into Gardner Canal occurs through Verney Passage and Ursula Channel rather than through Devastation Channel. Thus, the tidal currents in Devastation Channel should be much smaller than the currents in the 2 other channels and so tidal mixing is expected to have been correspondingly less. The interaction of tidal currents with the shallow sills which cross Verney Passage and Ursula Channel should have further enhanced tidal mixing in these 2 channels. The proportion of surface layer flow which continued along Verney Passage after crossing the sill and the proportion which branched towards the south into Ursula Channel is undetermined. From the observed distribution of salinities at 1 m depth in this area in July, 1977 and June, 1978, it is evident that at least some of this flow appeared in both channels.

5.3.4.2 Flow Across the Verney Passage Sill

Special studies were undertaken during the September and December, 1977 cruises to study the flow over the Verney Passage sill. In the September cruise, a series of 6 stations, V1 to V6 (see Figure 23) were occupied along the length of Verney Passage repeatedly over a period of 24 hours. To complete a pass of the stations took approximately 2 hours. The principal variation in the water structure was observed to occur over a semi diurnal period which is consistent with the dominance of the M_2 tide in the region. On both the flooding and ebbing tides, the isohalines rose slightly in depth as the sill was approached on the upstream side then were distinctly depressed after crossing to the downstream side of the sill. Further downstream, the isohalines decreased their depths to attain similar depths to what they had upstream of the sill. Figure 24 shows the depth behaviour of

the isohalines which crossed the sill near a fully flooding tide (an eastward current). In this example, the 31‰ isohaline was depressed by about 20 m when it crossed the sill. Unfortunately, the spacing of the CTD stations didn't permit delineation of the shape of the isohaline depression, so the point at which the isohalines began to descend and the point of maximum depression are both unknown. In a second time series which immediately followed the first, the "Sea Lion" was anchored a short distance from the peak of the Verney Passage sill on its western side (see Figure 23). CTD casts were taken from the ship to a depth of 30 m every 10 minutes for a period of 12 hours. The tide was ebbing for the first half of this period (0500 - 1100, October 4) and flooding for the second half (1100 - 1700, October 4). During the period of the ebb, the salinity profiles showed local inversions which were evidence that the flow on the downstream side of the sill was turbulent. When the flow reversed itself to the flood tide some local inversions were evident, but these were not so prevalent as they were on the ebb tide. The time series of isohaline depths derived from the second series of CTD casts is shown in Figure 24. During the period of measurement, the 31‰ isohaline underwent dramatic changes in depth which were not reflected by the 26‰ and 28‰ isohalines. Based upon the results of the first time series, the 'normal' depth of the 31‰ away from the sill was judged to be about 20 m. During the period of the ebb, this isohaline was depressed to over 35 m depth on 2 occasions, one of which preceeded the peak ebb at 0800 and the other which followed it. At peak ebb, the 31‰ isohaline rose to within 10 m of the surface. Throughout the ebb tide, the water surface was ruffled in a band which extended in a line along the estimated position of the peak of the sill. Following the change of the tide to flood at about 1100, the 31‰ isohaline remained between 10 m and 20 m in depth.

During the December, 1977 cruise, current meters were moored on the peak of the Verney Passage sill at depths of 5 m, 15 m and 25 m (mooring CM 10). Figure 25 shows a 3 day section of current record from the 15 m current meter and the corresponding temperature records from all 3 meters. The current record presented is the current component perpendicular to the orientation of the Verney Passage sill. Since the current records obtained from 5 m and 25 m are similar to it, the 15 m record is taken to be representative of the currents which crossed the sill. The amplitude of these currents was observed to be of the order of 100 cm/sec. Salinity data were not available from one of the current meters so temperatures have been presented instead. The comparison of the available salinity data with the temperature data indicated that temperature fluctuations were positively correlated with salinity fluctuations, a temperature fluctuation of $1^{\circ}C$ being close to a salinity fluctuation of 1‰. The structure of the water column underwent a cycle which repeated itself approximately every 12 hours. Generally, the thermal stratification was greatest when the tide was in full ebb or flood. Even though the 5 m temperatures increased somewhat during these times, the temperatures at 25 m depth remained high. In contrast, around the times of the slack water after both flood and ebb tides, the temperatures at 25 m depth suddenly decreased to values approaching those at 5 m depth. The average temperatures (and

salinities) and the average temperature gradients (and salinity gradients) in the water column experienced minima at these stages of the tide.

A possible explanation for the September and December, 1977 observations is that a standing internal lee wave or a standing internal hydraulic jump formed on the downstream side of the peak of the Verney Passage sill when the current was flowing strongly. Such phenomena have been observed by D. M. Farmer (private communication) when stratified flows passed over obstructions in test tank experiments and in the flow over the sill in Knight Inlet, British Columbia. In these flows, the interface between 2 density layers was suddenly depressed as it passed over the submerged obstruction to rise again further downstream. In the region formed by the depression of the isopycnals, a body of low density fluid accumulated which was relatively stagnant. This interpretation of the observations around the Verney Passage sill is schematicized in Figure 26. The ruffled band which appeared over the sill during the September cruise is interpreted as being the leading edge of the stagnant region where it met the flow coming over the sill. The boundary between the stagnant region and the main flow underneath it should have been a zone of large current shear and hence a source of turbulent mixing energy. CTD casts taken during the period of the depression of the 31‰ isohaline on the second time series of the September cruise did show that considerable mixing was going on at this time. The rise in isohaline depths upstream of the sill was observed directly in the time series of CTD casts taken along the channel during the September cruise and indirectly in the current meter measurements of the December cruise. The lowest surface temperatures (and salinities) were not generally seen over the sill when the current was flowing strongly, but rather when the currents were weaker. In other words, the near surface isohalines over the sill seemed to rise when the current was strong. Farmer has noted that as the flow over a submerged obstruction is reduced, the upstream edge of the stagnant region climbs upstream over the peak of the sill. When the flow is sufficiently reduced, the isohaline depression breaks free of the sill and propagates upstream as an internal wave. This behaviour seems to explain the second depression of the 31‰ isohaline following peak ebb in the September anchor station observations and the reduction in temperatures (and salinities) at 25 m depth over the sill when the tide slackened in the December current meter observations.

The details of the flow downstream of a sill are expected to depend on the density stratification and the strength of the flow. At lower flow speeds a standing internal lee wave should develop which changes its wavelength and amplitude as the flow speed is increased. A critical flow speed exists at which this wave becomes unstable and develops into an internal hydraulic jump. The streamlines will still be depressed after they cross the sill, but instead of rising smoothly downstream they will suddenly jump up. Farmer has observed that a flow tends to become critical when the internal Froude Number, which he defines as the ratio of the fluid velocity, V, to the phase speed of an internal wave, C, approaches 1. In the case of flow over a sill, V was taken to

be the flow over the peak of the sill and C was taken to be the phase speed of a long wavelength internal wave on either side of the sill. The phase speeds of the first and second modes of long wavelength internal waves on the September cruise were calculated to be approximately 100 cm/sec and 60 cm/sec, respectively. The phase speeds of these waves were similar on the December cruise. Since flows over the Verney Passage sill ranged up to around 100 cm/sec, the value of the internal Froude was roughly 1 for a first mode internal wave and was greater than 1 for a second mode internal wave. It is, therefore, likely that during part of the tidal cycle, at least, the flow over this sill was unstable.

5.3.5 Gil Island Area Observations

The channels on either side of Gil Island, namely Whale Channel and Squally Channel, are both wide and connect directly to Hecate Strait through Otter Channel and Campania Sound. Accordingly, it is expected that most of the freshwater which was discharged into Douglas Channel and Gardner Canal ultimately left the Kitimat system through these channels. The water structure of the channels on either side of Gil Island was characterized over most of the year by the existence of a near surface layer of low salinity. The salinity of this surface layer increased towards the south around the sides of Gil Island which suggests that the surface layer flow was southerly in both Squally Channel and Whale Channel. The prominence of the surface layer in the Gil Island area followed the seasonal cycle of freshwater discharge as it did in the channels to the north. At station CTD 9 in Campania Sound, the difference between the salinity at 1 m and at 50 m depths was 5.3‰ in July, 1977, whereas in March, 1978, this difference was only 0.05‰. Vertical salinity gradients in the top 50 m were even further reduced at station CTD 8 in Caamaño Sound. Tidal mixing appeared to play a prominent role in the regions near Otter Channel and Campania Sound. Tidal currents of greater than 35 cm/sec occurred in both channels. Evidence of intense mixing appeared in the temperature, salinity (T,S) curves obtained from CTD casts at stations CTD 6 and CTD 9. Figure 27 shows examples of 2 such curves taken from CTD casts in July, 1977. The jagged appearance of these curves indicates that the water at these locations was a complex mixture of water from inside the Kitimat system with water which was transported through the entrances of the system from outside. Both T,S curves show local density inversions at several depths which probably arise due to turbulence. A comparison of the near surface salinities on the 2 sides of Gil Island shows that these were higher on the western side. Likely, the eastward tidal flow through Otter Channel appeared as a turbulent jet in Squally Channel which increased surface salinities in that area by advection of high salinity water from outside the system and by inducing vertical mixing.

Current measurements were made at a depth of 35 m in Campania Sound (mooring CM 4) for the period July to September, 1977. Although variations in the low pass filtered currents were observed, the general flow at this depth was southerly, having an average speed of about 8 cm/sec. Deeper current measurements made at the same location

indicated a northerly flow which averaged around 15 cm/sec at a depth of 265 m and a flow which was neither consistently northerly nor southerly at 150 m depth. Although the depth of the upper, lower salinity layer was of the order of 15 to 20 m in thickness in the southern part of Whale Channel in July and September, 1977, the southerly flow in Campania Sound is presumed to have been associated with the estuarine circulation of the system. A net southerly flow averaging 5 cm/sec was also noted at a depth of 30 m during the period March to June, 1978 at a location half way along the length of Whale Channel (mooring CM 15). Net currents at depths of 245 m and 445 m at the same location were small during this time. Current measurements were made in Otter Channel (mooring CM 8) at depths of 40 m, 135 m and 230 m in the period December, 1977 to March, 1978. Non-tidal transports at 40 m depth averaged about 15 cm/sec over this period in a westerly direction, but these transports were over 40 cm/sec for several days. Average transports were less than 3 cm/sec at the other depths. Since the estuarine circulation should have been weak during the period when these measurements were taken, it is presumed that the large transports at 40 m depth were due either to the wind or to a net circulation induced by the tides.

5.3.6 Grenville Channel Circulation

Because of its length ($\sim$ 85 km) and its narrow width (average $\sim$ 600 m), Grenville Channel is probably of lesser importance to the circulation within the Kitimat system. The tidal model predicts that the channel only supplies 10% of the total tidal transport into and out of the system. At its northern end, Grenville Channel joins Chatham Sound near the mouth of the Skeena River which is the second largest river in British Columbia with a mean annual discharge rate of approximately 10^3 m^3/sec. The presence of such a large freshwater source near its northern end raises the possibility that an estuarine circulation could be driven from that end.

During the study, CTD measurements were taken along Grenville Channel as far north as Klewnuggit Inlet which is approximately half way along its length. Figure 28 shows the salinity profiles taken at stations CTD 3, CTD 4 and CTD 5 along the channel in July, 1977 and the corresponding T,S curves. The profiles at stations CTD 3 and CTD 4 both had a much more pronounced surface layer of lower salinity than did the profile at station CTD 5. The section of Grenville Channel between stations CTD 36 (not occupied on the July, 1977 cruise) and CTD 5 is particularly narrow ($\sim$ 400 m wide) and shallow ($\sim$ 100 m deep). Current measurements taken in the period March to June, 1978 at a location near station CTD 4 (mooring CM 12) indicated tidal currents of the order of 25 cm/sec in amplitude. Since the channel at station CTD 4 is more than twice as deep and is 50% wider than it is in the section between stations CTD 36 and CTD 5, tidal current amplitudes in excess of 50 cm/sec are expected in the latter section. The combination of high tidal currents in a narrow, shallow section of the channel are thought to have induced turbulent mixing which appears to have been responsible for the erosion of the surface layer between stations CTD 4

and CTD 5. The changes in the T,S relationships along Grenville Channel were not inconsistent with a general flow at all depths towards the north in July, 1977. The T,S curve at station CTD 5 cannot be a product of mixing along the T,S curve at Station CTD 4, assuming that temperature and salinity behaved as conservative properties. If it is assumed that solar heating of the surface water occurred as it flowed north, then the water at station CTD 5 could have been a mixture of water which originated at station CTD 4. The uplifting of T,S curves by solar heating was observed in July, 1977 in both Douglas Channel and Gardner Canal. It is not possible to say conclusively whether the flow was northerly because it is not known what the T,S relationships were at the northern end of Grenville Channel. Figure 28 also shows the salinity profiles and the T,S curves observed at stations along the channel in June, 1978. On this occasion, the salinity profile at station CTD 5 had a more pronounced surface layer with lower salinities than the next station further south along the channel, CTD 36. Further south than station CTD 36, the surface layer again increased in prominence. An examination of the T,S curves for the 4 stations shows that station CTD 5 had distinctly cooler temperatures at the same salinity values than the other stations. Since June was a time of surface water heating, the conclusion is drawn that the surface layer flow at station CTD 5 originated at the northern end of Grenville Channel. The appearance of the T,S curve at station CTD 36 suggests that the water there shared some common origin with the water in Wright Sound. Current measurements made at CM 12 between March and June, 1978 indicated generally increasing southerly flows at 25 m depth. In June, these flows attained an average speed of around 15 cm/sec. At 155 m depth, northerly currents having an average speed of around 1 cm/sec occurred during this month. One explanation of this observation is that a 3 layer flow prevailed in the southern end of Grenville Channel in June, 1978 in which a southerly flow from the northern end of the channel was sandwiched between a northerly, low salinity flow on the surface and another northerly, high salinity flow underneath.

5.3.7 Princess Royal Channel Circulation

Princess Royal Channel is one of the 4 entrances to the Kitimat system. It is slightly shorter than Grenville Channel, but is somewhat wider and deeper over most of its length. No current measurements were made in the channel, but the tidal model predicted transports through the channel to be similar to those through Grenville Channel. The tidal currents associated with the predicted transports may be of considerable importance in the mixing processes of Princess Royal Channel particularly in the more constricted sections such as in Hiekish Narrows near its southern end where the channel has a maximum depth of 80 m and a width of 300 m. CTD measurements made along the channel in July, 1977 indicated a general increase in surface layer salinities from north to south which suggests that the near surface flow occurred in a southerly direction. A comparison of the T,S curves observed at stations CTD 14 at the northern end of Princess Royal

Channel and at CTD 29 about 18 km down its length indicated that the water at the 2 stations shared a common origin. At the other end of the channel, the water characteristics could have been subject to influence by low salinity surface layer flows which originated in the inlet complex to the south. Differences in salinity profiles and T,S curves between stations at the south end of the channel and those further north suggest that this was the case. A year later in June, 1978, the salinities of the surface layer were again noted to increase from north to south, but this increase was less than it was in July, 1977. The differences in salinity at 1 m depth between the northern and southern ends of Princess Royal Channel were 6.2‰ in July, 1977 and only 1.8‰ in June, 1978. On the intervening cruises in September, 1977; December, 1977; and March, 1978, the salinities at 1 m depth at the northern end were higher than those at the southern end by 0.2‰, 0.5‰ and 0.7‰, respectively. It seems that during the cruises after the July, 1977 cruise, the estuarine component of the circulation in Princess Royal Channel was probably weak and may have proceeded in a northerly direction for some of the time.

5.4 Estuarine Circulation Model

5.4.1 Description of the Model

A 2 layer, time independent, numerical model has been developed to describe the flow in stratified fiords by Pearson and Winter (1978). A version of this model was adapted for the Kitimat system by Winter in order to quantify the flow rates associated with the estuarine circulation. A description of the model as it was developed for a 1 channel system, namely Knight Inlet, British Columbia, is available in the reference cited; its application to the Kitimat system is briefly described in the following.

The model idealized the observed water structure as having 2 layers, the top one being relatively thin and brackish and the bottom one being thicker and more saline. Any lateral variations in each channel were considered to have been averaged out. Thus, the salinities in each layer and the layer thicknesses were represented as functions only of the distance along each channel. Furthermore, all time derivatives of water structure or water movement were considered to be zero so that the model was in a steady state condition. This layered model included the important effects of variations in mass density and in channel width, and allowed for exchange between the surface and the deeper layer. Transfer of mass and momentum across the interface was parameterized by 2 interzonal exchange flux rates which represented the upward and downward rates of water flow per square meter of interfacial area. A freshwater discharge was input along the sides of the model's channels and a time independent wind stress was applied to its surface. The equations to be solved in each layer of the model were the conservation of mass equation, the conservation of salt equation and the momentum equation. The required input to the model included the specification of the observed upper and lower layer salinities, the surface wind stress and the freshwater input rate along

the channels represented in the model. The division between the upper and lower layers in the real system was taken to be the depth of maximum negative curvature of the salinity profile. For the purposes of the estuarine model, the effective depth of the inlet system was taken to be constant at 60 m. This was considered more realistic than taking the lower layer to extend to the bottom. Although the calculated velocities in the lower layer were altered by this change, the behaviour of the upper layer was little affected. The wind stress was taken to be the same in amplitude everywhere and was directed along the channel axes. Its amplitude was estimated from the north/south component of the wind velocity at Kitimat Townsite averaged over the period when the CTD measurements were taken during each cruise. The relationship used for calculating wind stress, T_w, from the wind velocity component, v, was:

$$T_w = 1.3 \times 10^{-3} \rho v^2$$

where ρ is air density. The freshwater discharge rates were estimated from the sizes of the drainage basin areas (see section 5.1) along the sides of the channels. These discharge rates were calculated for periods appropriate to each application of the model. Figure 29 shows a schematic of the inlet network considered by the model. The network has been simplified somewhat by the omission of minor constricted channels as, for example, those associated with small islands near inlet shorelines. It is felt that the main features of the estuarine circulation mode were not distorted by this idealization. The network system was divided into a series of segments; the solution for each of these segments was found by stepwise integration of the governing equations from one end of the segment to the other. The starting point for the scheme was chosen to be near CTD 28 in the south end of Douglas Channel. Data from the thermistor chain at TMS 2 close to station CTD 28 were used in conjunction with the data from the CTD cast to determine an upper layer thickness from which the worst effects of aliasing (due to fluctuations having tidal periods or less) could be averaged out. Once the solution had been advanced to the north end of Douglas Channel, the computed upper and lower layer thicknesses were used as the starting conditions for the determination of the solution of the next segment. It was postulated that at all the junctions the thicknesses and densities of the upper and lower layers were continuous. The computation process proceeded through the inlet segments in the following order: Douglas Channel, Devastation Channel, Gardner Canal, Upper Verney Passage, Lower Kitimat Arm, Upper Kitimat Arm, and Kildala Arm. Since the model required the cumulative runoff to be specified, it was necessary to postulate that a certain fraction, α, of the freshwater from Gardner Canal flowed into Upper Verney Passage, with the remainder flowing into Devastation Channel.

5.4.2 Model Results

The estuarine circulation model was run several times to simulate the inlet conditions encountered during the July, 1977; September, 1977; and June, 1978 cruises. The total runoffs into Douglas Channel and Gardner Canal, the wind stress, and the starting upper layer thicknesses

at the south end of Douglas Channel are listed in Table 5 for the model applications.

Table 5.

Estuarine Circulation Model Input Parameters

Time Period of CTD Data Collection	Total Freshwater Runoff (m^3/sec)		Wind Stress* (nts/m^2)	Starting Depth of Interface at CTD 28 (m)
	Douglas Channel	Gardner Canal		
July 12 to July 15, 1977	5.3×10^2	1.7×10^3	2.5×10^{-2}	11
Sept. 30 to Oct. 1, 1977	1.3×10^2	4.0×10^2	-6.5×10^{-3}	14
June 8 to June 13, 1978	8.2×10^2	1.8×10^3	4.8×10^{-3}	10

* Positive wind stress towards north in Douglas Channel and towards east in Gardner Canal.

The parameter, α, representing the fraction of Gardner Canal runoff flowing into Upper Verney Passage was given the values 0.0, 0.5 and 1.0 to investigate its importance.

Figure 30 compares the upper layer thicknesses computed with the different values of α for each of the 3 cruises which were considered. A striking feature of these plots is that they indicate the depths of the interface between the 2 layers changed very little with a change in α from 0 to 1. Also shown in Figure 30 are the upper layer thicknesses as they were measured on each cruise. When comparing the observed and calculated upper layer thicknesses, it should be noted that the observed upper layer thicknesses are subject to aliasing uncertainties. At TMS 2 in September, 1977 (see section 5.2), an isotherm at a comparable depth to the bottom of the upper layer at that location underwent short period (< 1 day) fluctuations over a 3 m depth range. Allowing for fluctuations in the observed upper layer thicknesses of several meters, the agreement between the observed and calculated upper layer thicknesses for the July period appears quite good in the Douglas Channel section. In the Gardner Canal section, the calculated values of the upper layer thicknesses tended to be low by 1 or 2 meters at this time. The September run had the best agreement in both the Douglas Channel and the Gardner Canal sections except that

the calculated thicknesses were about 3 m too low in Kitimat Arm. The June run produced close results in the Douglas Channel section although, once again, the observed thicknesses tended to be greater than the calculated ones in Gardner Canal.

A change in the value of α did have a large effect on the upper layer velocities as can be seen in Figure 31 which shows these velocities for α = 0.0, 0.5 and 1.0. An increase in the fraction of freshwater which flows out of Gardner Canal into Devastation Channel greatly increased the calculated southward speed of the upper layer in Douglas Channel. For example, the September current speeds at the south end of Douglas Channel in the upper layer increased by a factor of 4 when α was changed from 1.0 to 0.0. During the periods when the CTD measurements were being made in July and September, the velocities at 5 m depth in the south end of Douglas Channel (see Figure 20) were undergoing changes in magnitude which were larger than the model's calculated surface layer velocities. This situation makes a quantitative comparison of observed and calculated velocities meaningless.

One of the major problems with the running of this model was the insufficiency of the wind information required to calculate the wind stress used as input to the model. In several runs with varying wind stresses, it was evident that wind stress had a significant effect upon the current speeds and thicknesses of the upper layer. The effect of having a wind stress which depended on position was not investigated. However, it is likely that a differential in wind stress on either side of Hawkesbury Island, for example, would have a large effect on the model results.

6. DEEP WATER MOVEMENTS AND EXCHANGE

On the basis of bathymetry, 3 major basins were defined in the interior of the Kitimat system which will be termed the Gil Island, Douglas Channel and Gardner Canal basins (see Section 2.2). The movement of deep water between these basins is restricted by the sills which separate them. Figure 32 shows the salinity contours along the lengths of the 3 basins obtained from CTD casts taken during the September, 1977 cruise. Although the depths of the isohalines have a rippled appearance (probably due to aliasing problems), these contours illustrate features common to those observed on the other 4 cruises. As expected, the highest salinities within the system were observed in the bottom of the Gil Island basin. Further north, the sill across Douglas Channel appeared to obstruct the northward movement of deep water from the Gil Island basin into the Douglas Channel basin. During the July, 1977; September, 1977; and June, 1978 cruises, the salinities on the northern side of the sill below sill depth were of the order of 1‰ less than those on the southern side. Conversely, during the March, 1978 cruise salinities on the northern side were higher by about the same amount than those on the other side. Above the depth of the sill, the isohalines along the length of Douglas Channel through to Campania Sound changed depths fairly evenly. The general trend was a deepening of the isohalines in a northwards direction during the July, September and June cruises and for the opposite to occur during the December and March cruises. It was a feature of the salinity structures observed on all the cruises that higher salinity water was prevented from reaching the mouth of Gardner Canal by the sills on both sides of it. The salinities of the bottom water at station CTD 17, located just south of the mouth, were similar to those found above the depth of the sill in Devastation Channel. The salinities in the deep basin of Gardner Canal were lower than those found throughout the remainder of the system at equivalent depths.

The salinities of the deep water of the Kitimat system underwent significant changes over the year of the study. The maximum depth of free access of the interior of the Kitimat system with Hecate Strait occurs through Campania Sound. This access is limited to 150 m depth by the presence of the Aranzazu Banks which lie in Caamaño Sound. Through Grenville Channel, Princess Royal Channel and Otter Channel, the maximum depths of free access with Queen Charlotte Sound or Hecate Strait are 80 m, 80 m and 60 m, respectively. Thus, deep water exchange with the exterior of the system is likely to occur to the greatest depth through Campania Sound. All the entrances of the Kitimat system connect most directly to the Gil Island basin. Figure 33 shows the depth, time contours for isohalines observed at station CTD 12 in the Gil Island basin; Figure 34 shows the T,S curves obtained at the same station. Salinities were highest at all depths on the September cruise and lowest on the March cruise. The salinities at sill depth in Campania Sound during the July, September and June cruises were either higher or similar to the salinities in the bottom of the Gil Island basin so it is presumed that exchange to the bottom of the basin had either just taken place or was in the process of taking place during these cruises. The changes in the T,S relationship of the water below sill depth indicated that complete renewal of the basin water

had occurred between the July and the September cruises. The salinity record from a current meter moored at 445 m depth in the Gil Island basin (mooring CM 15) from March to June, 1978 showed gradually declining salinities up to early May. Presumably, the high salinity water left in the basin after an exchange in the previous summer was being mixed with less saline water above it. Between May and June, the salinity at 445 m depth increased by about 0.2‰. Such an occurrence would have been due to the intrusion of higher salinity water over the sill to at least the depth of the current meter. The salinities at sill depth during the December and March cruises had been about 0.5‰ lower than those at the bottom of the basin. The depths of isohalines inside the system above sill depth were similar to those outside at these times. It seems that the vigourous tidal currents through Campania Sound and Otter Channel ensured good exchange of water inside the system above the sill depth with water outside. With the exception of Gardner Canal, similar seasonal variations in the T,S curves from station CTD 12 were observed at the other locations in the Kitimat system. During the July and September cruises, the T,S curves had a negative slope; that is, temperatures decreased with higher salinities and hence with depth. The T,S curve for December had a temperature maximum at a temperature of 8.5°C and a salinity of 32.1‰. This maximum occurred in the water column at a depth of 160 m which is above the depth of the sill in Campania Sound, but which is about the same depth as the deepest connection to Hecate Strait. In the other parts of the Kitimat system except for Gardner Canal, a temperature maximum was observed for water whose properties fell in the temperature range 8.0°C to 8.5°C, in the salinity range 31.9‰ to 32.0‰, and in the depth range 100 m to 200 m. By the March cruise, this temperature maximum had largely disappeared and the slope of the T,S curve had become positive so that temperatures increased with depth. The return of higher salinity water apparent in June was accompanied by a return to a negative slope for the T,S curve.

Figure 35 shows the time, depth contours for isohalines observed at station CTD 26 which is just north of the sill across Douglas Channel. Also indicated are the oxygen values obtained by hydrocast at the same station. Above the depth of the sill (240 m), the seasonal salinity changes were similar to those observed at CTD 12. The failure of the 32.7‰ isohaline to have been depressed in March and to have risen in June is attributed to a trapping effect of the sill. The cycle of dissolved oxygen changes in the water column followed that of salinity. In July, 1977, the dissolved oxygens decreased from 6.6 mg/ℓ at 30 m depth to 6.0 mg/ℓ at 300 m depth. The appearance of higher salinity water in September coincided with a reduction in dissolved oxygen of about 1 mg/ℓ at all depths. With the depression of the isohalines in December, dissolved oxygen levels above sill depth increased. Further increases in dissolved oxygen were noted on the March cruise above sill depth, but the dissolved oxygen at 300 m depth remained constant. Dissolved oxygen levels in the top 100 m were at or above 9.0 mg/ℓ at this time. With the appearance of higher salinity water again in June, 1978, the dissolved oxygen levels decreased in the top half of the water column. The dissolved oxygen at 300 m depth, however, went from 4.4 mg/ℓ in March to 6.1 mg/ℓ in June. Evidently, the relatively high salinity, low oxygen water behind the sill had been mixed with lower salinity, higher oxygen water above it during this time period.

Figure 36 shows the time, depth isohaline contours and the accompanying dissolved oxygen values obtained by hydrocast from station CTD 33 in the Gardner Canal basin. The salinities in July, 1977 were less than 32‰ over the entire water column. Elsewhere in the Kitimat system, the 32‰ isohaline occurred at a depth of 70 m or less at this time. Within Gardner Canal, the salinities actually decreased slightly with depth between 200 m and 500 m. A slightly positive static stability was maintained in the water column by a temperature gradient with the same sign as the salinity gradient. Dissolved oxygen levels below the sill depth in Gardner Canal (100 m) were between 5.8 mg/ℓ and 6.0 mg/ℓ in July, 1977. By September, the water in the inner basin appeared to have been replaced by water of slightly higher salinity and lower oxygen content. The September salinities in the basin lay between 32.10‰ at 100 m depth and 32.28‰ at 400 m depth; dissolved oxygens in the same layer fell in the range 5.4 mg/ℓ to 5.6 mg/ℓ. The depth of the 32‰ isohaline increased on successive cruises from 75 m in September to 210 m in the following June. During this time, the salinities at 400 m depth gradually decreased having values of 32.24‰, 32.14‰ and 32.05‰ on the December, March, and June cruises, respectively. The changes in the T,S relationships in the water column below 100 m depth support the view that the salinity of the deep water was gradually being reduced by mixing with less saline water above it. The average dissolved oxygen value of the upper 100 m reached a maximum of over 8.5 mg/ℓ in March, 1978. Conversely, the dissolved oxygen levels of the water at depths of 300 m and 400 m were 5.1 mg/ℓ and 5.2 mg/ℓ, respectively at this time, which were their lowest values for the study period. It is thought that the oxygen reduction at these depths was due to a combination of mixing with lower oxygen water from lesser depths and to *in situ* biological respiration. By June, some of the water of high oxygen content present in the top 100 m of the inlet appears to have diffused downwards to slightly raise the dissolved oxygen levels at depth. It would appear from the observations that the inner basin of Gardner Canal underwent a complete water exchange sometime between July and September, 1977. By the following June, this exchange had not yet repeated itself, but perhaps in the following months it would have.

The seasonal cycles of salinities and temperatures in Hecate Strait described by Barber (1956) are qualitatively similar to the changes in water structure observed in the Gil Island area and in Douglas Channel. Barber notes that in the deep water there is an alternation between a summer and a winter water, the winter water being less saline than the summer water. He attributes the changes in water masses to changes in the seasonal wind climate. During winter, southeast winds predominate on the outside coast which tend to cause a convergence zone along the coast. Less dense water accumulating along the coast displaces denser, more saline water seaward, thus at a given depth, the water appears less saline. During the summer period, the southeast winds relax allowing more saline water to return toward the coast and the sea level to subside. Observations of sea level were taken by tide gauges in Campania Sound and in Otter Channel (TG 2 and TG 4). These data, filtered to remove the tidal fluctuations, are shown in Figure 37 together with the filtered salinity record obtained from the current meter at 165 m depth in Douglas Channel (mooring CM 2). Although there was considerable fluctuation in the sea levels at periods less than a week, these levels tended to be highest in the period between the beginning of November, 1977 and the end of February of the following year. The

salinities, which were highest in August and September, began to fall in the middle of October when the sea levels began to rise. Minimum salinities occurred in February and March which was the time period during which the sea levels had reached their peak and had then begun to fall sharply. After March, sea levels kept on falling as salinities rose. The observation that sea levels and salinities were roughly inversely correlated with one another supports Barber's explanation for the mechanism responsible for the seasonal salinity changes at depth within the Kitimat system

7. SUMMARY AND CONCLUSIONS

The physical oceanographic study of the Kitimat system by SEATECH between July, 1977 and June, 1978 has outlined major features of the tidal, wind driven, and estuarine circulations of the system.

The tidal circulation was described using a 1- dimensional barotropic tidal model which utilized tide gauge data collected in the 4 entrances of the system to drive it. The model was subsequently tuned with current meter and tide gauge data collected from the interior of the system. It was developed in 3 configurations, namely as a linear model, as a nonlinear model with linear friction, and as a nonlinear model with quadratic friction, but these 3 configurations gave almost identical results. The model results indicated that the flow north of Wright Sound was predominantly a standing wave; that is, tidal heights and transports were approximately 90° out of phase with each other. The tide which flooded south along Devastation Channel met the flood tide through Ursula Channel and Verney Passage just north of the mouth of Gardner Canal, thus the tidal transport into Gardner Canal occurred through the latter channels. In the region around Gil Island, the phase relationships of tidal height and transport were more complicated. The direction of the flood tide was into the Kitimat system through Campania Sound and Princess Royal Channel and out of it through Otter Channel and Grenville Channel. The tidal flow in this region appeared to be a combination of a standing wave and a travelling wave. In the region around Gil Island, the tidal model was less successful than it was in the sections of the Kitimat system north of Wright Sound. It is thought that in the Gil Island region a 2-dimensional barotropic model which includes rotational effects should be developed if greater predictive accuracy is required.

The analyses of current meter data from different locations throughout the Kitimat system indicated that the baroclinic component of the tidal current near the surface was sometimes larger than the barotropic component. The baroclinic currents observed in 4 consecutive, 3 month sections of record showed these currents to vary by an order of magnitude in amplitude. The apparent, near surface tidal current which is the sum of the barotropic and baroclinic components underwent major variations as a consequence. The time variability of the baroclinic currents limits the applicability of the tidal model for predictive purposes. Further investigation of the baroclinic currents is required to determine first, what their limits of predictability are at one location over several years, and second, if they are predictable, what their distributions of amplitude and phase are throughout the Kitimat system.

On the basis of the observed water structure, an estuarine circulation mode is presumed to have existed in the Kitimat system. Throughout most of the system, a brackish surface layer was evident whose definition varied with the seasonal cycle of freshwater discharge into Douglas Channel and Gardner Canal. At all times of the year, this surface layer was most sharply defined in Gardner Canal which had the largest freshwater input rate of any part of the system. Gardner Canal received its peak freshwater discharges in summer and it was in this season that surface layer salinities

were lowest. The freshwater discharge rate into Douglas Channel reached a maximum in the summer, but a second maximum occurred in autumn. Accordingly, the surface layer was most distinct during the cruises to the study area in summer and autumn. During these cruises, the surface layer salinities increased towards the south end of Douglas Channel suggesting a general southward surface layer flow. Direct observations of currents in this layer showed that the flow in summer and autumn was predominantly southwards, but the wind had an increasingly important effect as winter was approached. The wind caused several flow reversals in the summer months and by autumn the direction of the near surface currents appeared to be dominated by the wind. It seems that in the absence of an appreciable freshwater discharge into Douglas Channel in winter and spring, the near surface circulation is almost completely dominated by the wind.

To describe the estuarine circulations in Douglas Channel and Gardner Canal quantitatively, a 2 layer, time independent, estuarine circulation model was constructed of this part of the system including Devastation Channel and Verney Passage. Data on surface layer salinities and wind stress were supplied to the model which in turn calculated various parameters of the flow including surface layer thicknesses and surface layer velocities. The model was able to predict the observed thicknesses of the surface layer fairly well for most parts of the system. An arbitrary parameter which must be specified as input to the model, was the division of surface layer flow towards the north and south out of the western end of Gardner Canal. The variation of this parameter did not appreciably affect the surface layer thicknesses in Douglas Channel, but surface layer flow velocities were affected to a greater extent. Another difficulty encountered in applying the model was the proper specification of the wind stress. For want of better information, a uniform wind stress was applied over the whole of the area covered by the model. In reality, a differential in wind stress would likely have existed on the 2 sides of Hawkesbury Island which would have forced the circulation one way or the other around the island. A major difficulty is the compatibility of a model which is time independent with a physical system which has a large amount of variance at time scales of a few days or shorter. Also, it is evident that more observations of current velocities need to be made in the region covered by the model for its proper evaluation.

The shallow sills which cross Ursula Channel and Verney Passage appeared to cause particularly strong tidal mixing in their vicinity. The partial destruction of the surface layer of lower salinity by the mixing process is expected to have had a major influence on the estuarine circulation in the region. The interaction of the tidal flow when it crossed the sill in Verney Passage was studied in some detail. There is evidence that during both the flood and ebb flows across the sill an internal lee wave formed on the downstream side of the sill. The flows may have been strong enough that the internal lee wave became unstable and developed into an internal hydraulic jump.

In the channels to the south of Wright Sound, in Grenville Channel and in Princess Royal Channel, the surface layer of lower salinity was not as well defined as it was in the channels to the north of Wright Sound. The

nature of the circulation appeared complicated in these regions. For example, there is evidence that the surface layer movement in Grenville Channel in July, 1977 proceeded northwards, whereas the following June it proceeded in the opposite direction. It is possible that the estuarine circulation in Grenville Channel could have been driven from either end at different times of the year. However, in a double ended channel such as Grenville Channel, it is certain that the wind stress has a major influence on surface layer flow. Possibly, in this channel, a net circulation was also driven by the nonlinear interaction of the tidal currents with the topography. Similar considerations as these may have also applied to the flow through Princess Royal Channel. In the channels around Gil Island, the investigation of the circulation proved to be particularly difficult. Likely, most of the freshwater which flowed into Douglas Channel and Gardner Canal eventually left the Kitimat system through Campania Sound and Otter Channel. The interaction of such a flow with wind driven and tidal flows is sure to have been strong. Near Campania Sound and Otter Channel, there was strong mixing apparently induced by the tides. It is evident that in the channels around Gil Island it is not sufficient just to examine variations in water structure along the channel's axes, but lateral variations must also be considered.

The movement of deep water within the Kitimat system appears to have been restricted by a series of sills. Above 160 m depth, which is the maximum depth of free access from the interior of the system to Hecate Strait, vigorous tidal currents should have ensured a constant exchange of water in and out of the system. Below 160 m depth, exchange was probably more limited, but it did occur. The appearance of high salinity water in Campania Sound in summer caused an exchange to the bottom of the channels on either side of Gil Island which are the deepest sections of the Kitimat system. The summer appearance of high salinity water in Hecate Strait has been recognized by other investigators and attributed to seasonal changes in the wind climate along the British Columbia coast. Beacuse of the sills which cross its approaches, the inner basin of Gardner Canal was isolated to a large degree from the rest of the system. Exchange to the bottom of the basin did occur sometime between July and September of 1977, but it had not recurred by June of the following year.

The major difficulty in studying the circulation of the Kitimat system was the system's size and complexity. In defining the wind driven and estuarine circulations, in particular, both temporal and spatial aliasing problems were severe. For example, to complete a series of CTD casts throughout the system took a couple of days which is comparable to the time scales of circulation and water structure changes caused by the wind. Also, the use of data from individual CTD casts to represent the water structure in an area is subject to aliasing uncertainties arising from changes in the water structure occurring at tidal frequencies. Near channel junctions, tidal advection may be the primary cause of such changes, whereas elsewhere the influence of propagating internal tides may have greater importance. Unfortunately, to account for changes in water structure at tidal frequencies, a high density of data is required which, in turn, usually necessitates a limitation on the size of the region being studied. Accordingly, it is felt that future studies of the Kitimat system should be restricted to 1 or 2 phenomena in specific areas at a time.

The highest priority for further study should be assigned to determining more of the nature of the wind driven and estuarine circulations in the channels on both sides of Hawkesbury Island. Since changes in the water structure and circulation in this region occur over such short time periods, perhaps the only way to study them is through a high density of moored instrumentation in the top 50 m of the water column. Although current meter measurements taken in Douglas Channel did succeed in showing the importance of the wind for near surface water movements, it is still not known how the channel is flushed. Specifically, to what extent does the water pile up at the north end of Douglas Channel with a strong southerly wind and to what extent does such a wind cause a return flow south through Devastation Channel? The answer to this question has great significance for determining the fate of a hypothetical pollutant released either in Douglas Channel or near the port of Kitimat.

REFERENCES

Barber, F. G. (1957). The Effect of the Prevailing Winds on the Inshore Water Masses of the Hecate Strait Region, B.C., J. Fish. Res. Bd. Canada, Vol. 14 (6), pp. 945-952.

Mooers, C.N.K. (1973). A Technique for the Cross Spectrum Analysis of Pairs of Complex-Valued Time Series, with Emphasis on Properties of Polarized Components and Rotational Invariants. Deep Sea Research. Vol. 20, pp. 1129-1141.

Pearson, G. E. and D. F. Winter (1978). Two-Layer Analysis of Steady Circulation in Stratified Fjords. In Hydrodynamics of Estuaries and Fjords, Edited by J.C.J. Nihoul, Elsevier Scientific Publishing Co., Amsterdam. 546 pp.

Pickard, G. L. (1961). Oceanographic Features of Inlets in the British Columbia Mainland Coast. J. Fish. Res. Bd. Canada, Vol. 18 (6), pp. 907-999.

Phillips, D. W. (1977). A Marine Climatology of the Approaches to Kitimat, British Columbia. Project Report No. 34, Atmospheric Environment Service, Toronto, Ont. Unpublished manuscript.

Phillips, O. M. (1966). The Dynamics of the Upper Ocean. Cambridge University Press, Cambridge, 261 pp.

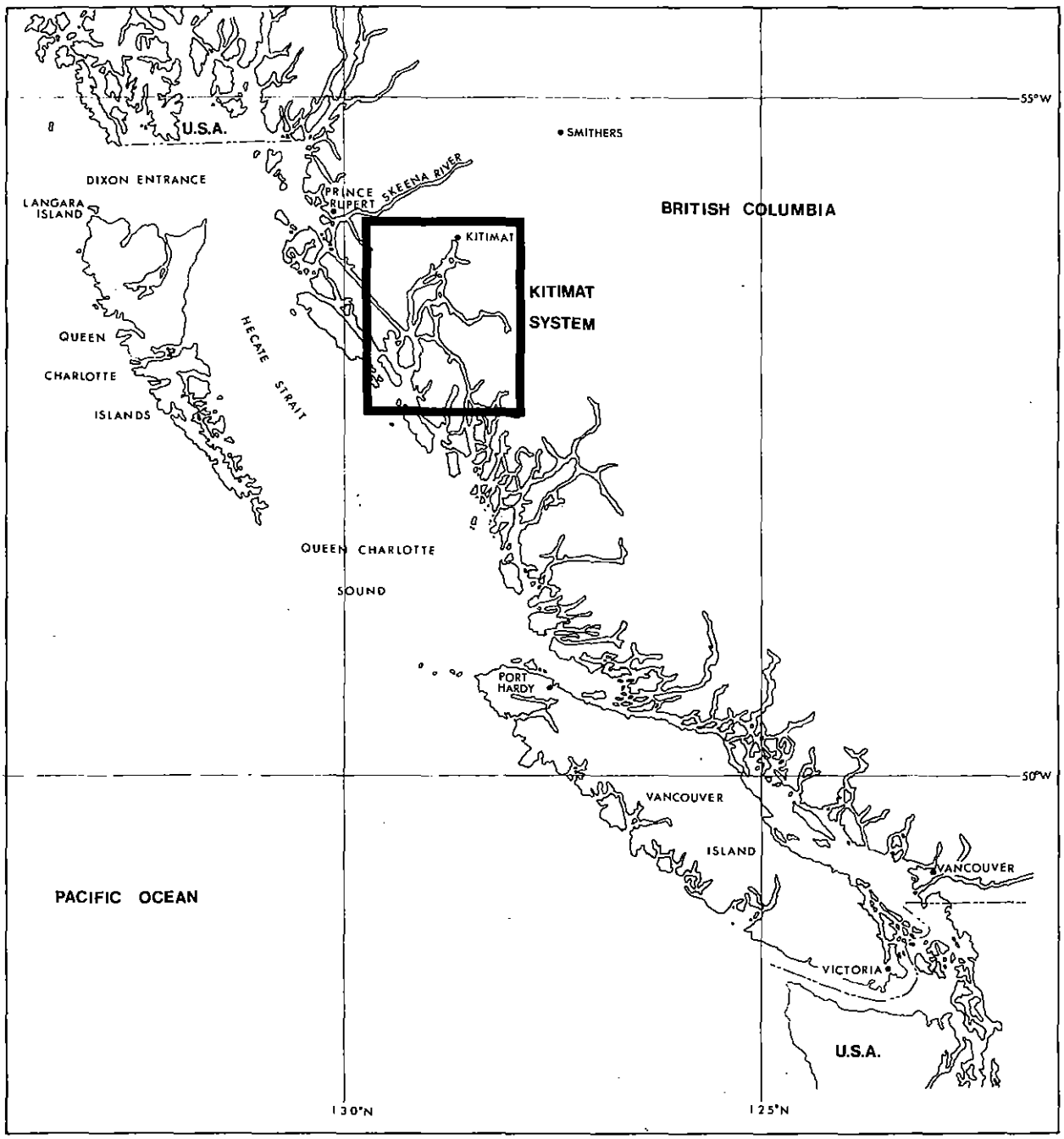

Figure 1. Location of Kitimat system.

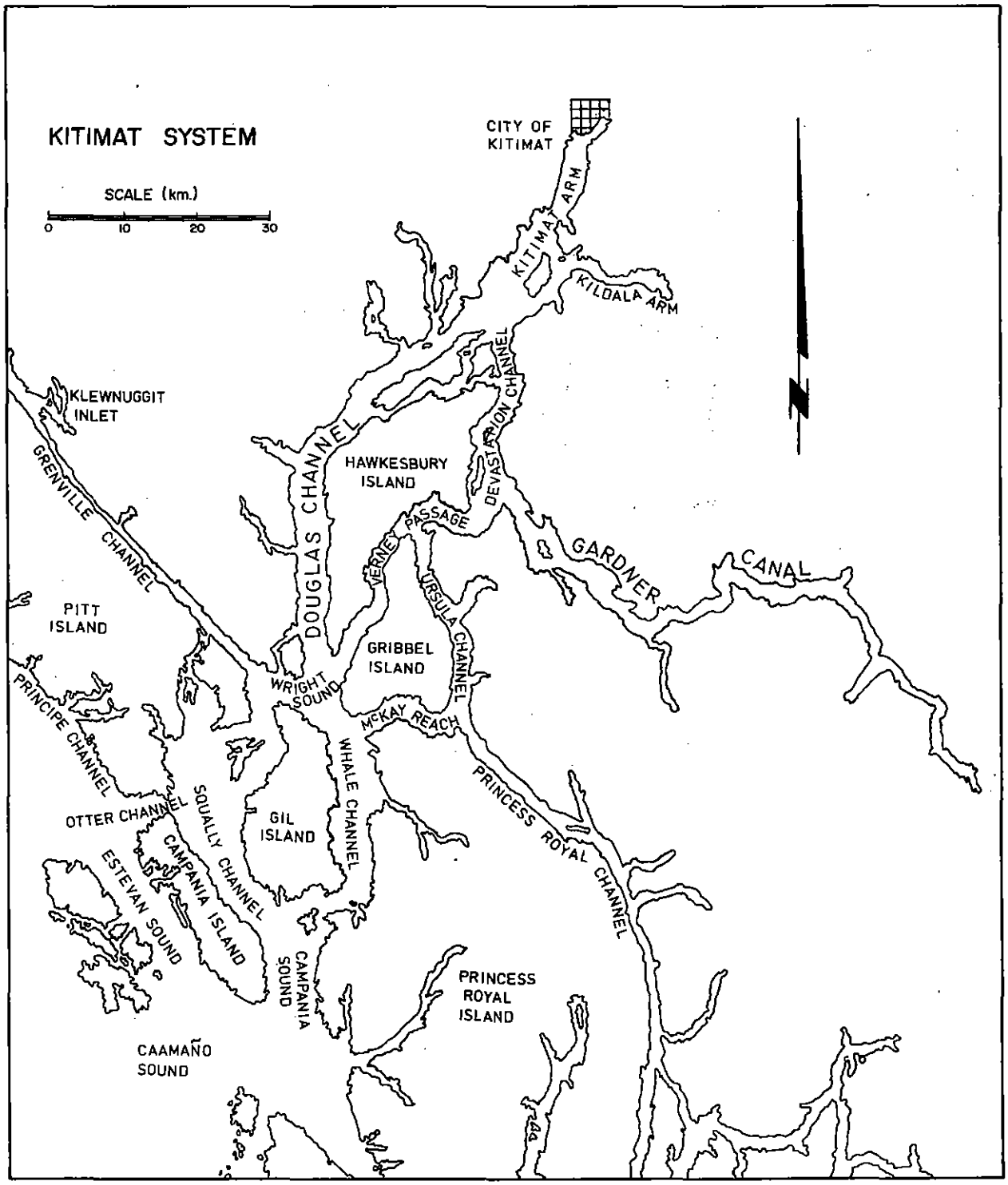

Figure 2. Map of Kitimat system.

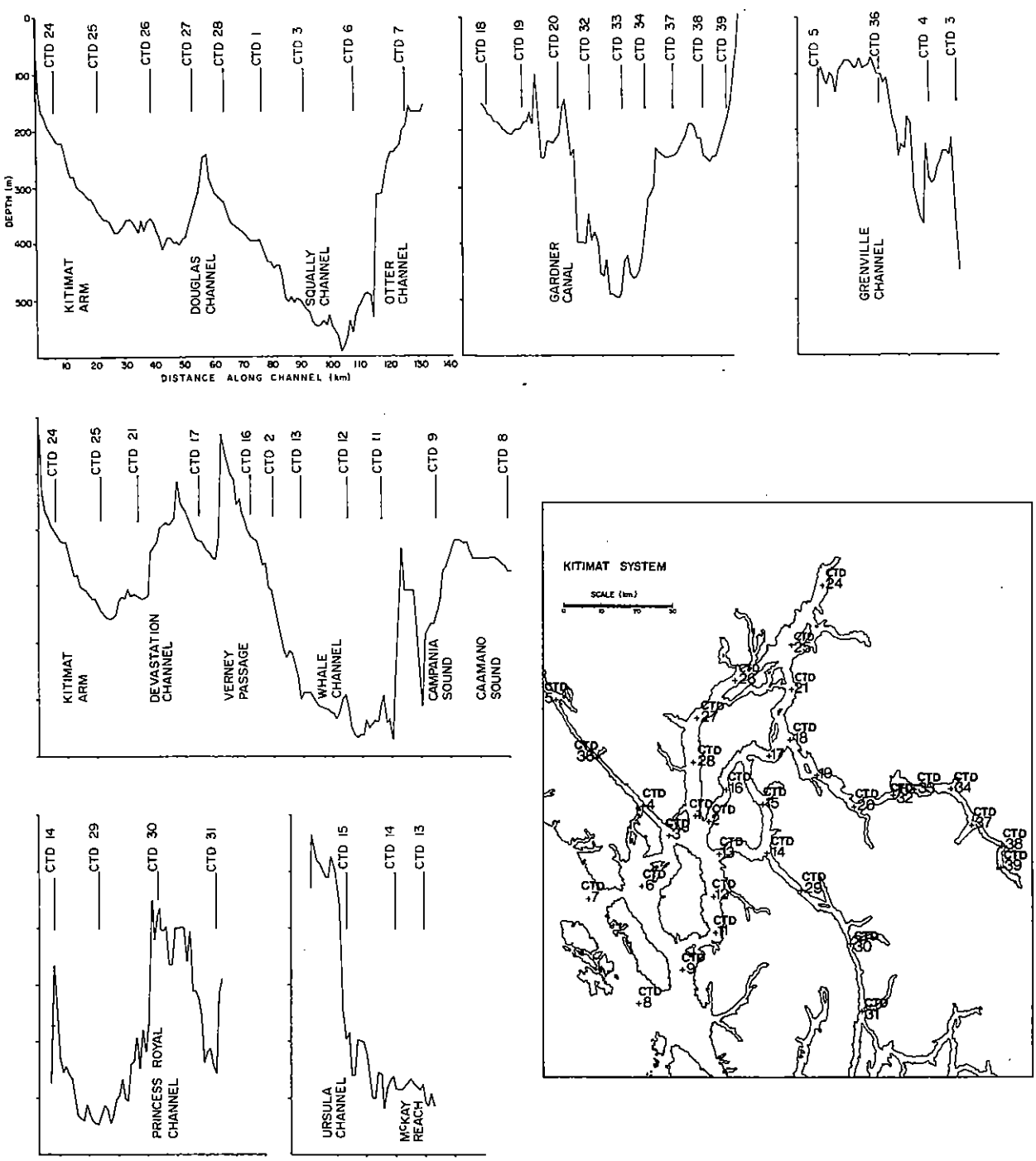

Figure 3. Bathymetry of Kitimat system.

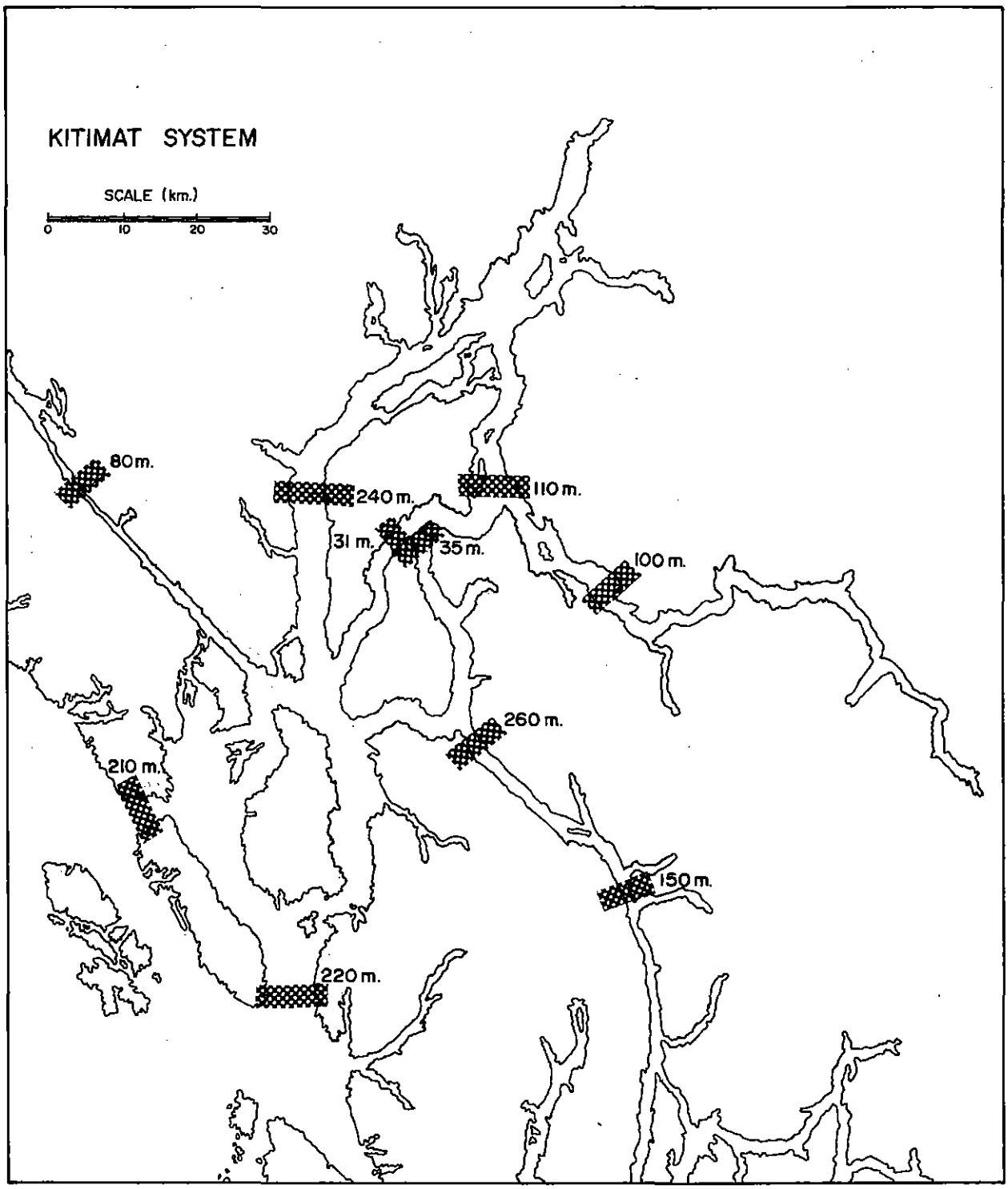

Figure 4. Depths of prominent sills throughout Kitimat system.

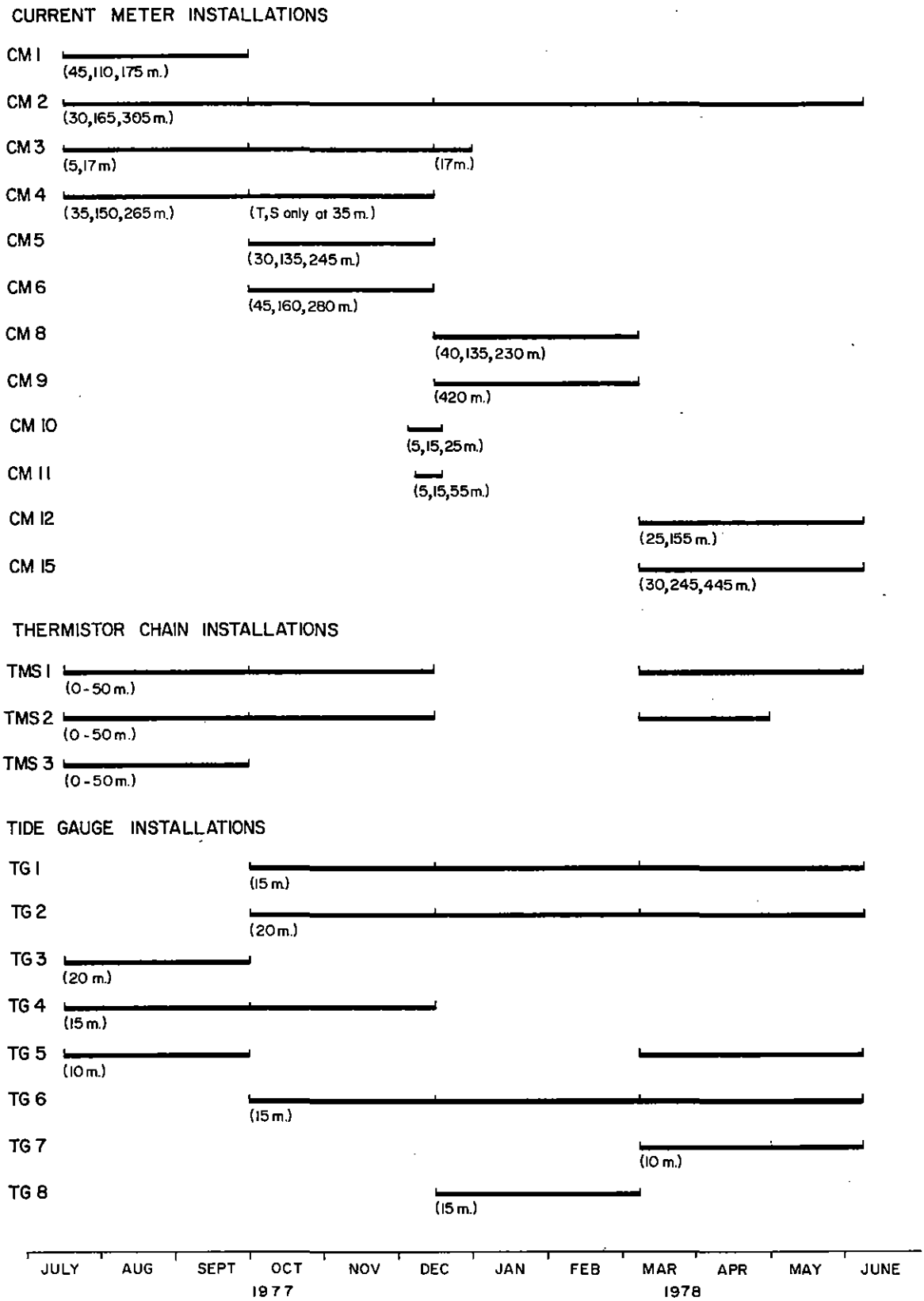

Figure 5. Installation periods of current meters, tide gauges, and thermistor chains.

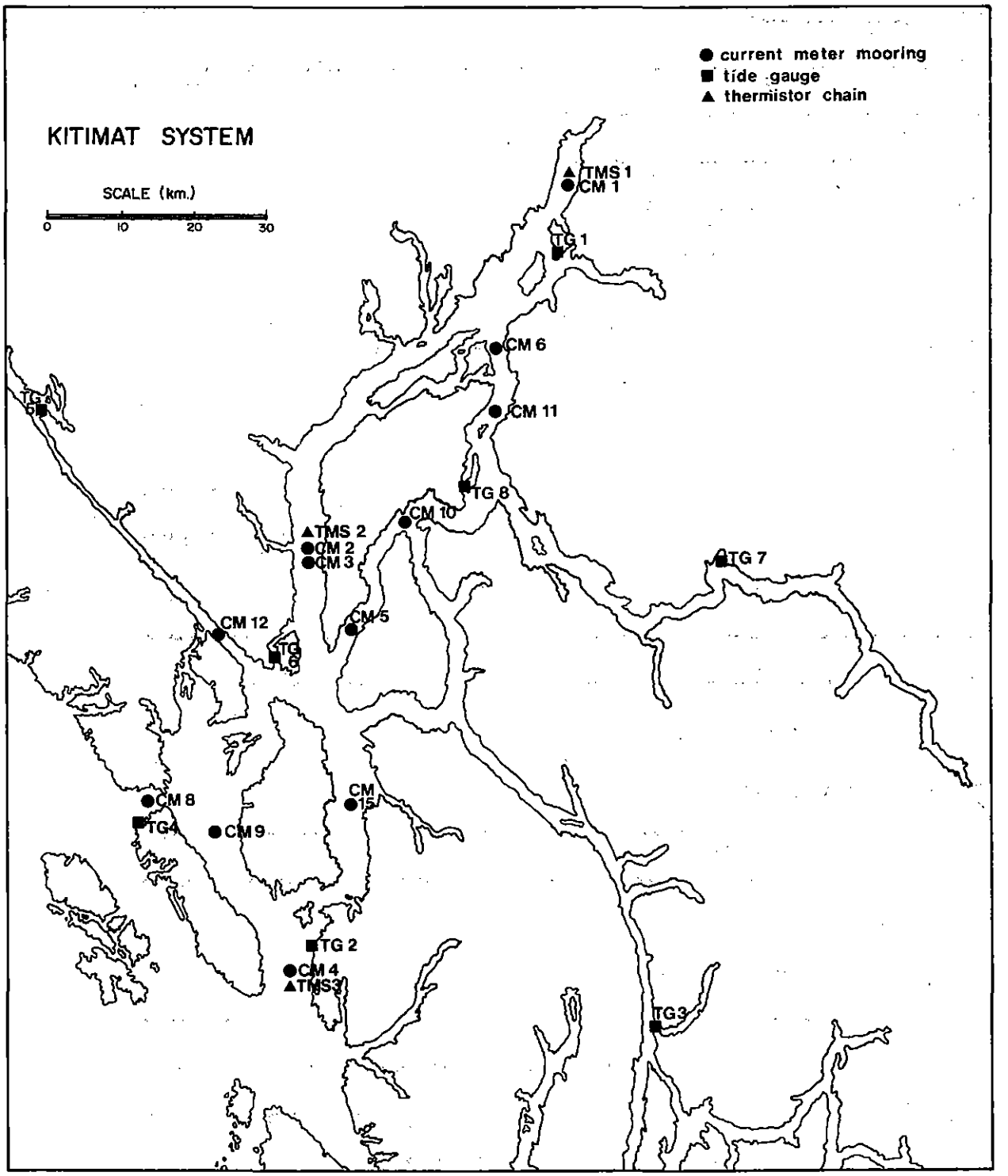

Figure 6. Installation locations of current meters, tide gauges, and thermistor chains.

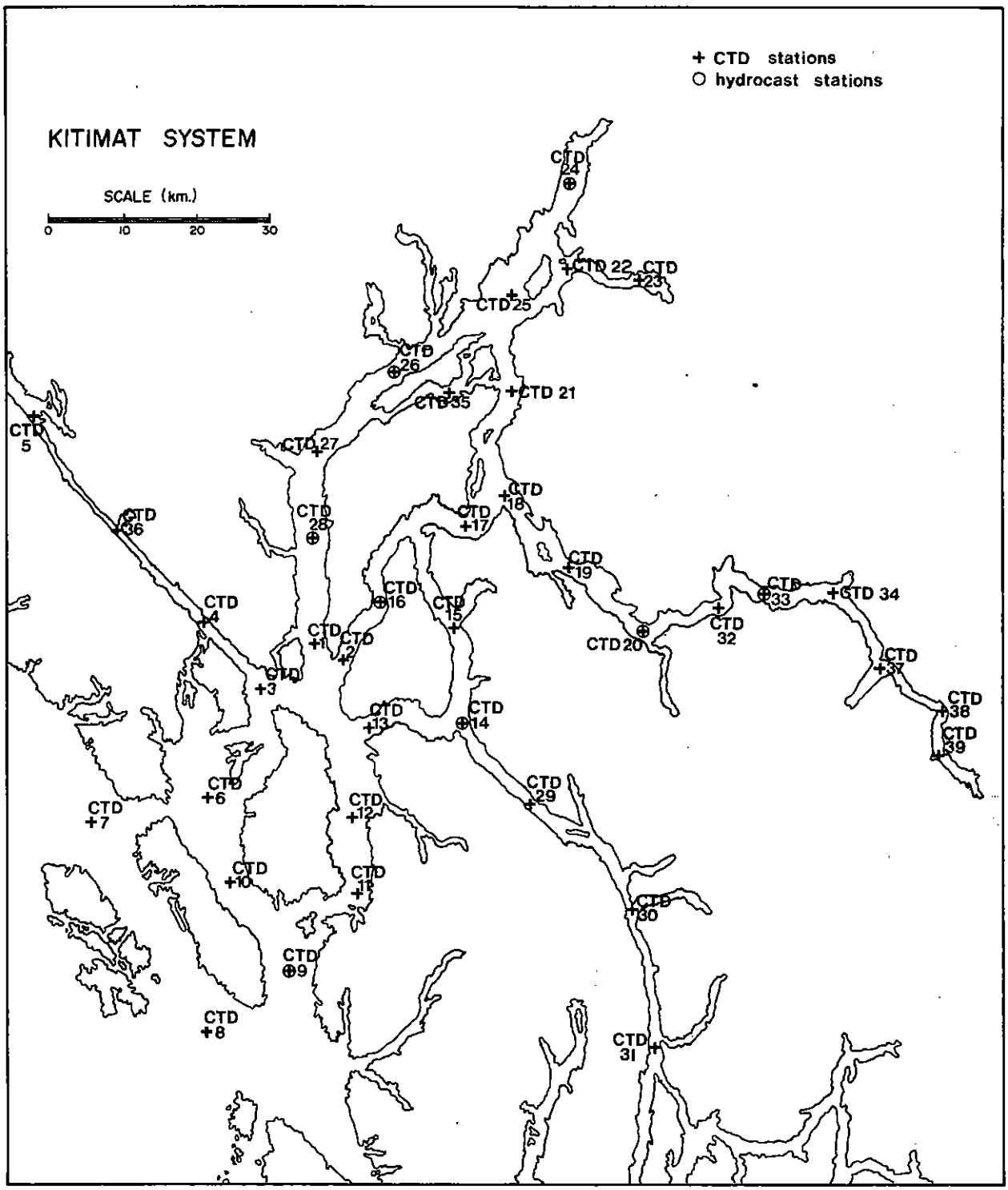

Figure 7. Locations of CTD and hydrocast stations.

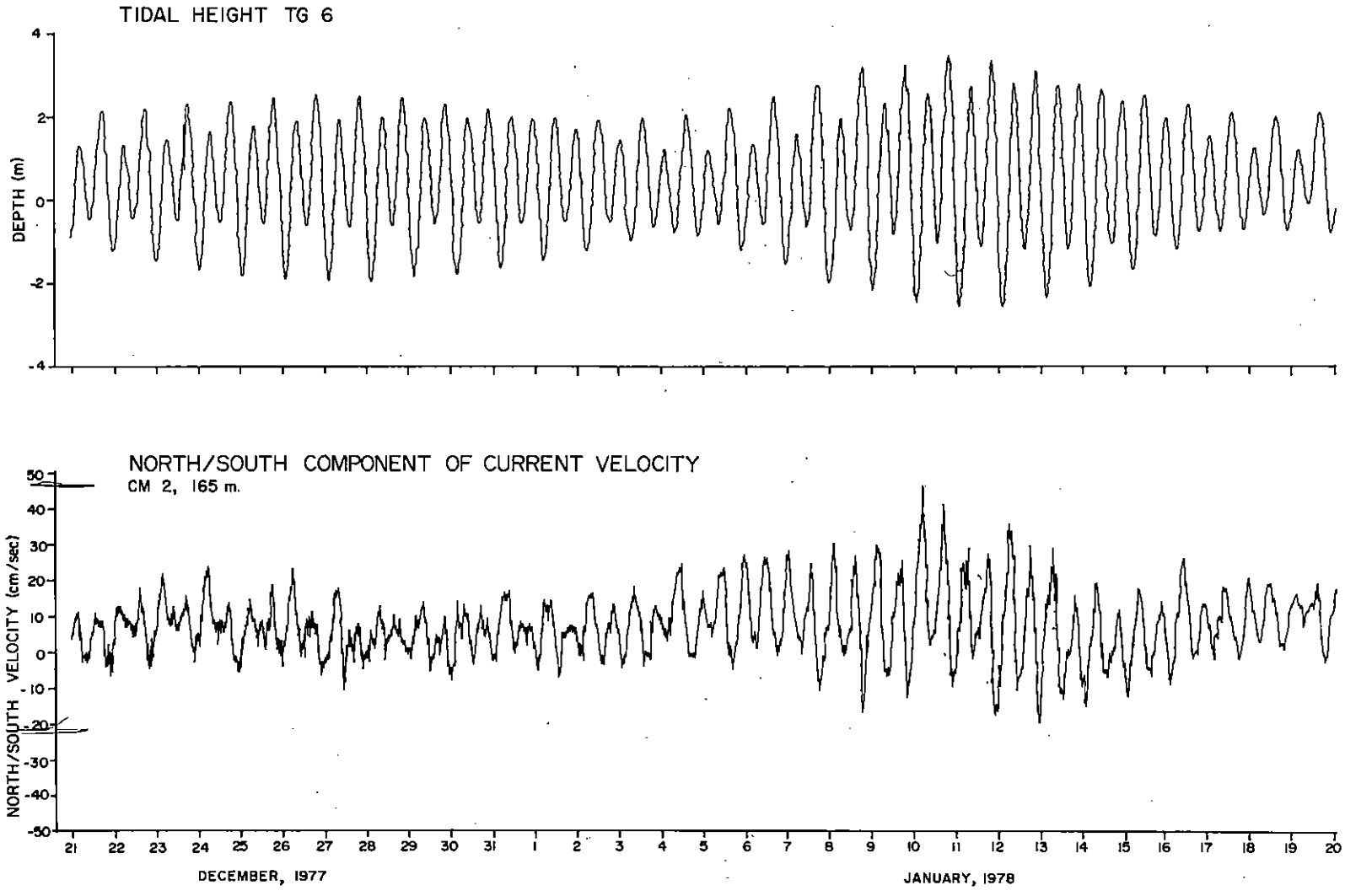

Figure 8. Example of a tide gauge and current meter time series.

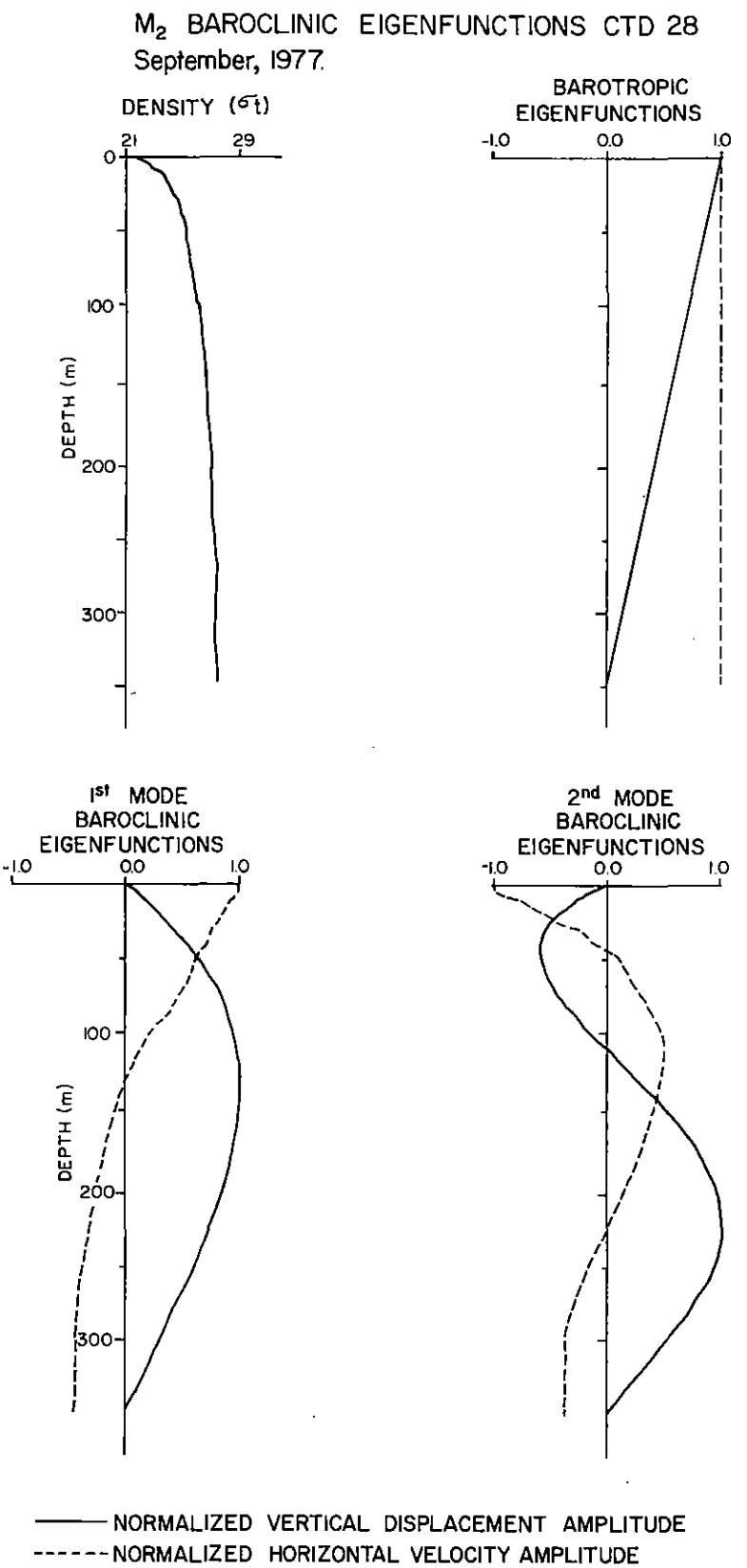

Figure 9. Normalized barotropic and baroclinic eigenfunctions, CTD 28 - September, 1977.

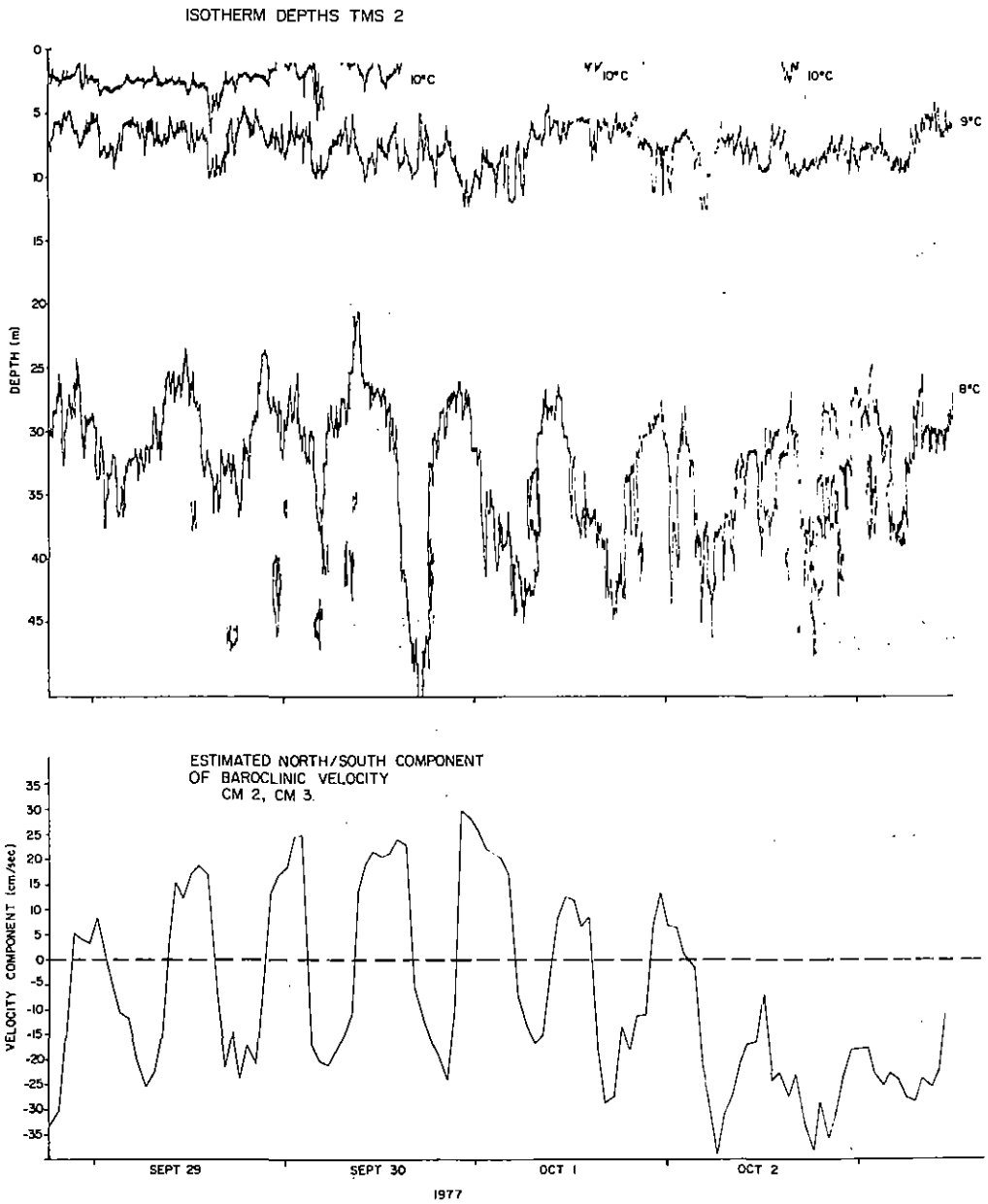

Figure 10. Isotherm depth time series, TMS 2 - September, 1977.

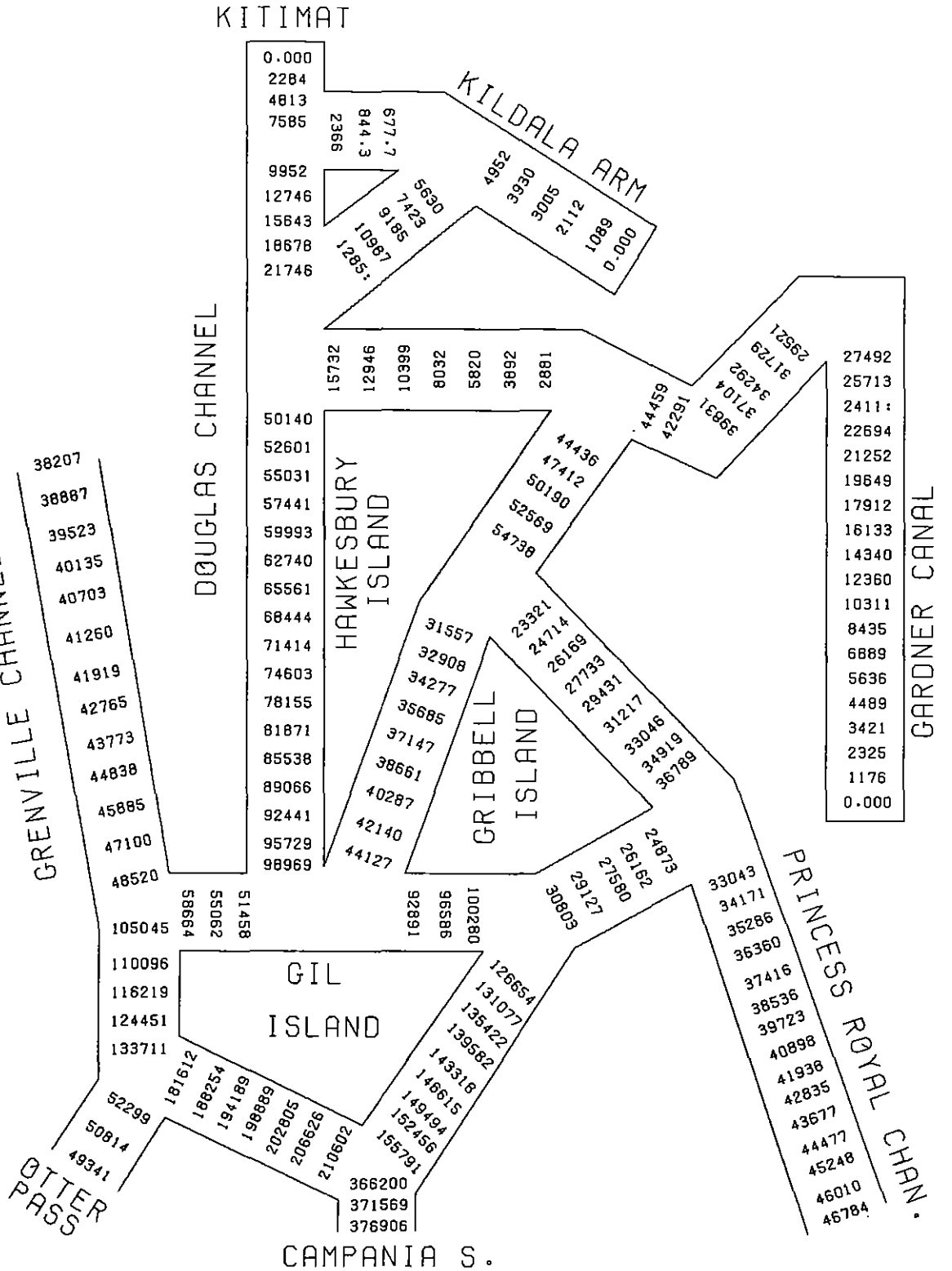

Figure 11. M_2 tidal transport amplitudes (m^3/sec), linear model.

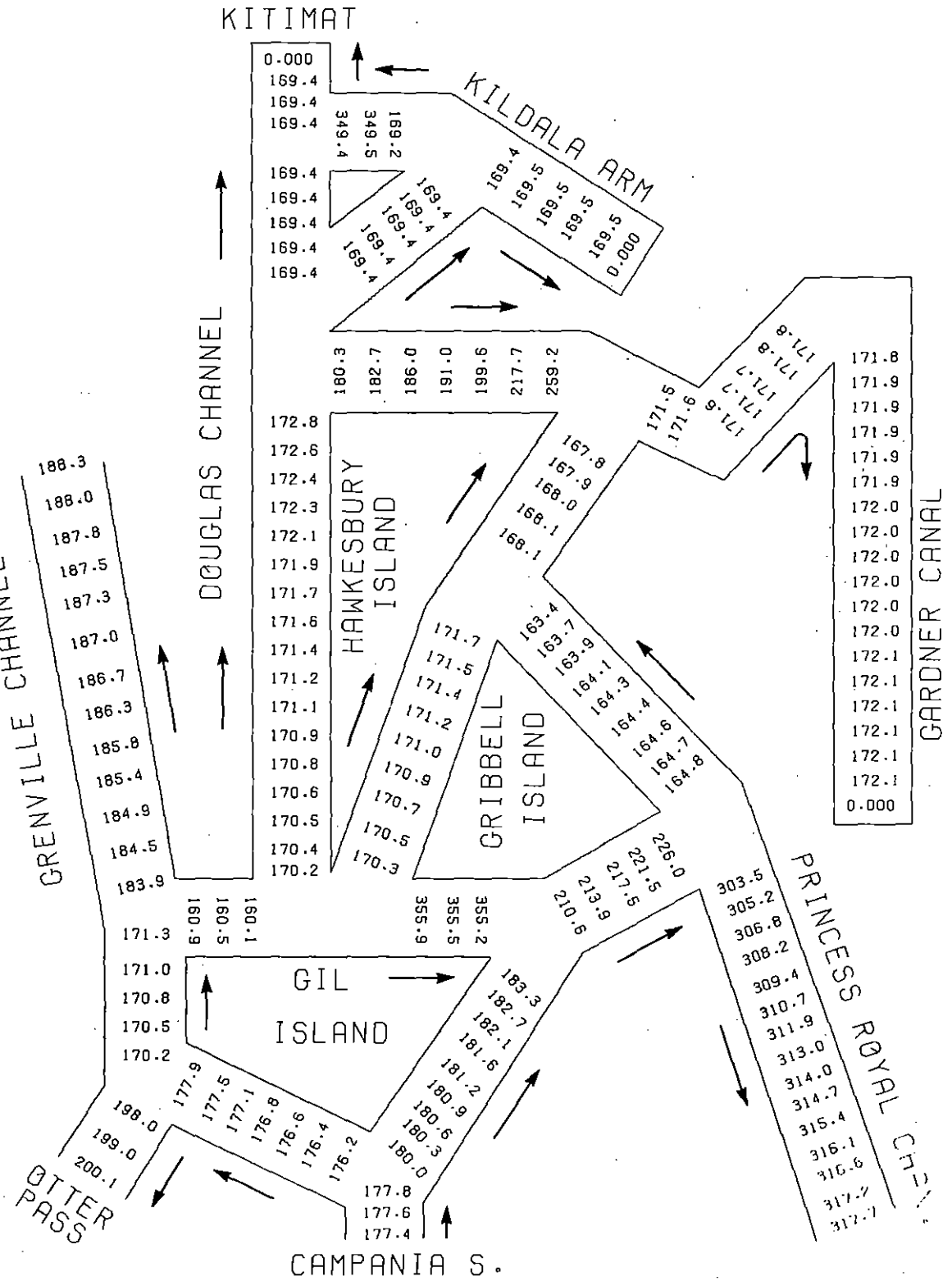

Figure 12. M_2 tidal transport phases (degrees), linear model (Note that the arrows represent the reference transport direction).

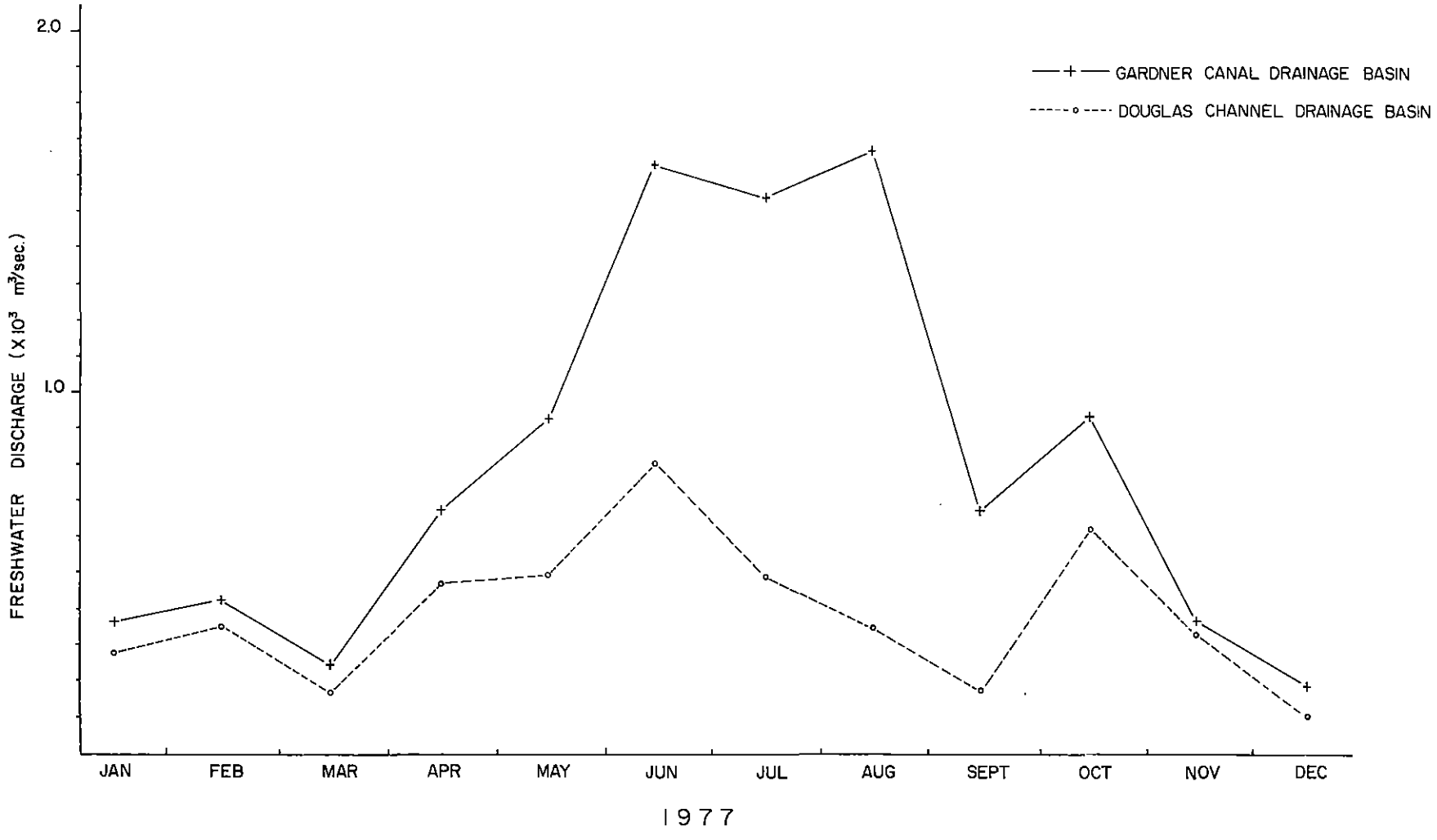

Figure 13. Monthly averaged freshwater dishcarges into Douglas Channel and Gardner Canal.

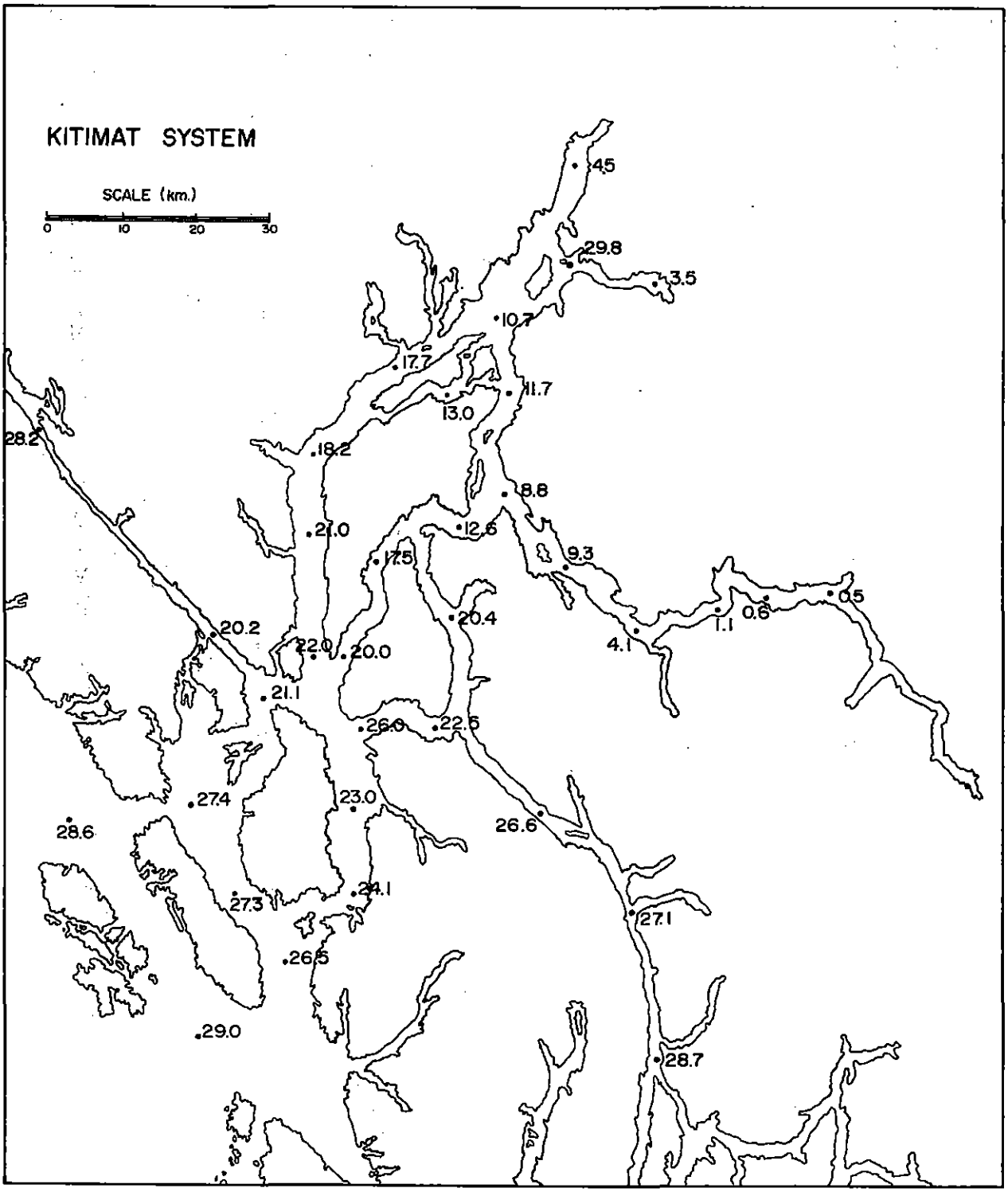

Figure 14. Salinities at 1 m depth - July, 1977.

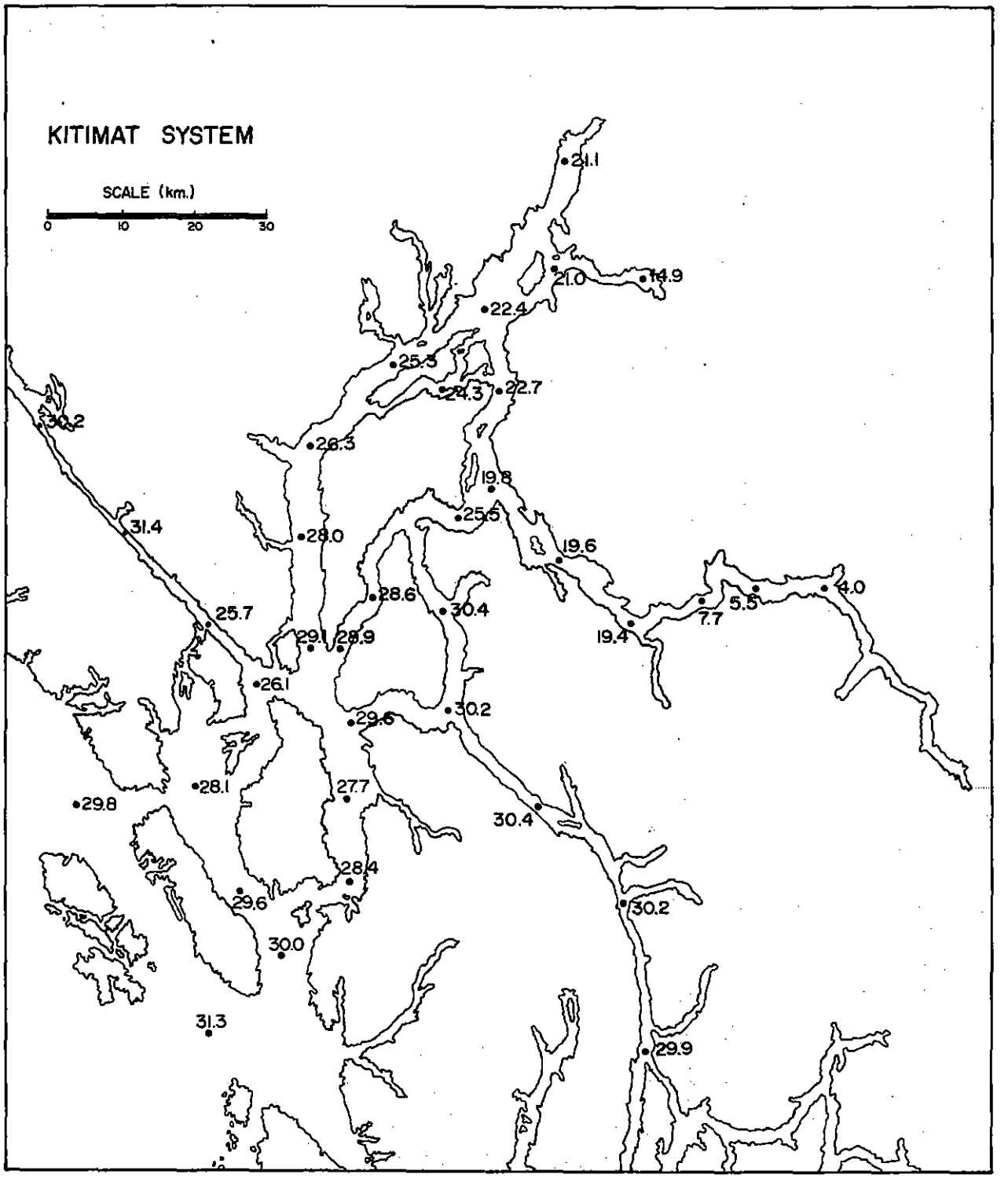

Figure 15. Salinities at 1 m depth - September, 1977.

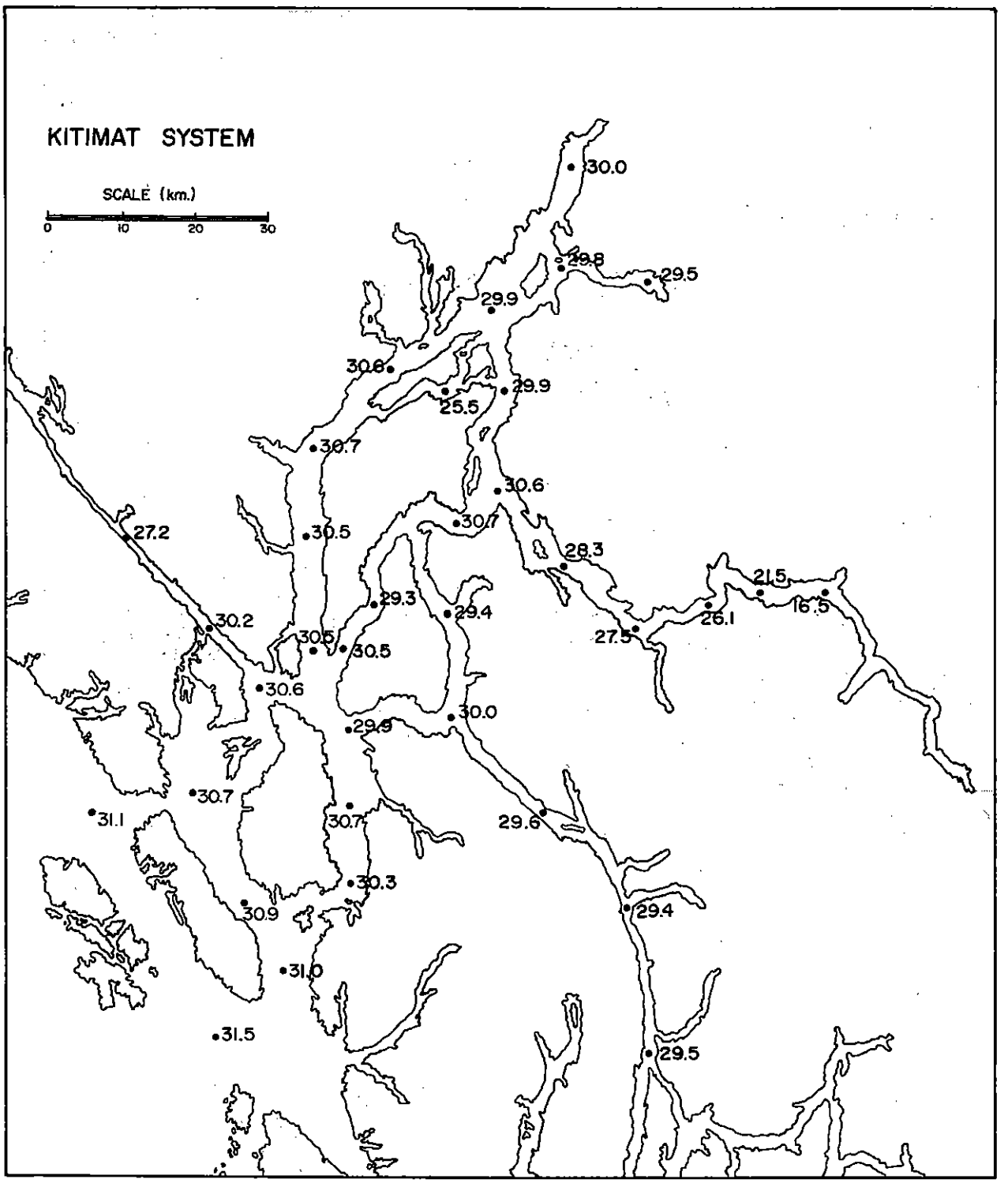

Figure 16. Salinities at 1 m depth - December, 1977.

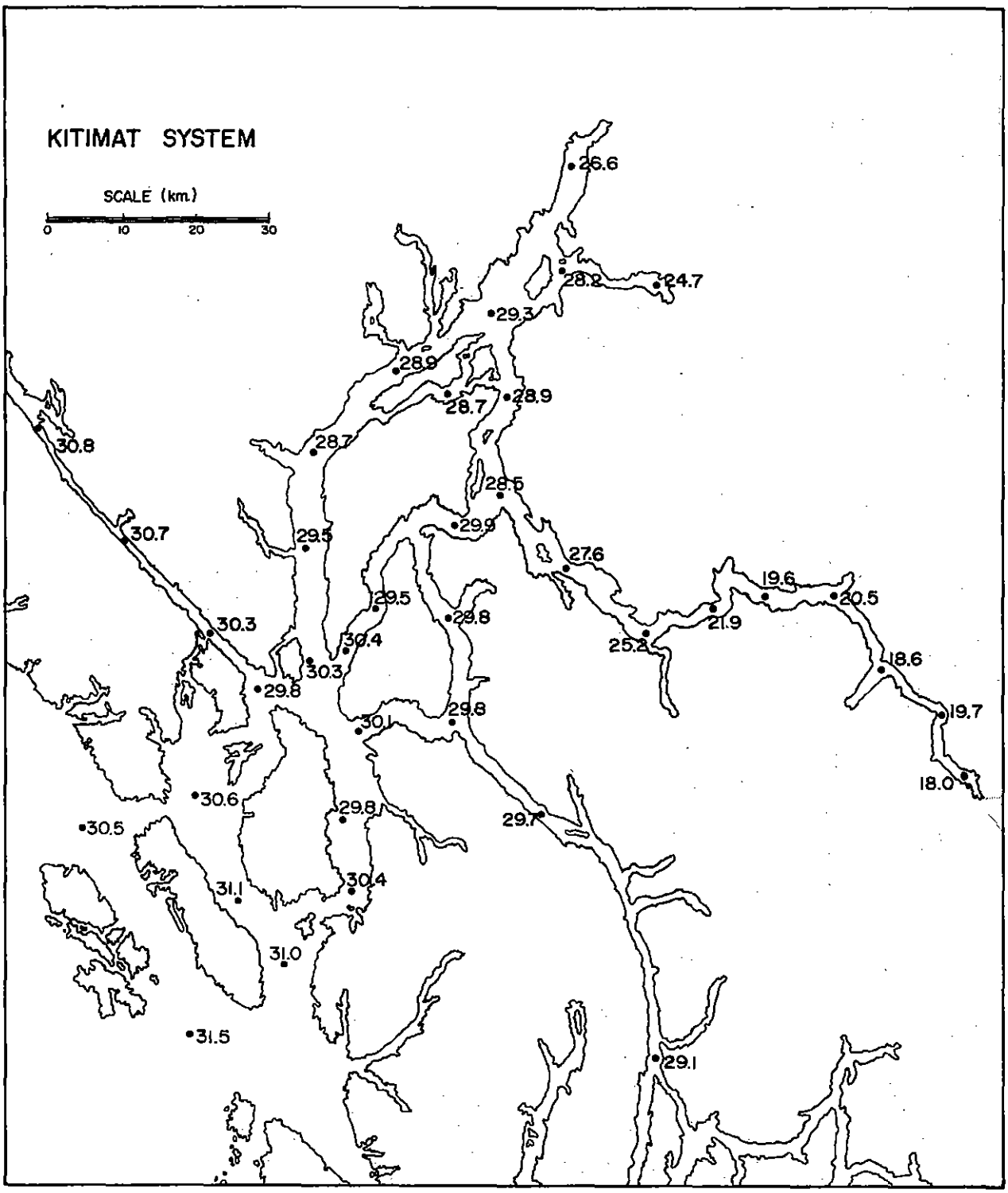

Figure 17. Salinities at 1 m depth - March, 1978.

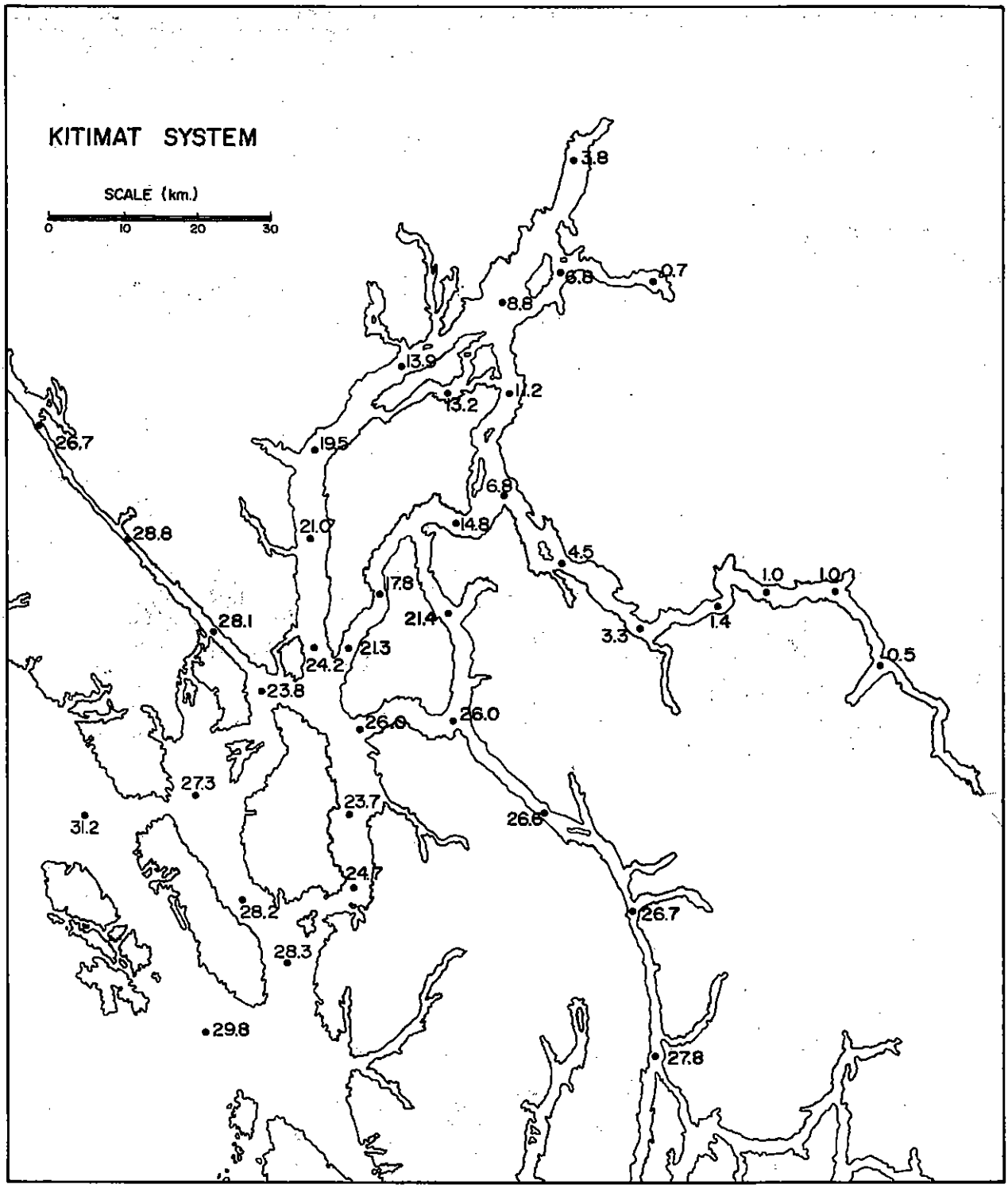

Figure 18. Salinities at 1 m depth - June, 1978.

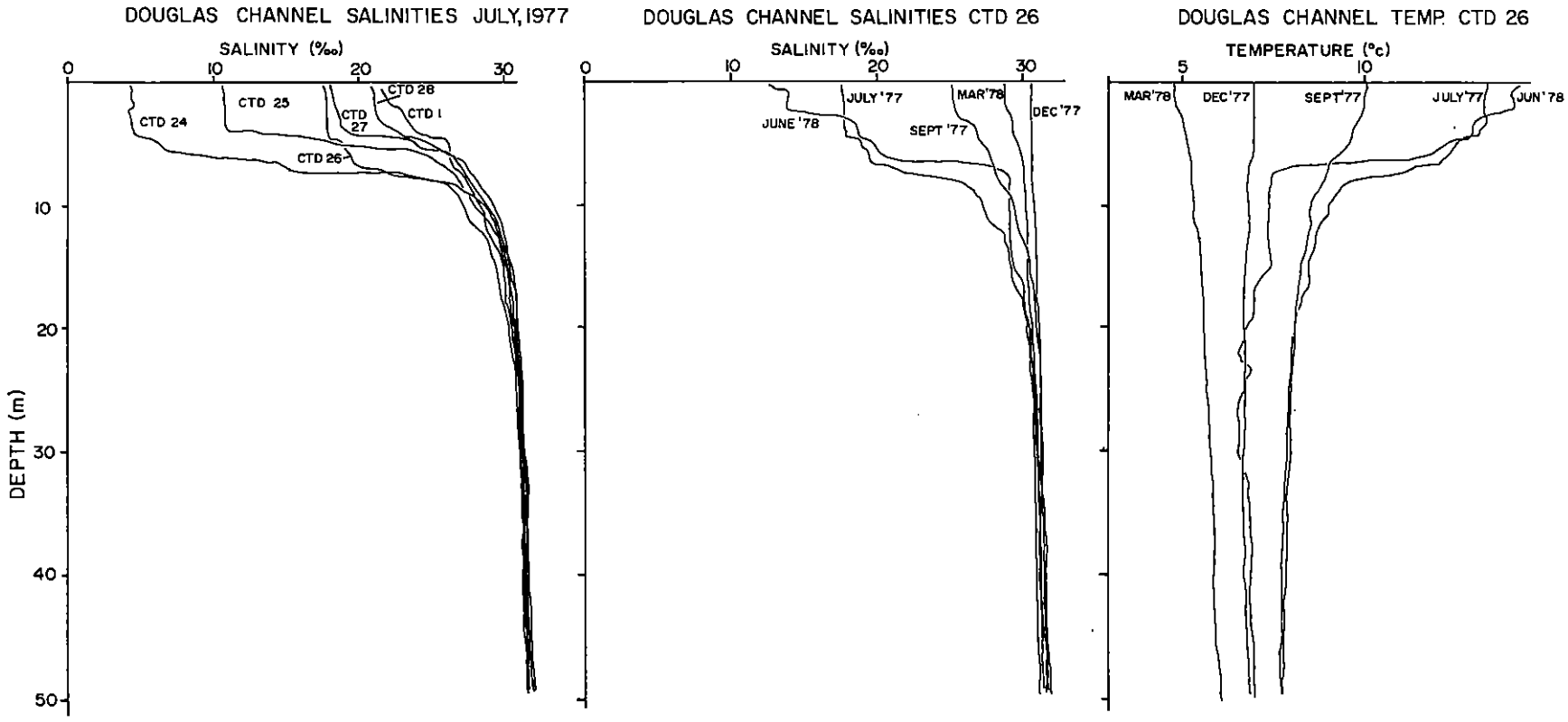

Figure 19. Salinities to 50 m depth along Douglas Channel - July, 1977; salinities and temperatures to 50 m depth at CTD 26 on each of the 5 cruises.

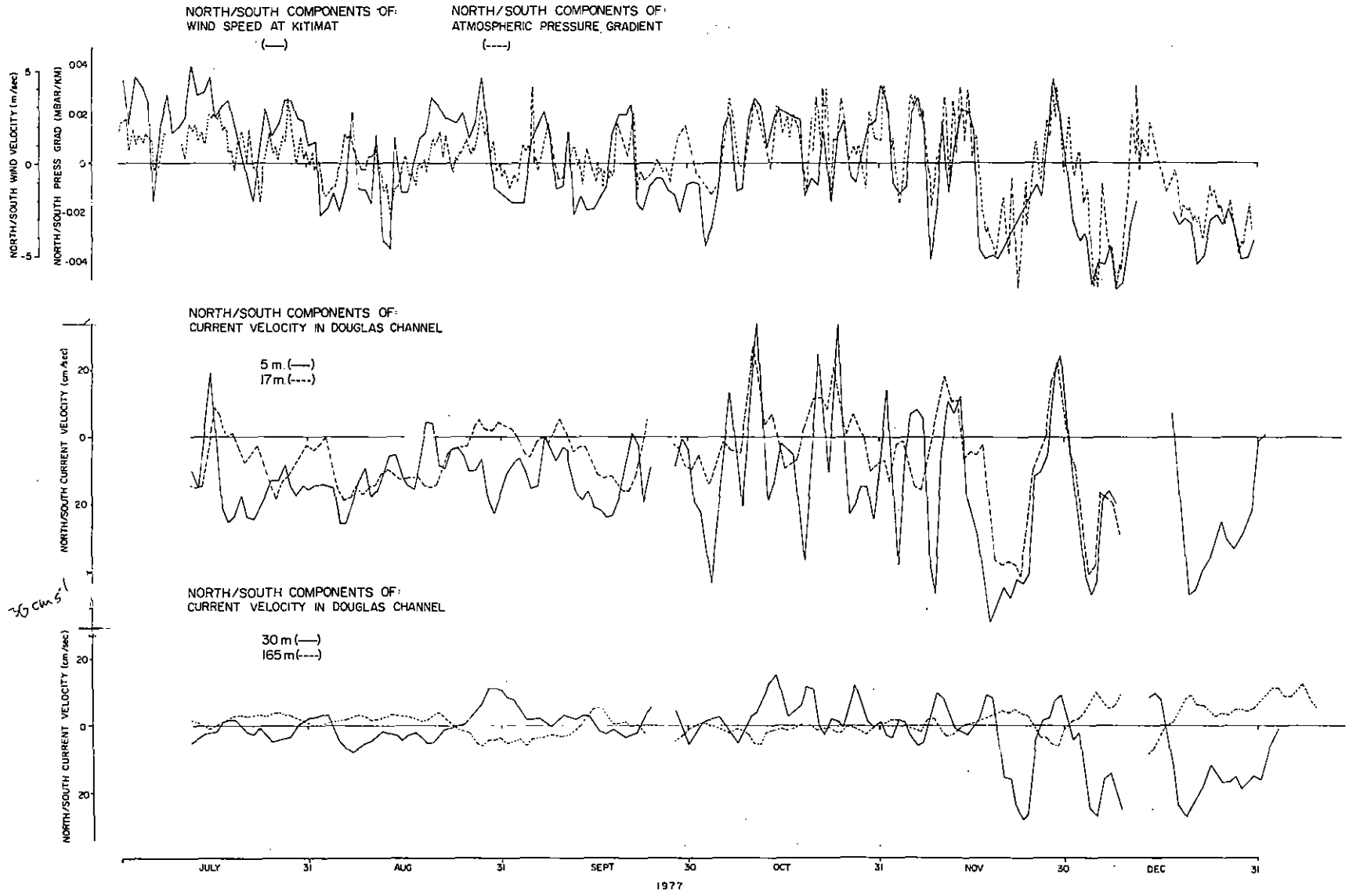

Figure 20. North/south components of wind velocity at Kitimat, of barometric pressure gradient, and of current velocities at 5 m, 17 m, 30 m and 165 m depths in Douglas Channel - July to December, 1977.

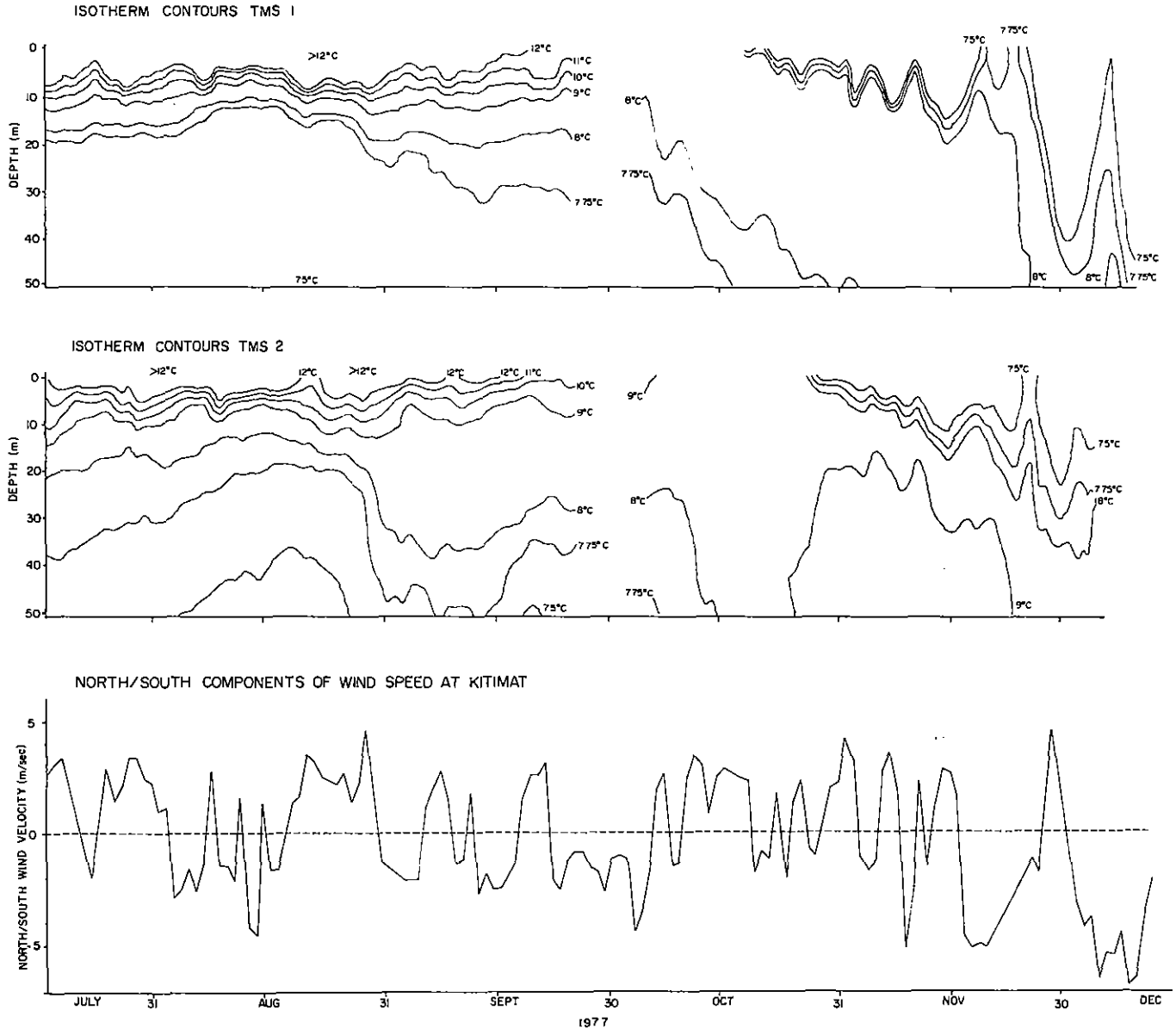

Figure 21. Contoured isotherm depths at TMS 1 and TMS 2 and north/south component of wind velocity at Kitimat - July to December, 1977.

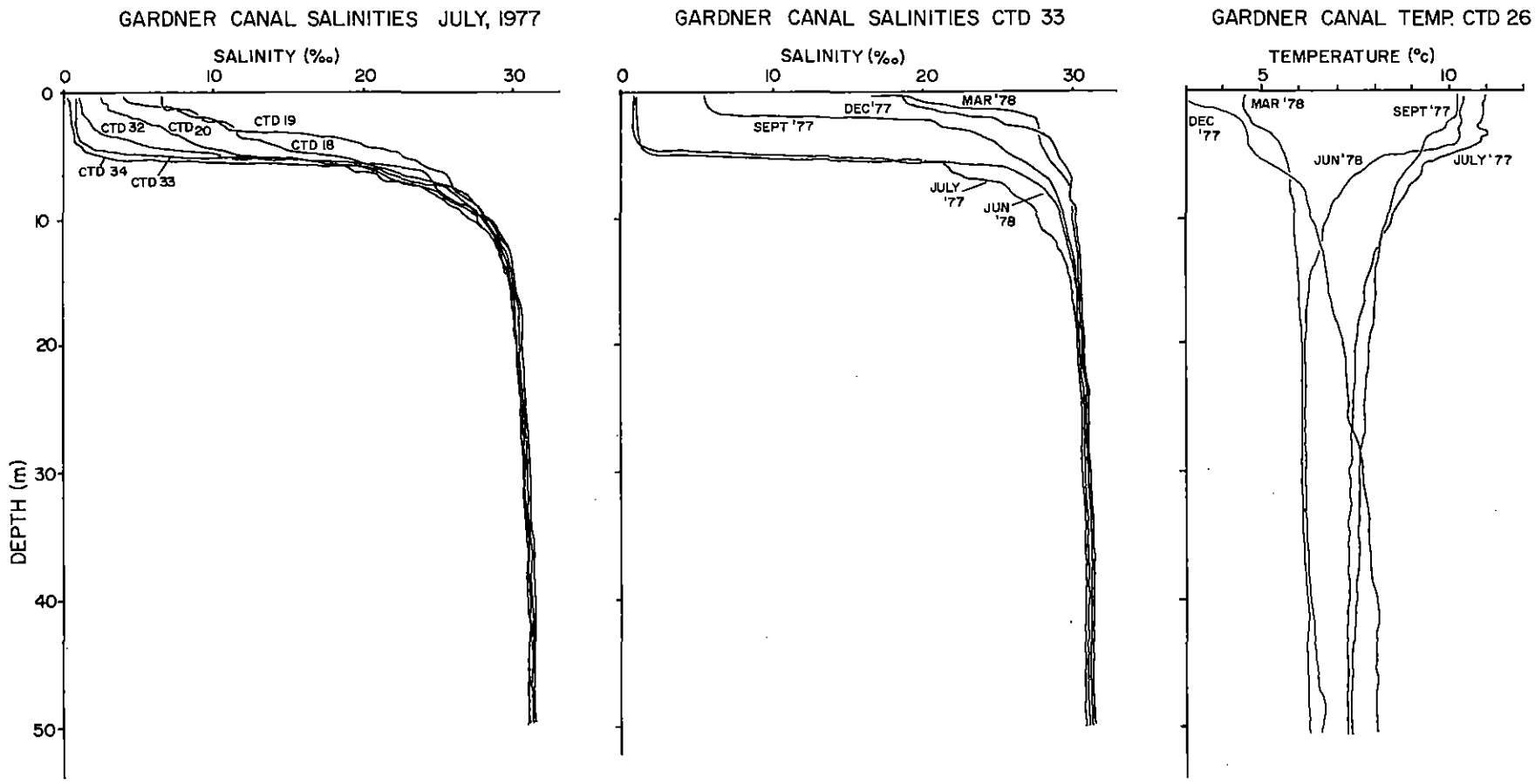

Figure 22. Salinities to 50 m depth along Gardner Canal - July, 1977; salinities and temperatures to 50 m depth at CTD 33 on each of the 5 cruises.

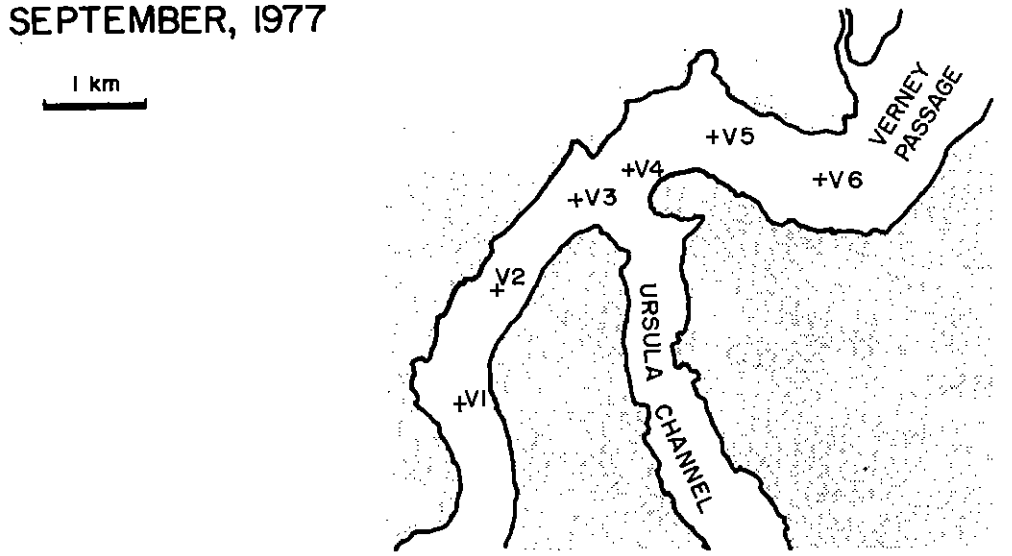

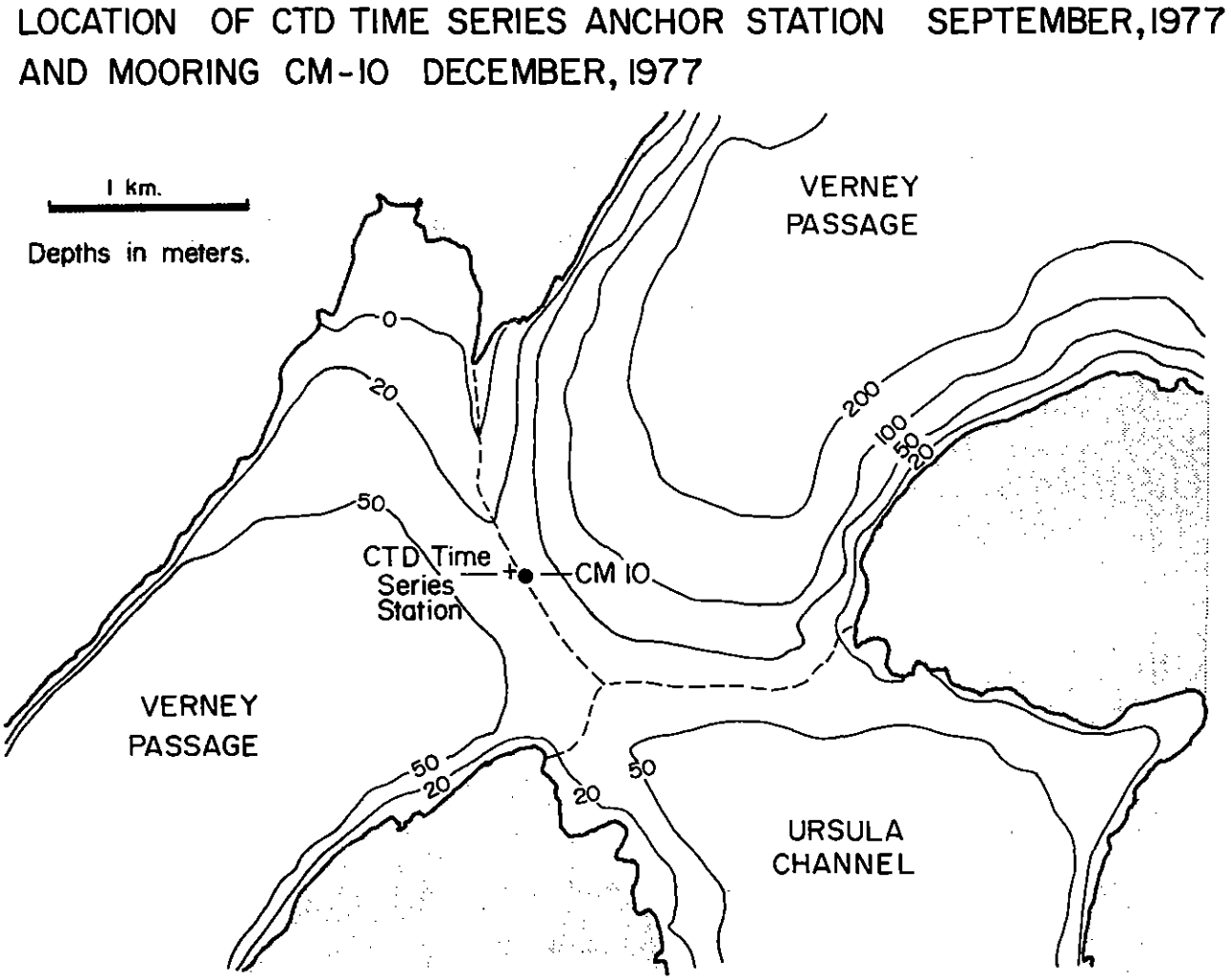

Figure 23. Locations of time series stations near Verney Passage sill.

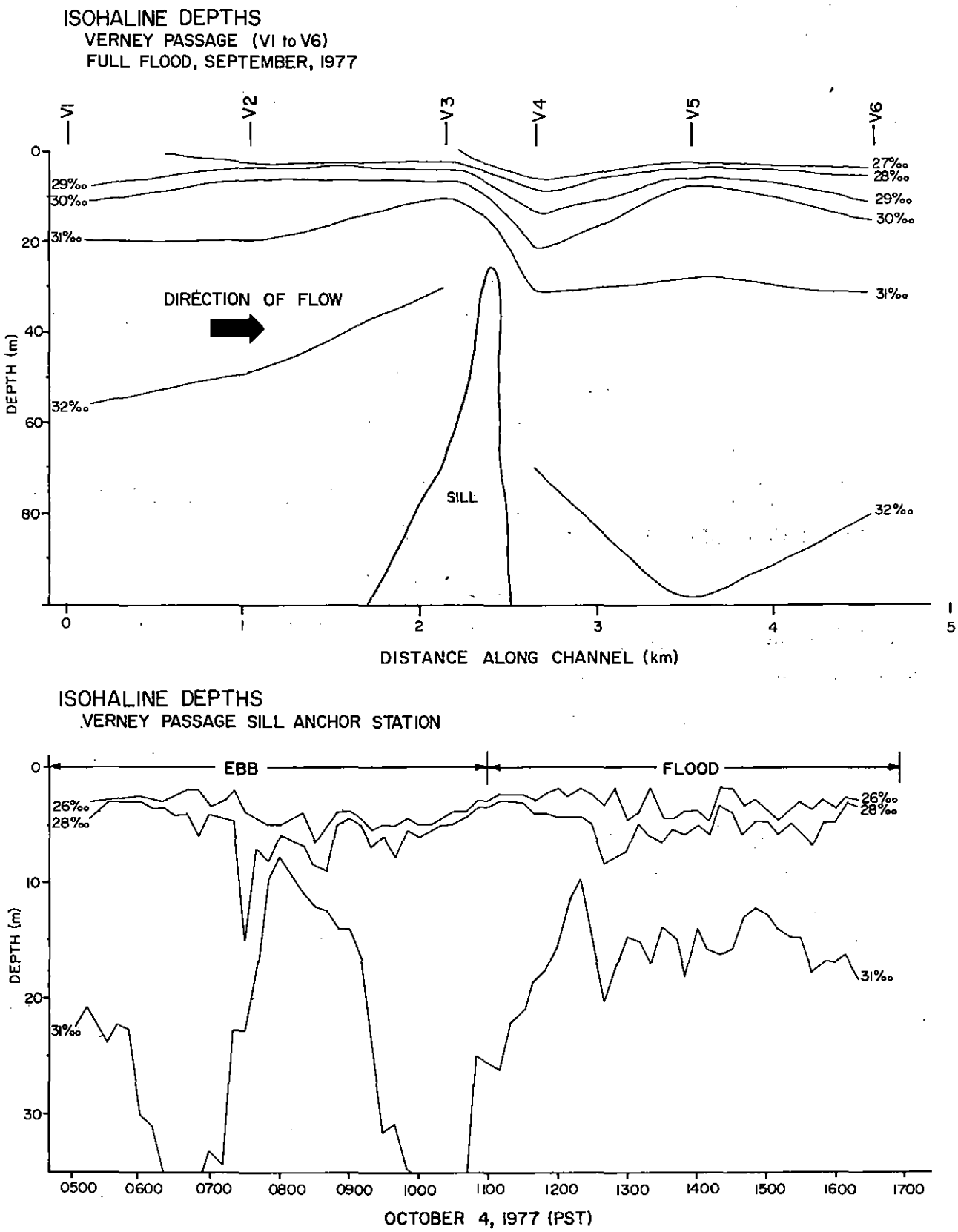

Figure 24. Depths of isohalines along Verney Passage - first time series - September, 1977; time series of isohaline depths second time series - September, 1977.

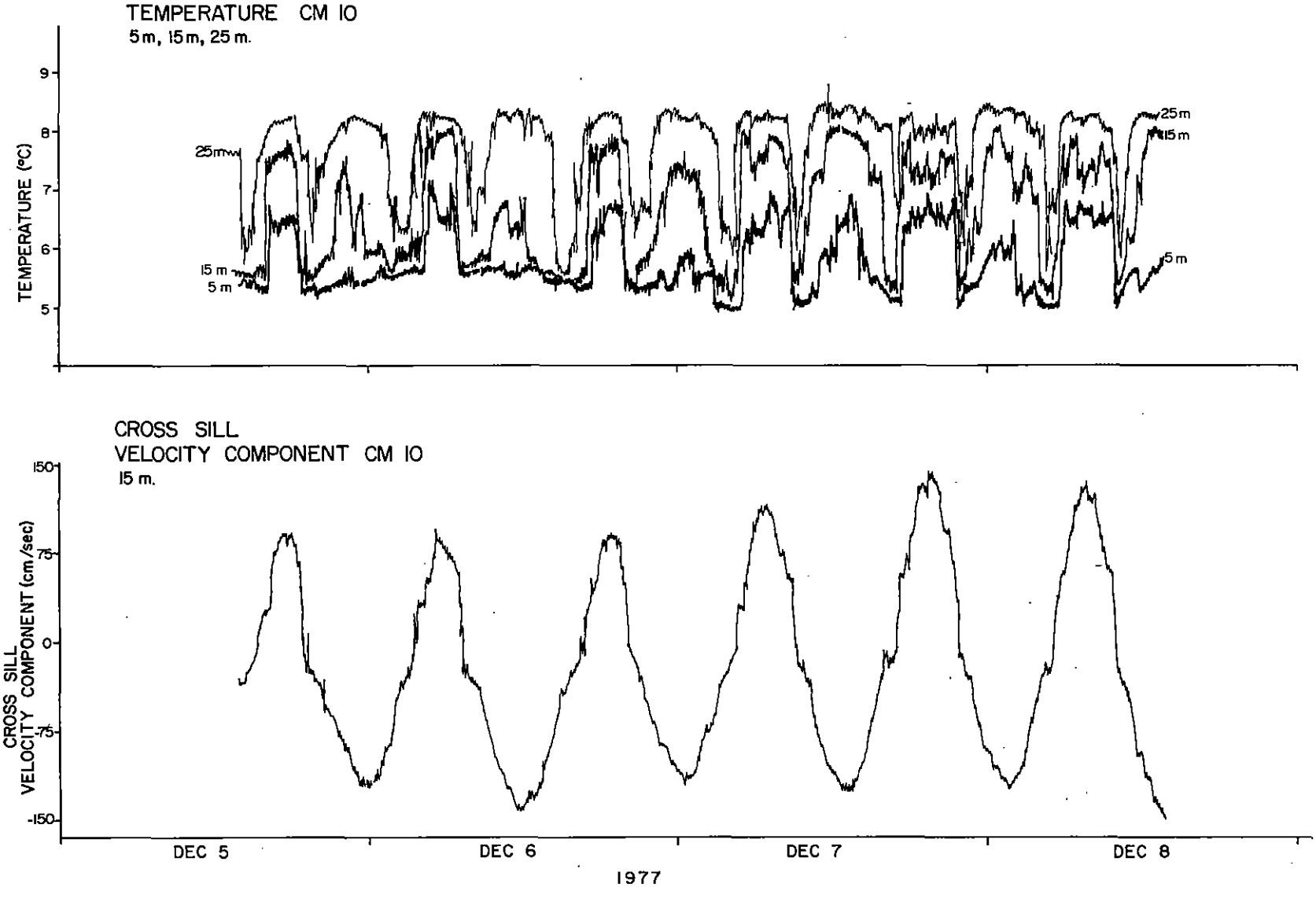

Figure 25. Temperature time series at 5 m, 15 m and 25 m depths and times series of cross sill current component, CM 10 - December, 1977.

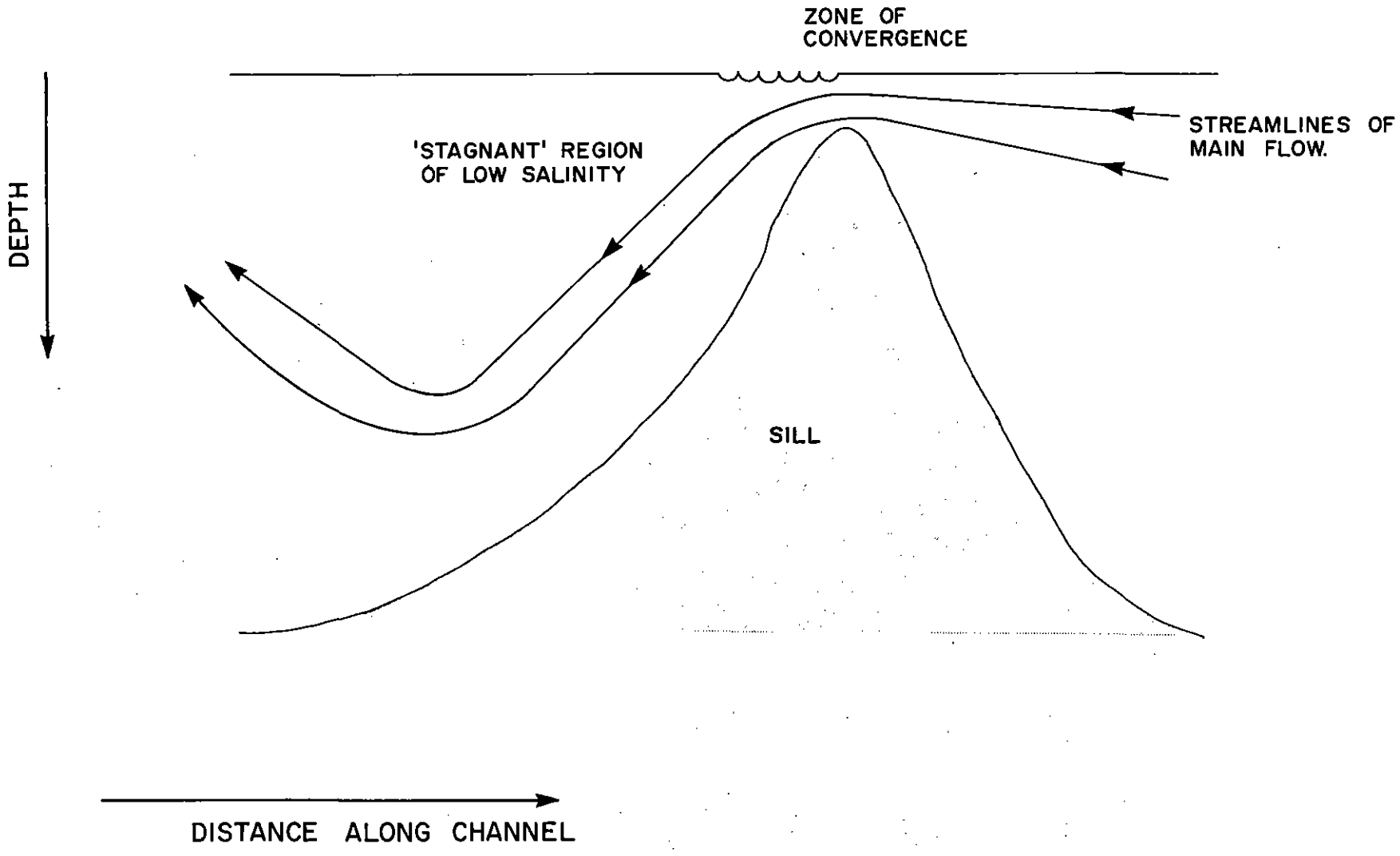

Figure 26. Schematic representation of flow over Verney Passage sill.

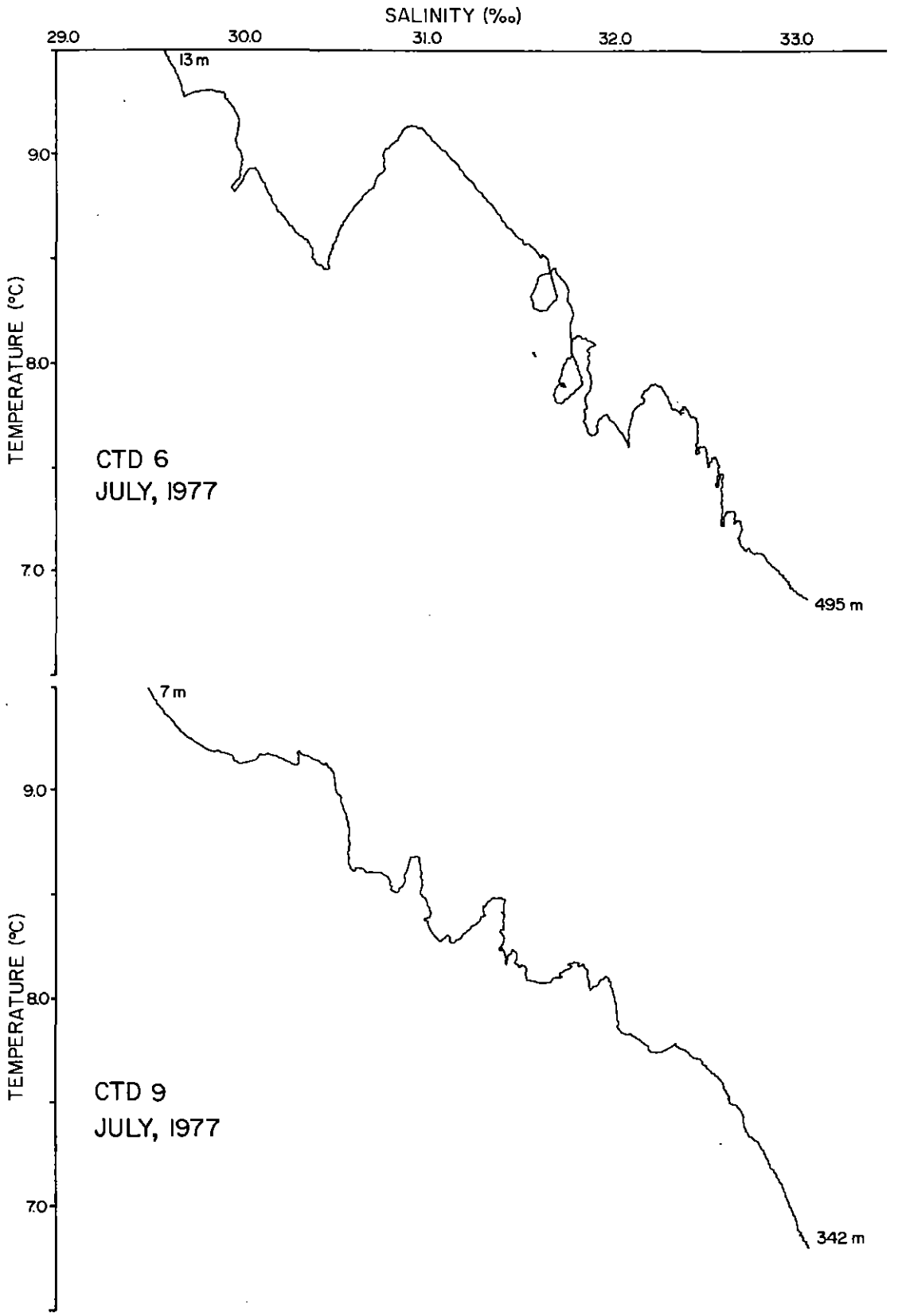

Figure 27. T, S curves from CTD 6 and CTD 9 - July, 1977.

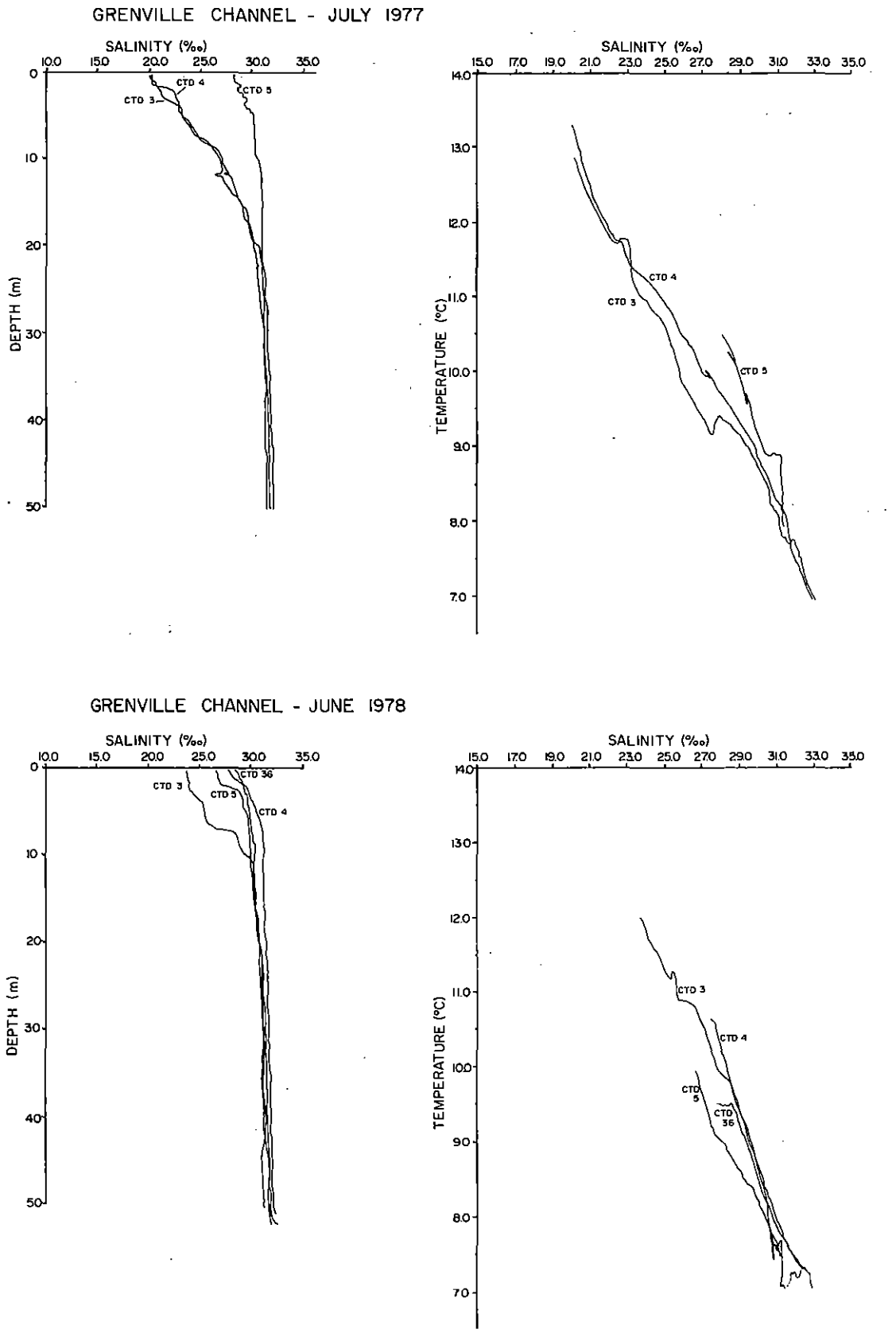

Figure 28. Vertical salinity profiles to 50 m depth and T, S curves from Grenville Channel - July, 1977 and June, 1978.

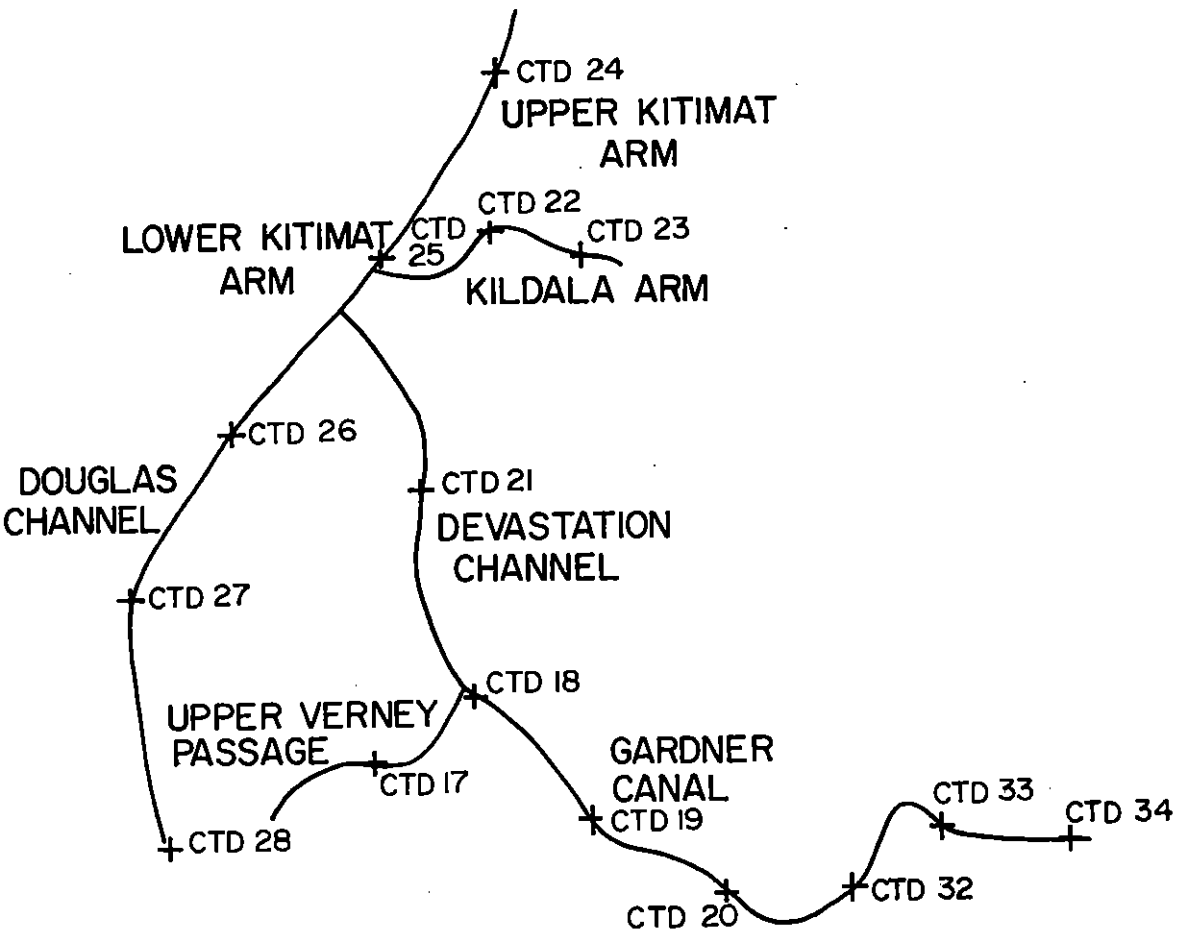

Figure 29. Schematic of inlet complex considered by Estuarine Circulation model.

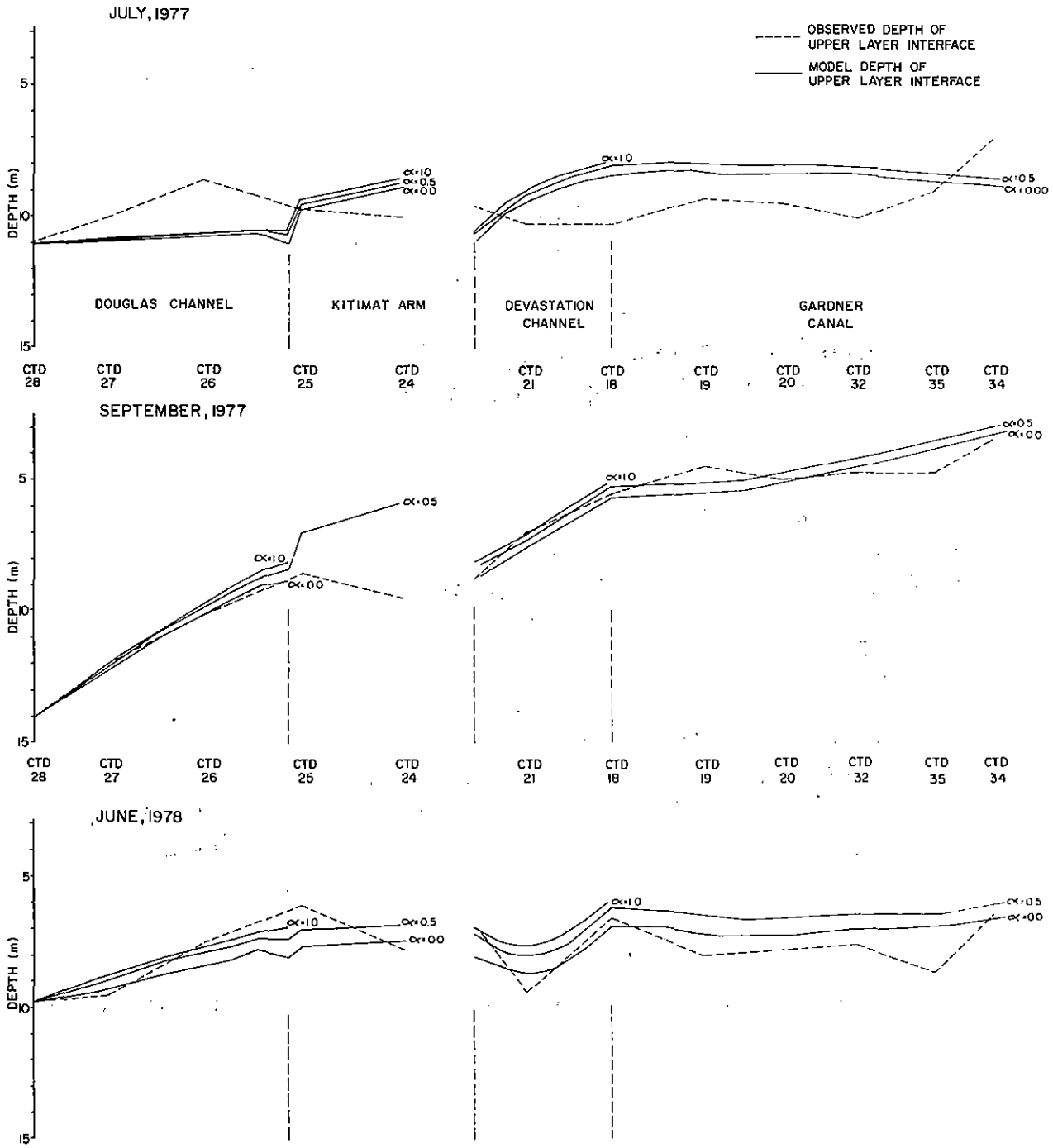

Figure 30. Computed upper layer thicknesses, Estuarine Circulation model - July, 1977; September, 1977; and June, 1978.

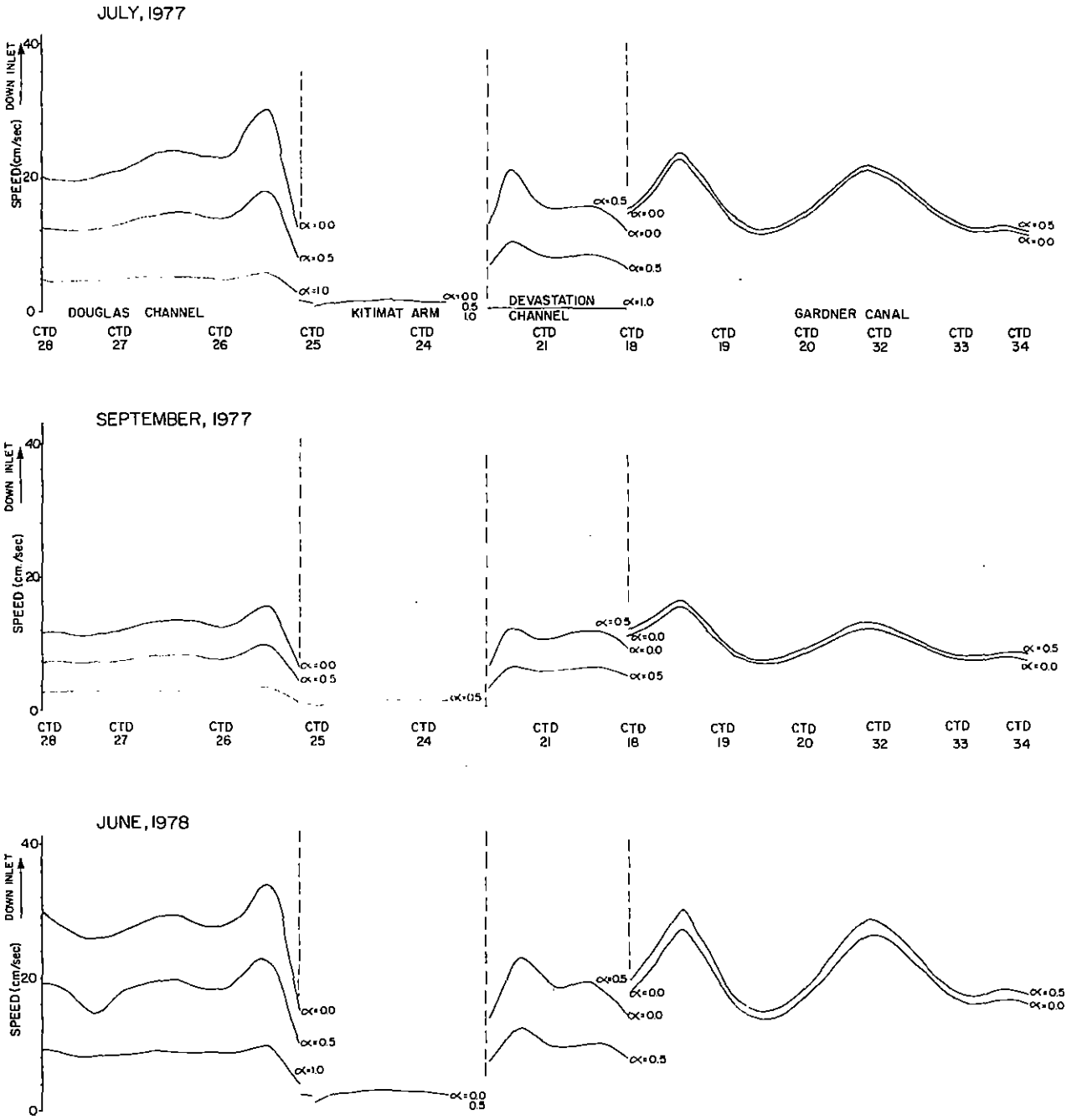

Figure 31. Computed upper layer velocities, Estuarine Circulation model - July, 1977; September, 1977; and June, 1978.

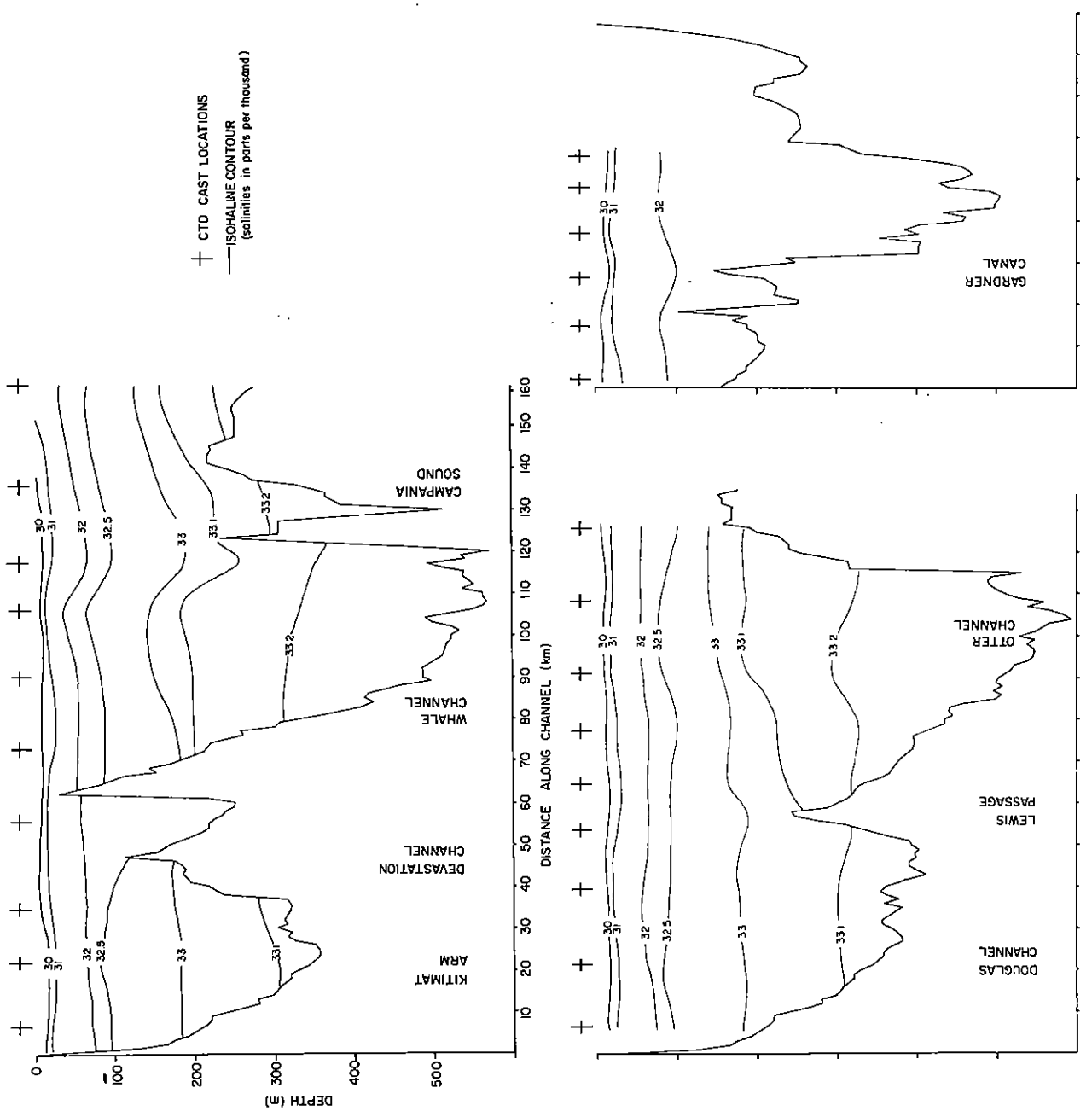

Figure 32. Depths of isohalines through 3 major basins of Kitimat system - September, 1977.

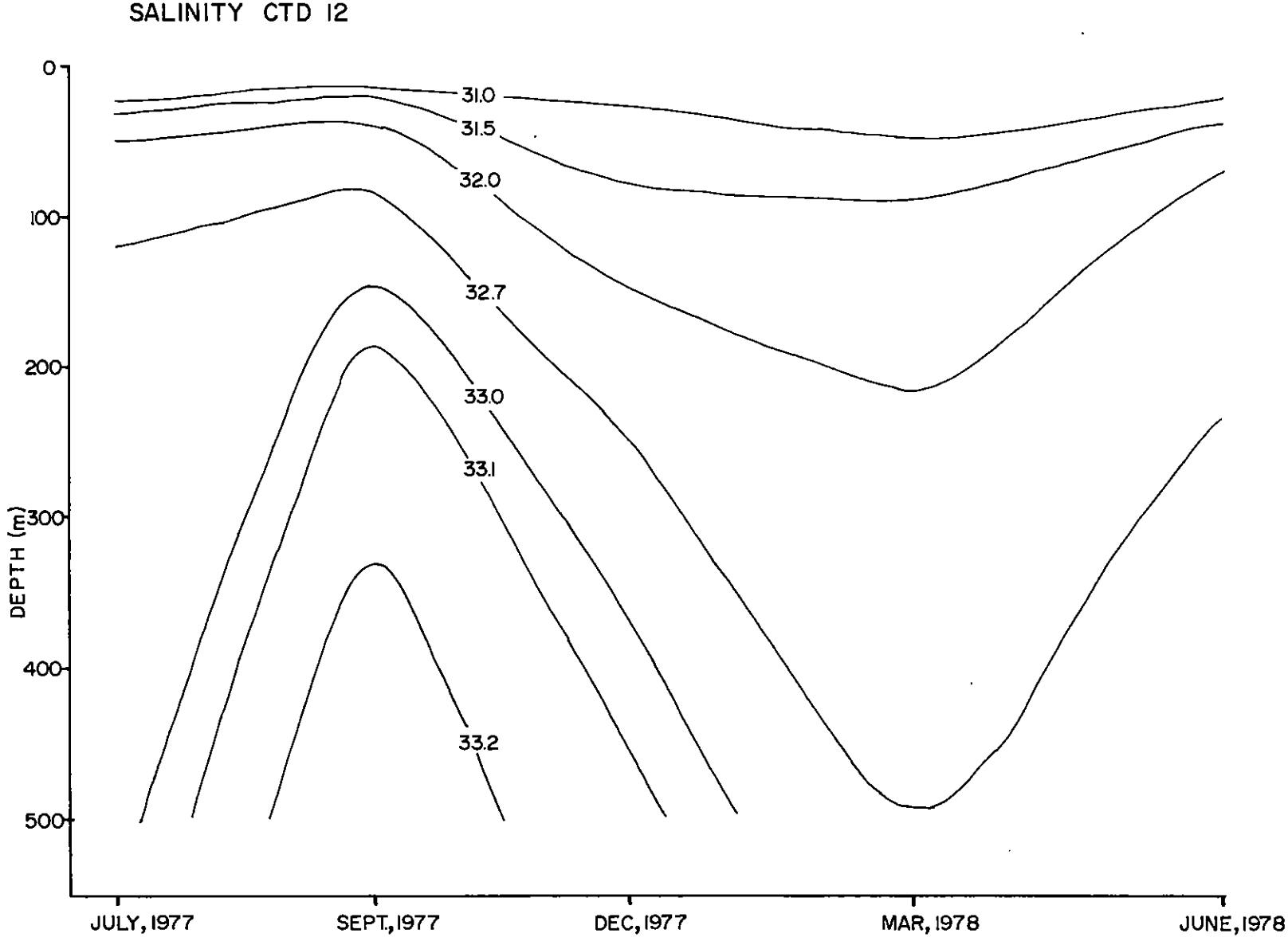

Figure 33. Depths of isohalines versus time at CTD 12.

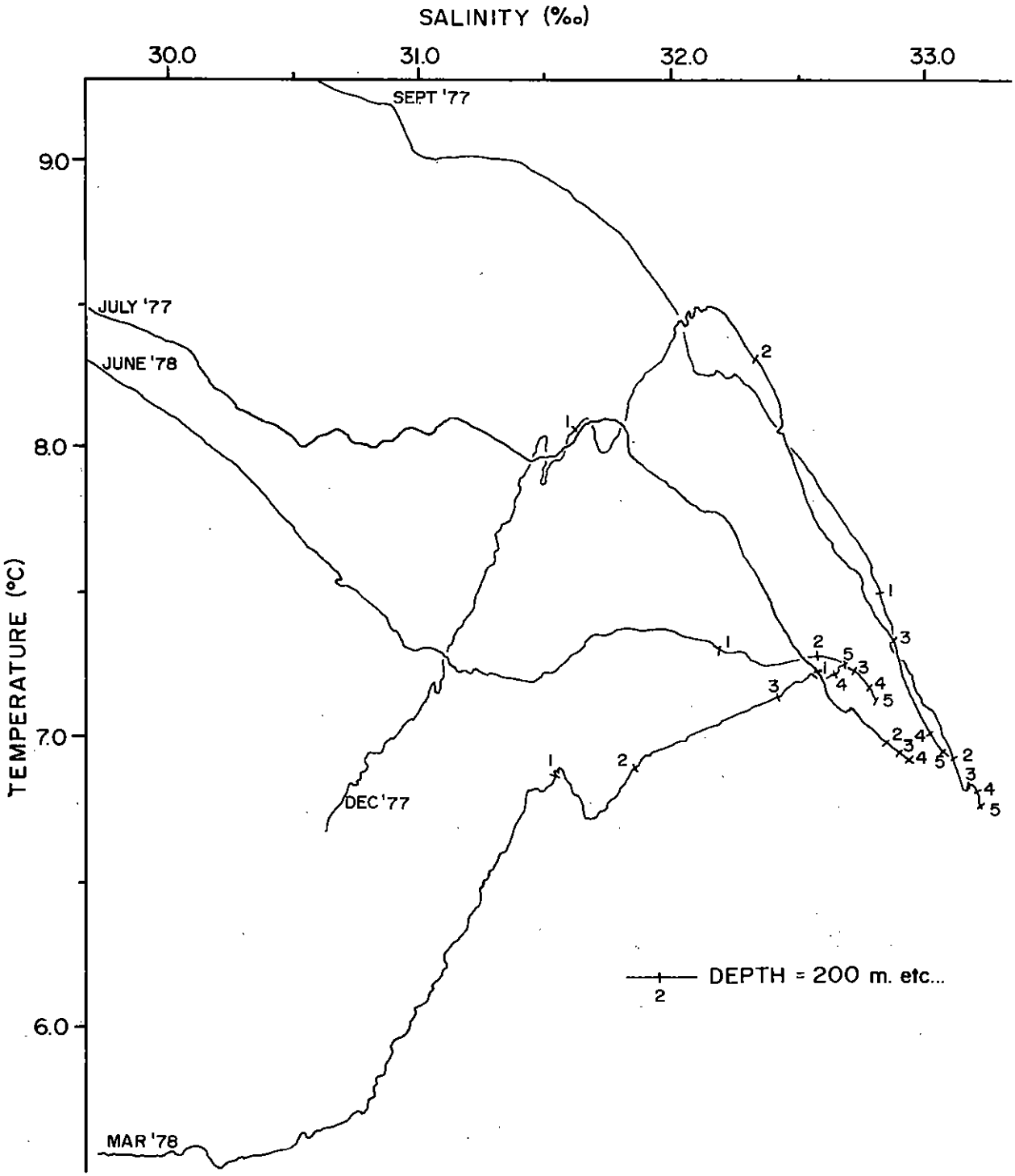

Figure 34. T, S curves from CTD 12 for 5 cruises.

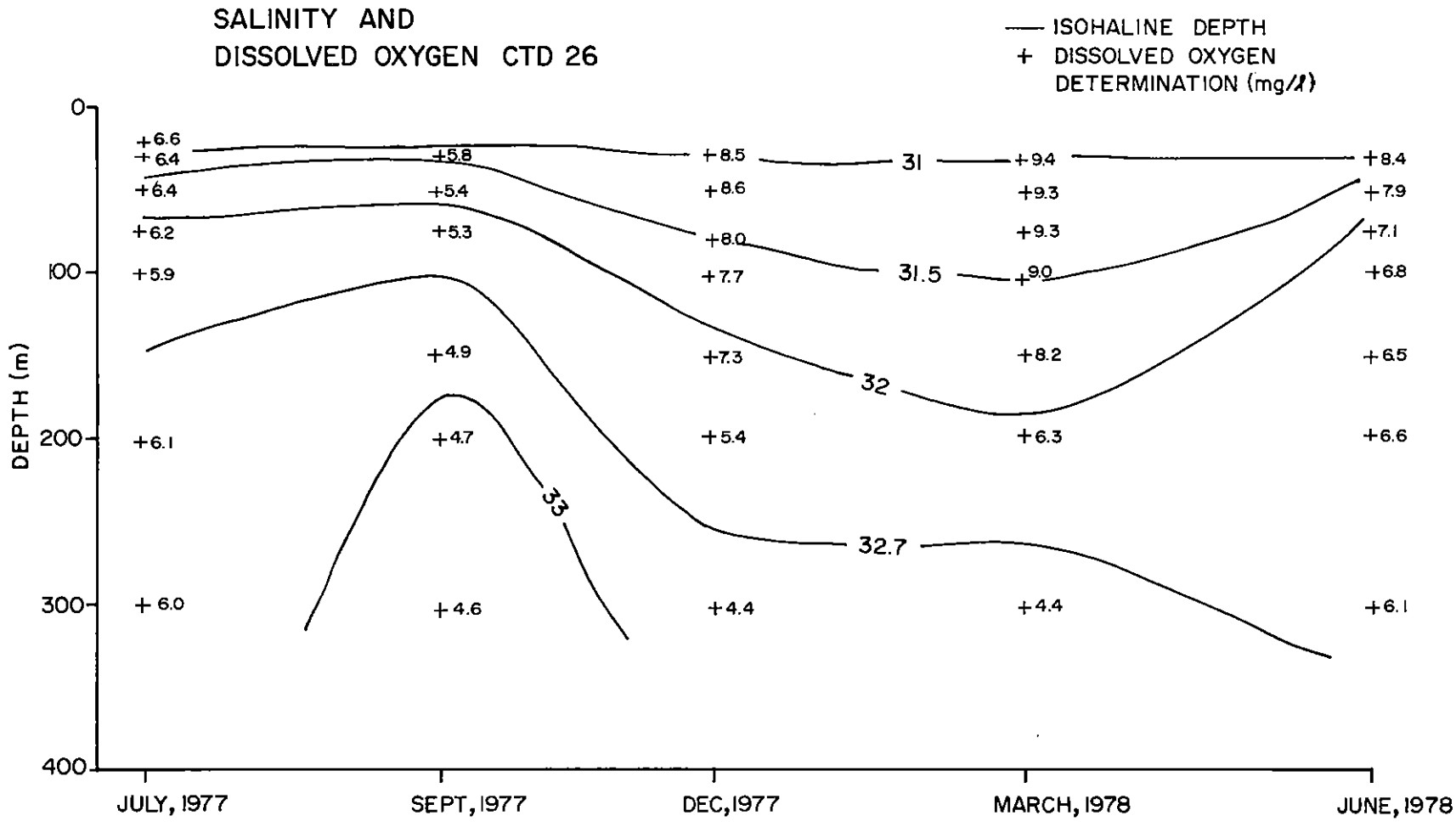

Figure 35. Dissolved oxygen levels and depths of isohalines versus time at CTD 26.

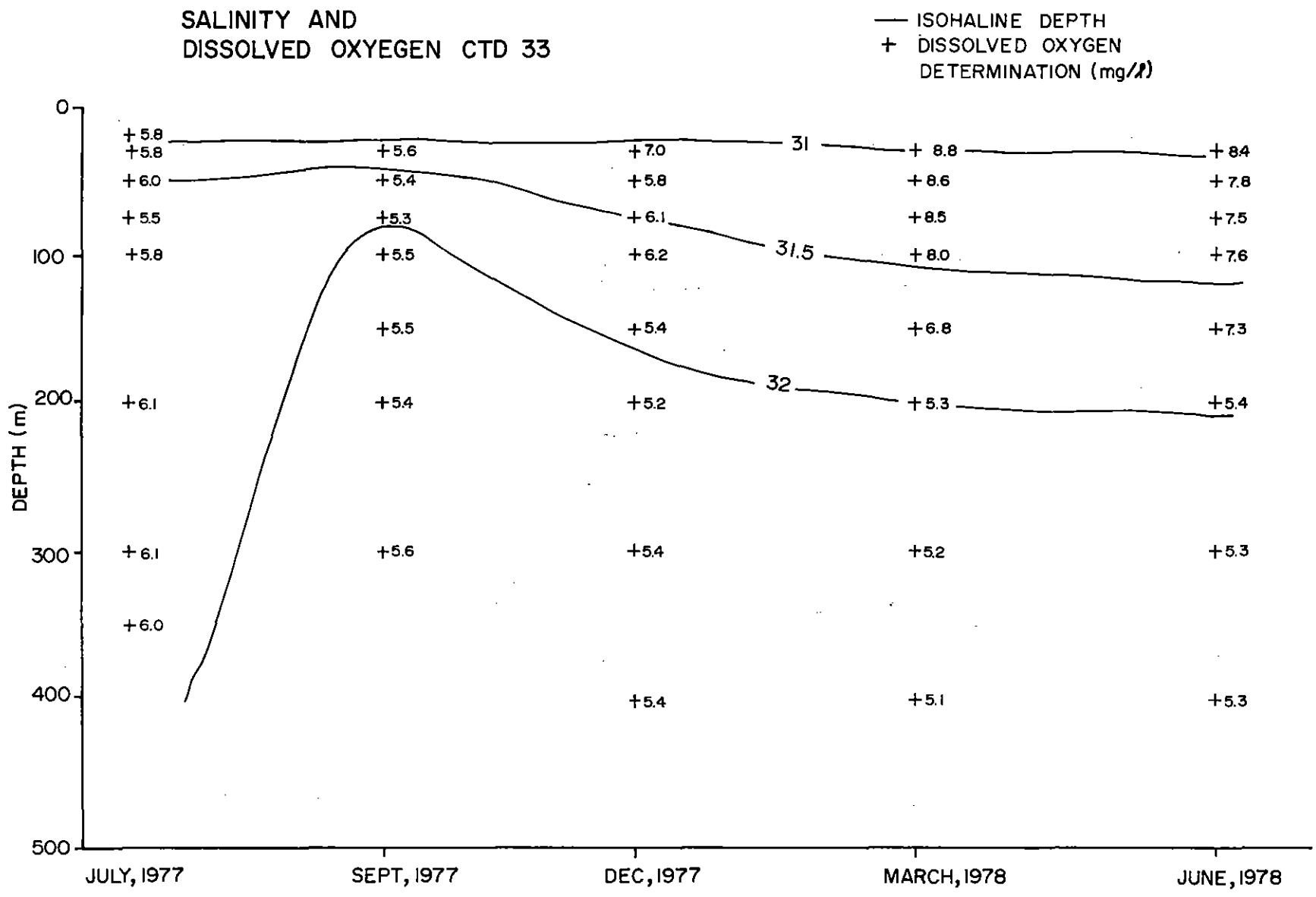

Figure 36. Dissolved oxygen levels and depths of isohalines versus time at CTD 33.

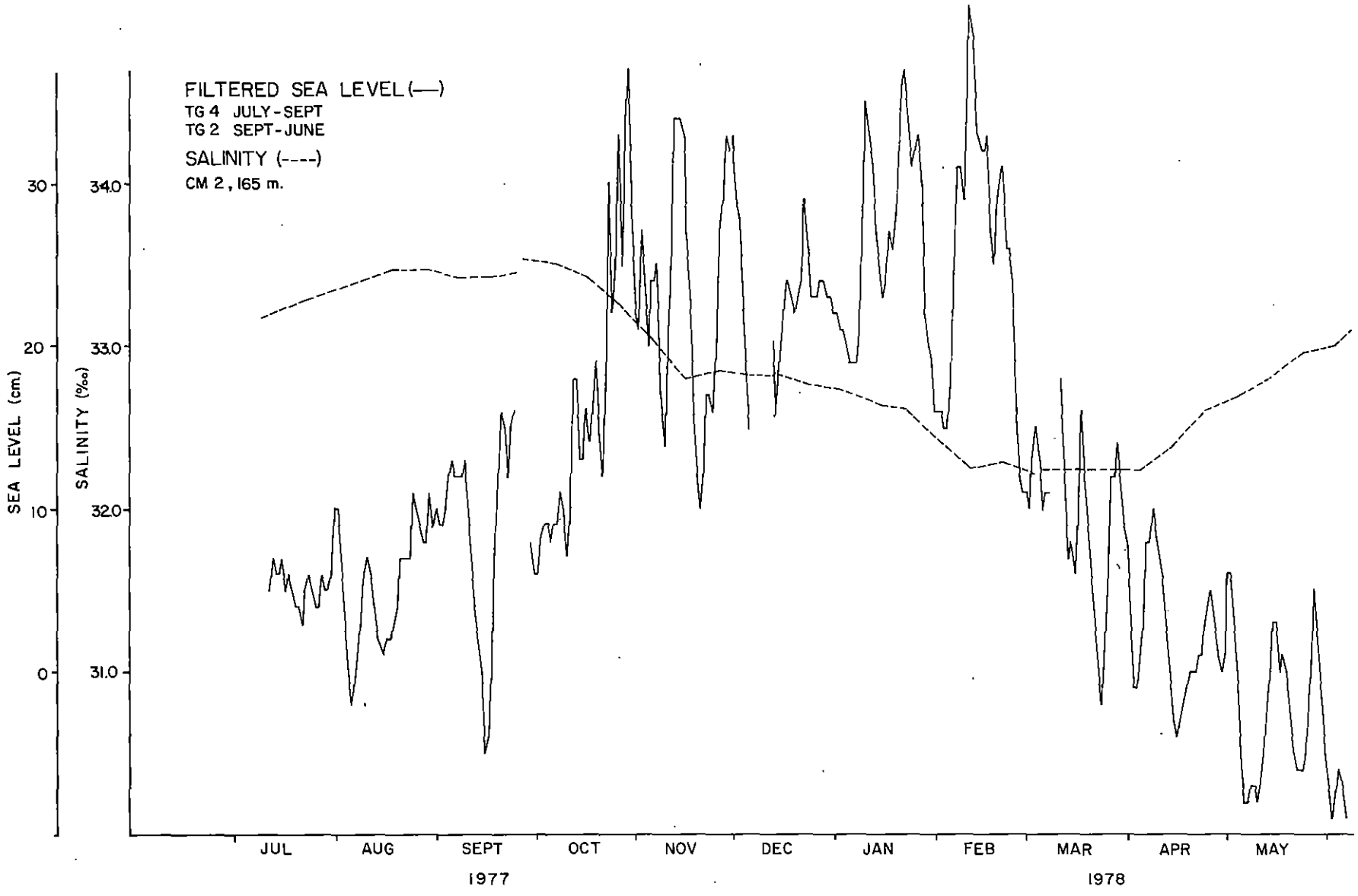

Figure 37. Observations of sea level (TG 2 and TG 4) and of salinity at 165 m depth (CM 2) - July, 1977 to June, 1978.